Regulation of Hop1 Function by Mec1/Tel1 Phosphorylation

Ana Raquel Penedos

A thesis submitted to University College of London in fulfilment of the requirements for the degree of Doctor of Philosophy

April 2012

Division of Stem Cell Biology and Developmental Genetics

National Institute for Medical Research

The Ridgeway; Mill Hill; London

NW7 1AA

Declaration

"I, Ana Raquel Penedos, confirm that the work presented in this thesis is my own. Where information has been derived from other sources, I confirm that this has been indicated in the thesis."

_____ _____

Abstract

Meiotic recombination is initiated with the formation of double-strand breaks (DSBs), which can be repaired by inter-sister (IS) or inter-homologue (IH) recombination. In most organisms, recombination between homologous chromosomes (homologues) is required to ensure the correct reductional segregation during meiosis I (MI). In contrast to mitotic recombination, during meiosis recombination between homologues is favoured over that between sister chromatids. This preference is referred to as IH bias.

Budding yeast Hop1 is an evolutionarily conserved meiotic chromosome axis phosphoprotein. It is required for three essential processes in meiosis: (i) catalysis of programmed meiotic DSBs, (ii) repair of DSBs via IH recombination, and (iii) activation of prophase I checkpoint.

Following Spo11-catalysis of DSBs, Hop1 is phosphorylated by Mec1/Tel1 at three serine (S) or threonine (T) residues within its SQ/TQ Cluster Domain (SCD), a Mec1/Tel1 and ATR/ATM target motif. The Mec1/Tel1 phosphorylation of Hop1 promotes the recruitment and activation of the effector kinase Mek1, which, in turn, are required for IH bias and meiotic checkpoint.

To better understand the molecular mechanism by which the Mec1/Tel1-phosporylation regulates Hop1 function, two alleles where either serine 298 or threonine 318 residues within Hop1's SCD were mutated to a non-phosphorylatable alanine (A) were characterised. Whilst both alleles confer a *dmc1*Δ arrest-deficient phenotype, *hop1-S298A* mutant, unlike *hop1-T318A*, produces highly viable spores at low temperature.

Further characterisation of these alleles suggests that T318 phosphorylation is required for efficient recruitment and initial activation of Mek1, essential for recombination, whilst S298 phosphorylation is necessary for the maintenance of Hop1-Mek1 interaction and hyperphosphorylation of Mek1, required for prophase checkpoint activation.

Table of Contents

List of Figures

List of Tables

List of Abbreviations

^{32}P	32-phosporous
A. thaliana	*Arabidopsis thaliana*
AAA+	ATPases associated
AE	axial element
Ahx	aminohexanoic acid
Amp	ampicillin
APS	ammonium persulphate
ATM	ataxia telangiectasia mutated
ATP	adenosine triphosphate
ATR	ataxia telangiectasia- and Rad3-related
ATRIP	ATR interacting protein
bp	base pair(s)
BSA	bovine serum albumin
BYTA	buffered yeast extract tryptone acetate
C. elegans	*Caenorhabditis elegans*
CDK	cyclin-dependent kinase
CDK-S	S-phase CDK
CE	central element
CEN	centromere
ChIP	chromatin immunoprecipitation
ChIP-chip	chromatin immunoprecipitation-on-chip
CO	crossover
Co-IP	co-immunoprecipitation
Cyh	cycloheximide
D. melanogaster	*Drosophila melanogaster*
DAPI	4,6-diamino-2-phenylindole
DDK	Dbf4-dependent kinase
dHJ	double Holliday junction
D-loop	displacement loop
DMSO	dimethyl sulphoxide
DNA	deoxyribonucleic acid
dNTP	deoxynucleotide triphosphate
DSB	double-strand break
dsDNA	double-stranded DNA
E. coli	*Escherichia coli*

ECL	enhanced chemiluminescence
EDTA	ethylenediaminetetra-acetic acid
EMS	ethyl methane sulphonate
FHA	forkhead-associated
GST	glutathione S-transferase
HJ	Holliday junction
HO	homothallic
Hyg	hygromycin
IH	inter-homologue
IS	inter-sister
JM	joint molecule
Kan	kanamycin
kb	kilo base (s)/ kilo base pair (s)
LB	Luria Bertani
LE	lateral element
LMP	low melting point
MAT	mating type locus
MI	meiosis I
MII	meiosis II
MOPS	3-(N-morpholino)propanesulphonic acid
NCO	noncrossover
NLS	nuclear localisation signal
OD_{600}	optical density at 600 nm
PAGE	polyacrylamide gel electrophoresis
PBS	phospho-buffered saline
PBS-T	PBS with Tween
PC	polycomplex
PCR	polymerase chain reaction
PEG	polyethylene glycol
PFG(E)	pulsed-field gel (electrophoresis)
P-Hop1	phosphorylated Hop1
RPA	replication protein A
rpm	revolutions per minute
S	DNA synthesis
S. cerevisiae	*Saccharomyces cerevisiae*
S. pombe	*Schizosaccharomyces pombe*
SC	synaptonemal complex
SCD	SQ/TQ cluster domain

SCE	sorbitol sodium citrate EDTA
SD	synthetic dextrose
SDS	sodium dodecyl sulphate
SDSA	synthesis-dependent strand annealing
SEI	single end invasion
SPM	sporulation medium
ssDNA	single-stranded DNA
TAE	Tris-acetate EDTA
TBE	Tris-borate EDTA
TCA	trichloroacetic acid
TE	Tris-EDTA
TEMED	N,N,N',N'-tetramethyl-ethylenediamine
WT	wild-type
YEP	yeast extract peptone
YPA	yeast extract peptone acetate
YPD	yeast extract peptone dextrose
YPG	yeast extract peptone glycerol

Acknowledgements

Firstly, I would like to thank Rita Cha, my supervisor, for accepting me into her group, giving me the opportunity to work on this project. Her guidance and advice were greatly appreciated and I have learnt a great deal from them. Her constant optimism and objective view on subjects and goals will always be for me an example to follow.

I am grateful to Anthony Johnson, Hideo Tsubouchi, Jesús Carballo and Marco Foiani for providing some of the strains and reagents used in this thesis. The meetings with the members of my thesis committee, Alastair Goldman, James Turner and Robin Lovell-Badge, were rich in ideas and valid input and have motivated me and challenged my views in all occasions. I am thankful to them for finding the time for them.

I would also like to say a big “thank you!!” to all present and former members of the Cha and Thorpe labs for discussions, ideas, constructive criticism, advice and laughter. I would especially like to thank Nadia for her support in the early days of my PhD and for her patience and understanding of my constant questions and preoccupations then and after. I would like to thank Jesús for discussions, suggestions and advice, and express my admiration for his infinite scientific knowledge. I also thank Tony for all his support in technique-, IT- and yeast-related issues and for sharing his “yeasty” and “non-yeasty” knowledge. Marco’s and Ad’s help on genetic manipulation and protein techniques is deeply appreciated. The insightful comments and suggestions offered by Jesús, Marco and Peter were also immensely valuable. On a less serious note, I thank Jesús, Rico and Alex for the many silly conversations and laughter-inducing moments that made days in the lab so much funnier.

Off the lab, I am grateful to my family, especially my mum, for all the support and to Ausrine and Steffani, the best flatmates ever, for being such fun and understanding friends. Also, I thank Amanda, Mónica, MunYee and Sahar for remembering me, despite my near-disappearance. Finally, I would like to thank Alex for his unequalled patience and kindness, and for making me smile in the last few months.

Chapter 1: Introduction

1.1. Overview

Meiosis occurs in a wide range of eukaryotes. In plants, complex fungi and yeast it leads to spore formation, while in animals it is the basis of gametogenesis. It comprises two rounds of chromosome segregation preceded by a single round of DNA replication. On the first division of meiosis (MI), homologous maternal and paternal chromosomes (homologues) are segregated, leading to the halving of the genetic material (reductional division). On the second meiotic division (MII), sister chromatids are separated in a manner similar to mitosis (equational division; Figure 1.1) (Zickler and Kleckner, 1998).

This process is highly conserved in sexually reproducing eukaryotes. It is through meiosis that the required ploidy reduction prior to fertilization is achieved so that genome size is maintained in sexually reproducing organisms (Zimmer, 2009). Meiotic recombination is also an important source of genetic variability in populations and, consequently, one of the causes of the prevalence of sexual reproduction amongst eukaryotes as it leads to improved population fitness (Paland and Lynch, 2006), higher adaptability (Goddard et al., 2005) and increased resistance to pathogens (Zimmer, 2009).

Up to 90% of the total time of meiosis in many organisms is taken in MI (Bennett, 1977) and most of this is spent on prophase I. This is due to the nature of the division. The separation of homologues in meiosis I presents its own challenges. While sister chromatids remain attached through centromere and inter-sister cohesion after DNA replication, homologous chromosomes are physically independent entities. Two distinguishing meiotic events that ensure correct segregation of homologues occur during prophase I: the programmed introduction of double-strand breaks (DSBs) throughout the genome and their repair via recombination with the homologous chromosome (Figure 1.1). This process, being potentially lethal for the cell, is tightly regulated (Phadnis et al., 2011).

Homologue missegregation is rare in most organisms. In budding yeast, the probability of meiotic nondisjunction is about 1 in 10,000. In *Drosophila melanogaster* it occurs in around 1 in 4,000 of the female germ line. Mammals, namely mice, seem to have a higher rate of meiotic errors leading to aneuploidies,

although less than 2%. However, in humans, meiotic defects appear to occur much more frequently and aneuploidies are detected in 5% of pregnancies or more. Common outcomes of meiotic defects in humans are infertility, miscarriage and genetic diseases such as Down syndrome and sex-chromosome aneuploidies, which most frequently result from homologue missegregation in meiosis I (Hassold and Hunt, 2001).

In this project, I will focus on the process of meiotic recombination and, particularly, on the mode by which it is regulated to favour DSB repair via inter-homologue (IH) rather than inter-sister (IS) recombination, the prevalent repair pathway in mitosis. The budding yeast *Saccharomyces cerevisiae* will be used as a model system, because of the ease of its genetic manipulation and induction of highly efficient and synchronous meiotic cultures.

Figure 1.1 Timeline of major meiotic events

(A) Following S phase, DSB catalysis occurs and COs are formed during prophase I. This allows accurate segregation of homologues in MI and formation of four haploid spores in MII.

(B) Prophase I is subdivided into four sub-stages. At leptotene DSBs are formed and repair is initiated. At the chromosomal level, axial elements start forming. During zygotene, invasion into the homologue occurs and formation of SCs is initiated. D-loops and dHJs are formed during pachytene. Complete SCs are detected at this sub-stage. DSB repair is completed at diplotene with the formation of COs, which are detected as chiasmata at the cytological level.

Figure adapted from (Hunter and Kleckner, 2001, Murakami and Keeney, 2008).

1.2. Meiotic recombination

1.2.1. Recombination in mitosis and meiosis

Mitotic recombination occurs throughout the proliferative cycle and is required for the repair of DNA damage resultant from exogenous and endogenous sources. Its objective is, therefore, the maintenance of genome integrity through efficient and accurate repair of lesions. In contrast, meiotic recombination is temporally confined to a particular period in meiosis (prophase I) and is essential for ensuring correct segregation of homologues at anaphase I (Andersen and Sekelsky, 2010).

The different functions of mitotic and meiotic recombination entail that their regulation and products are also distinct. In mitosis, DNA damage may be due to single- or double-strand breaks, stalled or collapsed replication forks or other deleterious structures resulting from harsh environments or cell metabolites. Repair can be achieved through several different mechanisms, depending on the type of damage (Andersen and Sekelsky, 2010).

In meiosis, DNA damage consists essentially of developmentally programmed DSBs. These are processed in a tightly regulated manner that ensures that a major fraction of breaks are repaired via IH recombination. This pathway can lead to the formation of crossovers (COs), required for the establishment of physical connections between homologous chromosomes. These are detected at the cytological level and referred to as chiasmata. The latter, in turn, are essential for accurate homologue segregation in MI (Andersen and Sekelsky, 2010).

1.2.2. Initiation via programmed DSB catalysis

Meiotic recombination is initiated by the induction of double-strand breaks (DSBs) at the onset of prophase I (leptotene) (Figure 1.1). These occur throughout the genome and are catalysed by the meiosis-specific Spo11, an evolutionarily conserved nuclease related to type II topoisomerases (Keeney et al., 1997). In order to be effective in cleaving DNA, Spo11 interacts with three other proteins: Ski8, Rec102 and Rec104 (Arora et al., 2004, Jiao et al., 2003, Kee and Keeney, 2002). The first interaction is required for chromatin association and, subsequently, is thought to mediate Spo11 interaction with a complex formed by Rec102 and Rec104 (Arora et al., 2004), both meiosis-specific and necessary for DSB formation (Bullard et al., 1996).

In addition to Spo11 and the above mentioned Spo11-interacting proteins, several other factors are required for DSB formation. One such factor is the MRX complex, composed of Mre11, Rad50 and Xrs2 proteins. Co-immunoprecipitation experiments have shown that Mre11 binds the two other components of the complex, allowing Rad50-Xrs2 interaction (Haber, 1998). Deletion of *RAD50*, *MRE11* or *XRS2* blocks DSB formation (Cao et al., 1990, Ivanov et al., 1992, Johzuka and Ogawa, 1995).

Another complex required for DSB catalysis is that formed of Mer2, Mei4 and Rec114. Absence of any of these proteins leads to undetectable levels of meiotic DSBs (Bullard et al., 1996, Jiao et al., 1999, Rockmill et al., 1995). Like Spo11 and MRX complexes, Mer2-Mei4-Rec114 complex localises to chromosomes, although no significant co-localisation between the three complexes is detected, possibly indicating that they are required at different stages in DSB induction (Li et al., 2006).

Two other meiosis-specific proteins, Hop1 and Red1, have also been shown to be required for DSB formation as DSB levels are substantially reduced in *hop1*Δ and *red1*Δ mutants (Mao-Draayer et al., 1996). Like the previously mentioned DSB factors, they localise to chromosomes. Interestingly, however, these proteins are components of characteristic structures that form along the axes of replicated meiotic chromosomes, the axial elements (AEs; Figure 1.2) (Hollingsworth et al., 1990, Rockmill and Roeder, 1990), constituting one of the links between DSB catalysis and chromosome structure.

Other structural proteins, such as cohesins, condensins and histones, also have a role in DSB formation, affecting the levels and sites at which breaks occur. Mutations in a histone deacetylase, Sir2, for example, affect the frequency of breaks at 12% of the genes in the budding yeast genome (Mieczkowski et al., 2007). Loci where high levels of DSBs are induced, referred to as DSB hotspots, are usually located in intergenic regions, where transcription factor binding sites can be found (Mizuno et al., 1997) and chromatin structure allows access of various proteins to DNA (Wu and Lichten, 1994, Wu and Lichten, 1995, Yamada et al., 2004).

In fact, DSBs appear to occur in regions corresponding to chromatin loops, although tethering of these regions to chromosome axes, where DSB catalysis takes place, must occur prior to or at the point of DSB formation. Evidence suggests that tethering of a DSB hotspot to the axis occurs through the action of the Mer2-Mei4-Rec114 complex and in the presence of axes components Hop1, Red1 and

cohesins (Berchowitz et al., 2009, Blat et al., 2002, Glynn et al., 2004, Panizza et al., 2011).

Finally, DSB induction is also temporally regulated so that breaks do not occur in unreplicated chromosomes, with the onset of DSB induction coupled to the completion of the genome replication (Borde et al., 2000). Mer2 phosphorylation by two cell cycle regulators, Cdc28 and Cdc7 kinases, is thought to have a prominent role in the temporal regulation of DSB formation. This phosphorylation is DSB-independent and mediated by the CDK-S (Cdc28+Clb5/6) and DDK (Cdc7+Dbf4) complexes (Henderson et al., 2006, Sasanuma et al., 2008). These seem to act jointly in the activation of Mer2 (Wan et al., 2008), allowing its interaction with Mei4, Rec114 and Xrs2 (Arora et al., 2004), likely timing DSB catalysis with completion of DNA replication in this way (Murakami and Keeney, 2008).

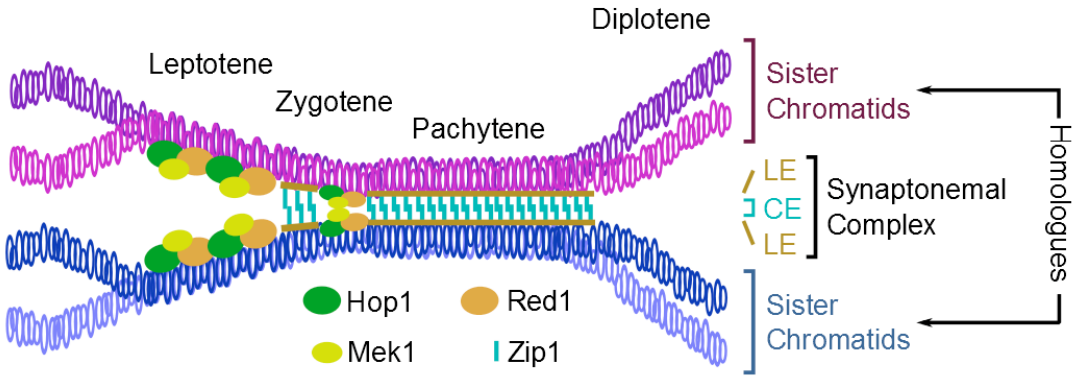

Figure 1.2 Meiotic chromosome structure

Budding yeast Red1, Hop1 and Mek1 are major components of the axial elements (AEs) that form along each homologous chromosome during prophase I of meiosis. During zygotene and pachytene, AEs of each homologue pair are juxtaposed by dimers of Zip1. This characteristic meiotic structure is referred to as the synaptonemal complex (SC) and is composed of the two axial elements, now named lateral elements (LEs), and a central element (CE), of which Zip1 is the major component.

1.2.3. DSB repair

1.2.3.1. Overview

Following DSB formation, Spo11, covalently bound to DSB ends, is removed through resection from the 5' ends of the breaks, generating 3' single-stranded DNA (ssDNA) ends (Figure 1.3A and B). The MRX complex is required for this step in meiotic recombination (Garcia et al., 2011, Sun et al., 1991). In *rad50S* mutants, for example, DSBs are formed, but not resected, leading to the accumulation of unrepaired breaks in the cell (Alani et al., 1990). In *mre11-58* mutants, where interaction with Rad50 and Xrs2 is disrupted, DSB processing is also blocked, as it is in the *mre11S* and *mre11-H125N* mutants (Moreau et al., 1999, Nairz and Klein, 1997, Tsubouchi and Ogawa, 1998).

Mre11 co-localises with Sae2/Com1 (Terasawa et al., 2008) and the absence of the latter leads to a phenotype similar to that of the *mre11* or *rad50* mutants described above, with accumulation of unresected breaks and delays in meiotic progression (McKee and Kleckner, 1997, Prinz et al., 1997). Similarly, *sae2* mutants where phosphorylation by CDK-S or Mec1/Tel1 does not occur are also defective in DSB processing (Baroni et al., 2004, Cartagena-Lirola et al., 2006, Manfrini et al., 2010).

Upon Spo11 removal from the ends of DSBs, further resection is carried out via two redundant pathways, one involving the exonuclease Exo1 and the second requiring the nuclease Dna2 and the helicase Sgs1 (Figure 1.3C) (Manfrini et al., 2010, Mimitou and Symington, 2008, Tsubouchi and Ogawa, 2000). The long 3' ssDNA tails thus generated serve as a substrate for Rad51 and Dmc1, yeast orthologues of the bacterial recombinase RecA, which promote DSB repair via homologous recombination (Bishop et al., 1992, Shinohara et al., 1997a, Shinohara et al., 1992).

During meiosis, DSB repair occurs through two major pathways, the first involving the homologous chromosome, inter-homologue (IH) recombination (Figure 1.3E), and the second using the sister chromatid as the repair template, inter-sister (IS) recombination (Figure 1.3D). Since only IH recombination has the potential to generate crossovers, which allow accurate homologue segregation in anaphase I, this pathway is favoured and intermediate products of IS recombination events are detected at only 13-25% of the levels of those ensuing from IH recombination. The

preference for IH recombination in meiosis is referred as IH bias (Allers and Lichten, 2001, Schwacha and Kleckner, 1994, Schwacha and Kleckner, 1997).

Both Dmc1 and Rad51 are required for homology search and invasion into the undamaged recombination template (homologous chromosome or sister chromatid), with the meiosis-specific Dmc1 playing a central role in the establishment of IH bias (Bishop et al., 1992, Shinohara et al., 1997a, Shinohara et al., 1992). Following invasion into the homologue by a single-stand end of the DSB (single end invasion, SEI), a D-loop structure is formed (Figure 1.3G). DNA synthesis takes place and two situations can occur (Figure 1.3H and I) (Allers and Lichten, 2001, Borner et al., 2004, Hunter and Kleckner, 2001):

(i) The invading strand detaches from the donor sequence, reannealing to the complementary single strand on the other side of the break (Figure 1.3H), a mechanism known as synthesis-dependent strand annealing (SDSA). In this manner, no exchange of sequences flanking the DSB occurs and a noncrossover (NCO) is made;

(ii) The second DSB strand is captured, leading to the formation of a joint molecule (JM) (Figure 1.3I). Next, ligation of damaged and donor strands results in the formation of a double Holliday junction (dHJ) (Figure 1.3J), which can then be resolved into a crossover (CO) (Figure 1.3L), resulting in the exchange of genetic material between homologues, or, less likely, into a NCO (Figure 1.3K).

Resolution of dHJs can be achieved by two sets of nucleases: Mus81 and Mms4 or Msh4 and Msh5 (Argueso et al., 2004). When resolution is carried out by the latter nucleases, the presence of one CO inhibits the occurrence of a second one in close vicinity, a phenomenon referred as crossover interference (Nishant et al., 2010, Shinohara et al., 2008), a tendency that is not detected in Mus81/Mms4-dependent crossovers (de los Santos et al., 2003, Ehmsen and Heyer, 2008).

Msh4 and Msh5 belong to the ZMM group of proteins (Zip1-4, Msh4-5, Mer3), involved in meiotic recombination and crossover control. *zmm* mutants show reduced CO levels and defects in homologue pairing or synapsis, due to inefficient assembly of a meiosis-specific structure, the synaptonemal complex (SC). All ZMM proteins and a full SC are required for crossover assurance, the mechanism by which at least one CO (obligatory crossover) is ensured between homologous chromosomes in order to allow correct homologue segregation in MI (Shinohara et al., 2008). Zip2 and Zip4 have also been implicated in crossover homeostasis, a

process that promotes the increase of the proportion of CO to NCO in situations of reduced DSB levels so that the obligate crossovers are formed (Chen et al., 2008).

SC assembly is tied in with the meiotic DNA recombination events described above. In early prophase I, leptotene, the meiosis-specific structural proteins Red1, Hop1 and Mek1 are loaded onto chromosomes, forming the axial elements (AEs) (Bailis and Roeder, 1998, Hollingsworth et al., 1990, Smith and Roeder, 1997). At zygotene, when DSBs progress to SEIs, AEs are juxtaposed through dimers of Zip1 (a ZMM protein), which align perpendicularly to the axes, forming a zip-like structure (Padmore et al., 1991). The synaptonemal complex is fully assembled at pachytene, when the late stages of recombination take place, being formed of the two AEs, now named lateral elements (LEs), and a central element (CE) that holds them together (Figure 1.2) (Page and Hawley, 2004, Sym et al., 1993). The axial element proteins, similarly to Dmc1, play key roles in promoting IH bias during meiosis (Hollingsworth and Byers, 1989, Niu et al., 2007, Schwacha and Kleckner, 1997, Shinohara et al., 1997a).

Figure 1.3 Major pathways for repair of programmed DSBs in budding yeast meiosis

(A) DSB catalysis is mediated by Spo11 and requires several additional proteins, including the MRX complex and the axial element proteins Red1 and Hop1. **(B)** Spo11 molecules covalently linked to the DSB ends are removed by resection of the 5' ends of DSBs by Mre11, Rad50 and Sae2. **(C)** Further resection by Exo1, Dna2 and Sgs1 leads to the formation of long 3' single-stranded DNA tails. Homology search is then carried out by two RecA orthologues: Rad51 and Dmc1. Meiotic DSB repair can be carried out using two major pathways for homologous recombination. One of these pathways uses the sister chromatid as a template for DSB repair, inter-sister (IS) recombination, and is mediated by Rad51 **(D)**. The preferred DSB repair pathway in budding yeast meiosis uses the homologous chromosome as a template for DSB repair: inter-homologue (IH) recombination. Invasion into the homologue is mediated by Dmc1 and Rad51 in this case **(E)**. Red1, Hop1, Mek1 and Hed1 are some of the proteins required for the establishment of the bias towards IH recombination (IH bias). Noncrossovers (NCOs) are mainly generated by synthesis-dependent strand annealing **(H)**. See Section 1.2.3 for a more complete description of the meiotic DSB repair process. Figure adapted from (Phadnis et al., 2011).

1.2.3.2. IH bias

As previously mentioned, in meiosis DSBs are preferentially repaired via inter-homologue recombination. It is only by this pathway that physical connection between homologous chromosomes (chiasmata), through the formation of crossovers, can be achieved (Schwacha and Kleckner, 1994, Schwacha and Kleckner, 1997, Tsubouchi and Roeder, 2003). While recent findings have suggested that inter-sister recombination events may be more frequent in meiosis than previously thought, they are still less frequent than those with the homologue, with an estimated IS:IH ratio of 1:1.7 to 1:2.5, still much higher than that observed in mitosis, where IS recombination is the favoured pathway (Goldfarb and Lichten, 2010, Oh et al., 2007). In most organisms this bias towards IH recombination is observed. A notable exception so far is *Schizosaccharomyces pombe*, where IS recombination is the predominant pathway in meiotic DSB repair, with IS Holliday junctions outnumbering those forming between homologues on a ratio of approximately 4:1 (Phadnis et al., 2011).

In order to establish IH bias, several structural modifications and events must occur during meiotic prophase. Firstly, the meiosis-specific structural proteins Red1 and Hop1, the kinase Mek1 and the cohesin Rec8, major components of the axial elements, must be present. Absence of any of these components leads to reduced IH and increased IS recombination, although IH bias seems to be lost at different stages. While IH bias is lost from early stages in recombination in *red1*Δ and *mek1*Δ mutants, in *rec8*Δ it appears to be established but then later lost at the SEI to dHJ transition (Figure 1.3) (Hollingsworth and Byers, 1989, Kim et al., 2010, Niu et al., 2007, Schwacha and Kleckner, 1997, Shinohara et al., 1997a, Woltering et al., 2000).

The presence of Red1 at chromosome axes is required for efficient Hop1 recruitment and subsequent phosphorylation by Mec1/Tel1 upon DSB formation. Mek1 interaction with Red1 and phosphorylated Hop1 is then necessary for its loading onto chromosomes, dimerization and activation, essential for its roles in IH bias (Bailis and Roeder, 1998, Carballo et al., 2008, de los Santos and Hollingsworth, 1999, Niu et al., 2005, Rockmill and Roeder, 1990, Wan et al., 2004) and checkpoint (Section 1.3.2). It has been suggested that the complex formed by Red1, Hop1 and Mek1 is required to locally inhibit Rec8, which would normally favour IS recombination by keeping sister chromatids close together and therefore

more likely to be used as templates for homologous recombination (Kim et al., 2010).

Once activated, Mek1 phosphorylates Rad54, a partner of Rad51 in strand-exchange, to down-regulate Rad51's activity. This, in turn, allows Dmc1 to take the pivotal role in homology search and single-end invasion (Niu et al., 2009). Rad51, however, is still required for meiotic recombination: in *rad51*Δ mutants spore viability is reduced, recruitment of Dmc1 to chromosomes compromised and hyperresected DSBs accumulate, triggering the prophase I checkpoint (Bishop, 1994, Bishop et al., 1992, Shinohara et al., 1992). Rad51 or Rad54 overexpression can also suppress *dmc1*Δ defects, while the reverse is not true (Bishop et al., 1999, Tsubouchi and Roeder, 2003).

Limiting Rad51 activity while favouring that of Dmc1, and its partner Rdh54/Tid1, is crucial in meiosis (Klein, 1997, Shinohara et al., 1997b). In addition to Mek1-mediated Rad54 phosphorylation, a second mechanism mediated by the meiosis-specific protein Hed1 is in place to down-regulate Rad51's activity. Hed1 binds specifically to Rad51, reducing its recombinase activity. Deletion of *HED1* partially rescues the spore viability defect of *dmc1*Δ mutants in a manner similar to Rad51 or Rad54 overexpression (Busygina et al., 2012, Busygina et al., 2008, Tsubouchi and Roeder, 2006). It has been proposed that Rad51 activity may be inhibited in meiosis to allow Dmc1/Rdh54-mediated IH recombination, but, once the obligate crossovers have been formed, the excess of DSBs (140-170 breaks formed per budding yeast meiosis) must be repaired via IS recombination. Rad51 and Rad54 are required for the latter (Arbel et al., 1999, Buhler et al., 2007, Goldfarb and Lichten, 2010, Mancera et al., 2008, Oh et al., 2007).

Pch2, a member of the AAA+-ATPase family, associated with roles in remodelling multicomponent complexes, is another axis component. It localises to putative crossover sites and regulates the levels and distribution of the LE protein Hop1 and the CE protein Zip1 (Borner et al., 2008, Joshi et al., 2009). In *pch2*Δ mutant, crossover interference seems to be reduced and crossover distribution is affected, with more COs being detected in larger chromosomes while little or no effect is found in smaller chromosomes. These defects do not reflect on spore viability of the single mutant, but combination of *PCH2* deletion with mutations that confer reduced DSB levels leads to a reduction in spore viability (Joshi et al., 2009, Zanders and Alani, 2009). The *pch2*Δ *dmc1*Δ double mutant also shows reduced IH

recombination events and an increase in IS recombination, suggesting a role for Pch2 in IH bias, possibly by promoting full Mek1 activation (Zanders et al., 2011).

Mec1 and Tel1, orthologues in yeast of the mammalian ATR/ATM, are key regulators of meiotic recombination, phosphorylating targets such as Mre11 and Hop1 (Carballo and Cha, 2007, Carballo et al., 2008). In *mec1-1 sml1*Δ double mutant (where *SML1* deletion rescues the lethality conferred by the *mec1-1* allele), IH recombination is reduced while ectopic and IS recombination events increase (Grushcow et al., 1999, Thompson and Stahl, 1999). Mec1 has also been shown to affect crossover distribution through the phosphorylation of replication protein A (RPA) (Bartrand et al., 2006).

1.2.4. Meiotic recombination in other organisms

Initiation of meiotic recombination through DSB formation appears to be universal, with orthologues of Spo11 found in *Schizosaccharomyces pombe* (Rec12) (Sharif et al., 2002), *Arabidopsis thaliana* (SPO11-1) (Grelon et al., 2001), *Caenorhabditis elegans* (SPO-11) (Dernburg et al., 1998), *Drosophila melanogaster* (Mei-W68) (McKim and Hayashi-Hagihara, 1998) and *Mus musculus* (Spo11) (Romanienko and Camerini-Otero, 2000). Resection of DSBs in most organisms also requires a MRX-like complex, MRN, where Mre11 and Rad50 are highly conserved between species, while Xrs2 is replaced by Nbs1 in mammals and fission yeast (Andersen and Sekelsky, 2010, Mimitou and Symington, 2009).

Similar to budding yeast, RecA orthologues in fission yeast, plants, nematodes, flies and mice are also responsible for strand invasion (Andersen and Sekelsky, 2010). However, later recombination steps are less conserved amongst the different organisms. As in budding yeast, in *Arabidopsis* and mice most COs depend on Msh4-Msh5, being therefore subject to crossover interference. Some COs also arise in a Mus81-Mms4-dependent manner in these organisms. In *C. elegans*, all crossovers are Msh4-Msh5-dependent and only one CO is formed between each bivalent. Contrastingly, no Msh4 or Msh5 orthologues are found in *S. pombe*, most COs being Mus81/Mms4-dependent and not affected by CO interference (Berchowitz et al., 2007, Phadnis et al., 2011).

dHJs appear to be a common recombination intermediate in *S. cerevisiae* and *C. elegans*, generally associated with Msh4-Msh5 activity. In *D. melanogaster*, however, dHJs are detected despite the absence of these two proteins (Andersen and Sekelsky, 2010). In *S. pombe*, single rather than double HJs are observed

(Cromie et al., 2006). The requirement for recombination also differs between organisms. Whereas in plants, mice, budding or fission yeast, recombination is essential for synapsis and correct homologue segregation, in flies and worms synapsis occurs independently of recombination. However, synapsis appears to be required for CO formation in nematodes (Colaiacovo et al., 2003, Roeder, 1997).

1.3. Meiotic checkpoint

1.3.1. Mec1 and Tel1

S. cerevisiae Tel1 (telomere maintenance) and Mec1 (mitosis entry checkpoint) are orthologues of the mammalian signal transduction proteins ATM (ataxia telangiectasia mutated) and ATR (ataxia telangiectasia- and Rad3-related), which are also found in *A. thaliana* (ATM and ATR), *C. elegans* (ATM-1 and ATL-1), *D. melanogaster* (Tefu and Mei-41) and *S. pombe* (Tel1 and Rad3) (Carballo and Cha, 2007, Navadgi-Patil and Burgers, 2011, Phadnis et al., 2011). These chromosome-associated proteins play crucial roles in DNA damage and replication stress responses (Nyberg et al., 2002), as well as in unchallenged cell cycle in processes such as DNA replication and meiotic IH bias (Carballo et al., 2008, Cha and Kleckner, 2002, Hashash et al., 2011). Their inactivation confers sensitivity to genotoxic agents and genome instability (Novak et al., 2001, Zhou and Elledge, 2000).

Activation of Mec1/ATR and Tel1/ATM is mediated by ssDNA, coated by RPA and the 9-1-1 checkpoint clamp. In budding yeast, the clamp is composed of Ddc1, Rad17 and Mec3 (Hong and Roeder, 2002, Navadgi-Patil and Burgers, 2011). Interaction of the C-terminus tail of Ddc1 with Mec1 leads to the activation of the kinase domain of the latter (Navadgi-Patil and Burgers, 2009). Mec1 forms a heterodimer complex with Ddc2, the orthologue of human ATRIP (ATR interacting protein), which regulates its DNA binding affinity and, consequently, its kinase activity (Navadgi-Patil and Burgers, 2011).

Mec1/Tel1 kinase activity in yeast leads to phosphorylation of many targets, including mediator proteins like Rad9, which then leads to the activation of effector kinases, such as the key proteins Chk1 and Rad53 (orthologue of human Chk2) (Navadgi-Patil and Burgers, 2011). The consensus target sequences for these proteins consist of serine or threonine residues followed by glutamine residues (SQ/TQs). The presence of three or more of these motifs within 100 amino acids is

referred as a SQ/TQ cluster domain (SCD) and constitutes a hallmark for Mec1/Tel1 (ATR/ATM) targets (Traven and Heierhorst, 2005).

1.3.2. Hop1 and Mek1

Rad9 and Rad53 are two major targets of Mec1 (Section 1.3.1). Rad9 phosphoprotein contains multiple SQ/TQ sites, which, upon Mec1-dependent phosphorylation, allow its interaction with Rad53 and phosphorylation of the latter by Mec1/Tel1. A Rad53 transphosphorylation cascade mediated by Rad9 (Navadgi-Patil and Burgers, 2011, Usui et al., 2009) results in the full activation of Rad53 kinase. This leads to the phosphorylation of many downstream targets, important in the regulation of several cellular processes, such as DNA metabolism and checkpoint (Friedel et al., 2009).

During meiosis, checkpoint activation in response to defects in recombination (e.g., *dmc1*Δ) or synapsis (e.g., *zip1*Δ) is dependent on Hop1 and Mek1, but not on Rad9 and Rad53 (Carballo and Cha, 2007, Usui et al., 2001). Indeed, Rad53 has been shown to be phosphorylated during meiosis in response to accidental breaks, but not *SPO11*-dependent DSBs, potentially a consequence of Rad53 being blocked from accessing the latter due to the altered meiotic chromosome axis structure (Cartagena-Lirola et al., 2008).

In fact, Hop1 and Mek1 proteins could be considered meiotic counterparts of Rad9 and Rad53, based on the following considerations (Carballo and Cha, 2007, Cartagena-Lirola et al., 2008):

i) Both Rad9 and Hop1 are Mec1 targets, being phosphorylated at SCD residues (Carballo et al., 2008, Sweeney et al., 2005);

ii) Rad53 and Mek1 are kinases and contain FHA (forkhead-associated) domains that are autotransphosphorylated, leading to kinase activation (Niu et al., 2009, Usui et al., 2009);

iii) Rad9-Rad53 interaction occurs via the phosphorylated SCD of Rad9 and the FHA domain of Rad53 (Usui et al., 2009). Hop1-Mek1 interaction also requires phosphorylation of Hop1 SCD and, particularly, of the threonine residue 318 in this domain (Carballo et al., 2008). FHA domains are known to interact with phosphorylated threonine residues (Durocher and Jackson, 2002), therefore suggesting that the mechanism of Hop1-Mek1 interaction is similar to that in their mitotic counterparts;

iv) Like Rad53, Mek1 acts as a Mec1 effector kinase (Niu et al., 2009, Rockmill and Roeder, 1991).

1.3.3. *rad50S/sae2Δ*

In a *rad50S* or *sae2*Δ mutant, a delay in the exit of both meiotic divisions is observed (Hochwagen and Amon, 2006). In these backgrounds, DSBs are formed to normal levels, but Spo11 remains covalently attached to the DSB ends, blocking break resection and further processing, therefore leading to the accumulation of unresected DSBs (Alani et al., 1990, Prinz et al., 1997). This situation triggers a checkpoint response that requires Tel1 and Pch2 (Lydall et al., 1996, Usui et al., 2001). Since no ssDNA is generated in these mutants, recruitment of damage-sensing proteins to DSB sites requires factors that are unique to this checkpoint (Hochwagen and Amon, 2006).

Observations that *mre11-58* single mutant, which also accumulates unprocessed breaks (Tsubouchi and Ogawa, 1998), and *tel1*Δ *rad50S* double mutant proceed through meiosis with no delays have led to the proposal that both Tel1 and MRX complex are sensors of protein-linked DSBs (Usui et al., 2001). Recent data reveals that Pch2 and Tel1 act on a pathway that specifically signals unresected DSBs (Ho and Burgess, 2011). Furthermore, Pch2's role in triggering *rad50S/sae2*Δ checkpoint was shown to require interaction with the N-terminus of Xrs2, consistent with the earlier hypothesis that Tel1 and the MRX complex are required for signalling of unresected DSBs.

Taken together, these observations suggest that the activation of *rad50S*/*sae2*Δ checkpoint relies on Tel1, Pch2 and the MRX complex. Additionally, the meiosis-specific structural proteins Red1, Hop1 and Mek1 are also required for arrest in *rad50S/sae2*Δ (Hochwagen and Amon, 2006, Longhese et al., 2008). Activation of Mek1 kinase following interaction with phosphorylated Mec1 target Hop1 is also necessary, suggesting that Mek1 may take on roles typically associated to Rad53 during mitosis (Carballo et al., 2008, Niu et al., 2007, Wan et al., 2004, Woltering et al., 2000, Xu et al., 1997).

1.3.4. *dmc1Δ*

As mentioned above, Dmc1 (disrupted meiotic cDNA) plays a crucial role in the formation of SEIs. In the absence of this protein, DNA is continuously resected, generating long segments of ssDNA (Bishop et al., 1992, Bishop, 1994). This

triggers a checkpoint response that is stronger than that observed in *rad50S* or *sae2*Δ mutants and results in meiosis arrest in prophase I (Bishop et al., 1992).

Arrest in *dmc1*Δ involves Rad24, the DNA damage sensor 9-1-1 and Mec1/Ddc2 complexes. Unlike in *rad50S/sae2*Δ checkpoint, Tel1 is not required (Hochwagen and Amon, 2006, Lydall et al., 1996). Hop1, along with Mek1 and Red1, is also required for this checkpoint response (Carballo et al., 2008, Eichinger and Jentsch, 2010, Niu et al., 2007, Wan et al., 2004, Woltering et al., 2000, Xu et al., 1997). However, the lack of checkpoint response observed in *hop1* or *mek1* mutants is due, not to the bypass of the checkpoint pathway, but to the inappropriate repair of DSBs by IS recombination (Carballo et al., 2008, Hollingsworth and Byers, 1989). Pch2 has also been shown to be required for *dmc1*Δ arrest in some yeast strain backgrounds (Borner et al., 2008).

1.3.5. *zip1Δ*

Cell cycle progression is similarly arrested/delayed in the absence of synaptonemal complex components, such as Zip1, Zip2 and Zip3 (Hochwagen and Amon, 2006). Zip1 is the major component of the central element of the synaptonemal complex. In *zip1*Δ mutants, axial elements may line up side by side, but the distance between them is greater than that between lateral elements in a mature SC (Nag et al., 1995, Sym et al., 1993, Sym and Roeder, 1995).

The extent of cell cycle arrest in *zip1*Δ is variable, albeit generally less robust than in *dmc1*Δ. It requires Mec1, Rad24, Rad17, Ddc1, Mec3, Hop1, Mek1 kinase and Red1 (Hochwagen and Amon, 2006, Roeder and Bailis, 2000). Pch2 has also been shown to be required for the synapsis checkpoint response in *zip1*Δ and *zip2*Δ mutants (Borner et al., 2008, Hochwagen and Amon, 2006, Shinohara et al., 2008).

1.3.6. Meiotic checkpoint in higher eukaryotes

Checkpoint mechanisms monitoring meiotic DSB repair have been primarily studied in budding yeast, but can also be found in several other model organisms, including flies (Ghabrial and Schupbach, 1999), nematodes (Bhalla and Dernburg, 2005) and mice (Gartner et al., 2000).

Disruption of *RAD51*-like genes in *Drosophila*, *spnA*, *spnB* or *spnD*, leads to defects in the formation of the karyosome, a meiosis-specific structure in flies, and in eggshell patterning. These defects are suppressed in mutants lacking *Mei-W68*,

the *SPO11* orthologue in flies. The observation of these defects is also dependent on the presence of Mei-41 and Chk2, orthologues of the budding yeast Mec1 and Rad53 (Abdu et al., 2002, Ghabrial and Schupbach, 1999).

In the female germline of *C. elegans* hermaphrodites, cells with defects in DSB repair are removed by apoptosis, which occurs at prophase I, requiring the orthologues of yeast Rad17 and Rad24, MRT-2 and HUS-1, respectively (Colaiacovo et al., 2003, Gartner et al., 2000, Romanienko and Camerini-Otero, 2000). The nematode orthologue of budding yeast Hop1, HIM-3, appears to be required for checkpoint as well, since oocytes lacking this protein are not eliminated by apoptosis, despite defects in synapsis (Alpi et al., 2003).

In *M. musculus*, some differences are detected in terms of meiotic prophase checkpoints. Spermatocytes of *Rad50*$^{S/S}$ mice, for instance, do not suffer a permanent meiotic block, but are instead eliminated through apoptosis, leading to a depletion in mature spermatocytes in these mutants' testes (Bender et al., 2002). Although absence of DMC1 in mice produces a meiotic arrest as in yeast (Baudat et al., 2000), inactivation of ATM (the Tel1 orthologue in mammals) in *Dmc1*$^{-/-}$ mice produces a phenotype different from that observed in *S. cerevisiae*, as it does not bypass arrest. This is possibly due to functions of ATM in DSB repair (Libby et al., 2002, Romanienko and Camerini-Otero, 2000). As in yeast, however, *Spo11* inactivation leads to the bypass of arrest in *Dmc1*$^{-/-}$ (Barchi et al., 2005, Di Giacomo et al., 2005, Reinholdt and Schimenti, 2005).

1.4. Hop1

1.4.1. Cloning

In 1989, a screen designed to identify meiotic mutants that conferred pairing defects was carried out. This experiment used a haploid *S. cerevisiae* strain disomic for chromosome III and carrying the *spo13-1* mutation (Hollingsworth and Byers, 1989). Sister chromatid cohesion is lost during MI in these mutants and they undergo a single division that can be: (i) reductional (31%), (ii) equational (46%) or (iii) aberrant (23%) (Figure 1.4B), where aberrant designates situations where one spore is trisomic for chromosome III and the second is haploid. Mutants defective in IH bias but proficient in DSB repair can therefore give rise to viable diploid spores in this background (Klapholz and Esposito, 1980b, Klapholz and Esposito, 1980a).

The chromosome III homologues carried by the strain used were heterozygous, with one of them carrying a 11.4 kb duplication between *LEU2* and *HIS4* flanking the genes *URA3* and *CYH2* (Figure 1.4A). Intrachromosomal replication leads to the loss of the replicated sequence, hence *URA3* and *CYH2*, while *LEU2* and *HIS4* are conserved. Thus, mutants that undergo intrachromosomal recombination are able to synthetize leucine and histidine but require a uracil-rich medium to grow and are resistant to the drug cycloheximide (Cyh^R) (Hollingsworth and Byers, 1989).

Upon mutagenesis with ethyl methane sulfonate (EMS), colonies were screened for elevated production of His^+ Leu^+ Chy^R progeny after sporulation (Figure 1.4C), which would result from increased intrachromosomal recombination and/or higher proportion of cells going through an equational division, suggestive of pairing defects (Hollingsworth and Byers, 1989).

One mutant was isolated in which cycloheximide resistance was significantly increased, *hop1-1* (homologue pairing). Homozygous diploids for this allele produced largely inviable spores as a result of reduced crossover levels. Replicating plasmids containing random yeast DNA inserts were then screened for complementation of the spore viability defect of this mutant, allowing the cloning of the *HOP1* gene, which has been mapped to the left arm of chromosome IX and encodes a 69 kDa, protein composed of 605 amino acids (Hollingsworth and Byers, 1989, Hollingsworth et al., 1990).

Transcription of *HOP1* is limited to meiosis as its expression is dependent on heterozygosity at the *MAT* locus, one of the conditions required for meiosis in yeast, and no effects of *hop1* mutations are observed in mitosis. In fact, it has been demonstrated that *HOP1* is repressed in mitosis and activated in meiotic cells (Hollingsworth et al., 1990, Vershon et al., 1992). Gene expression has been shown to occur prior to meiotic DSB formation, consistent with the roles of the encoded protein in recombination and pairing (Carballo et al., 2008, Hollingsworth and Byers, 1989, Hollingsworth et al., 1990).

Figure 1.4 Screen for the identification of pairing-defective mutants through increase in intrachromosomal recombination

(A) A haploid strain carrying the *spo13-1* mutation and disomic for chromosome III was used in a screen to identify mutants defective in homologue pairing during meiosis. The constructs carried by each heterozygous chromosome III homologue are indicated.

(B) *spo13-1* strains can undergo reductional, equational or aberrant chromosomal segregation. In the absence of intrachromosomal recombination, none of the spores produced is His^+ Leu^+ Cyh^R.

(C) When intrachromosomal recombination events occur, His^+ Leu^+ Cyh^R spores are produced when equational or aberrant chromosome segregation occurs, but not when mutants are proficient in homologue pairing and can thus undergo reductional segregation of chromosome III.

Figure adapted from (Hollingsworth and Byers, 1989).

1.4.2. Structure/function studies of Hop1

Hop1 localises to the core of meiotic chromosomes at leptotene, prior to DSB formation, being one of the components of the axial elements (Figure 1.2) (Carballo et al., 2008, Hollingsworth et al., 1990, Smith and Roeder, 1997). During zygotene and pachytene, its localisation alternates with that of Zip1. This Hop1-Zip1 alternating hyperabundance is dependent on the activity of Pch2 and required for appropriate crossover distribution (Borner et al., 2008). Pch2 is a member of AAA+-ATPases family, involved in remodelling of multicomponent complexes (Section 1.2.3.2). Mutations in *HOP1* lead to defects in synaptonemal complex assembly, with reduced pairing of homologous chromosomes (30% of WT levels in *hop1-1*) and an increase in the formation of polycomplexes (PCs), disordered agglomerates of SC components (Carballo et al., 2008, Loidl et al., 1994, Nag et al., 1995).

Analysis of the amino acid sequence of Hop1 reveals the presence of a conserved Cys2/Cys2 zinc finger motif (Figure 1.5), characteristic of DNA binding proteins. This motif spans residues 343 to 378 and mutation of one of the conserved cysteine residues into a serine residue confers a *hop1*Δ phenotype (Hollingsworth et al., 1990). An *in vitro* study suggests that Hop1's zinc finger motif confers the protein its ability to bind GC-rich regions of dsDNA and to mediate the pairing of DNA double helices, consistent with its role in homologue pairing (Anuradha and Muniyappa, 2004, Kironmai et al., 1998, Muniyappa et al., 2000). A predicted nuclear localisation signal (NLS) sequence, PAKIRKI, is also found in the C-terminus of Hop1, between residues 588-594 (Figure 1.5) (Lange et al., 2007).

Comparison of DSB levels at a known recombination hotspot, *HIS2*, revealed that in a *hop1*Δ *rad50S* double mutant DSBs are reduced over 10-20 fold when compared to a *rad50S* strain. Since DSB repair is blocked in *rad50S* mutants, this result revealed a role of Hop1 in DSB formation (Carballo et al., 2008, Mao-Draayer et al., 1996, Schwacha and Kleckner, 1994). Recently, chromatin immunoprecipitation-on-chip (ChIP-chip) experiments have shown that Hop1 and Red1 interact with another meiosis-specific protein, Mer2, which in turn recruits Mei4 and Rec114 (Section 1.2.2). Recruitment of Mei4 and Rec114 by Mer2 leads to the tethering of DSB hotspots to the chromosome axis before or at the time of DSB formation (Panizza et al., 2011).

Intrachromosomal recombination events were shown to occur at normal levels in the first isolated allele of *HOP1*, *hop1-1*, while crossover formation was

decreased to 10% of the levels observed in wild-type. The deletion of *HOP1* results in a further reduction in interchromosomal recombination to approximately 1% of WT levels and a 60-fold reduction in CO levels relatively to *HOP1* (Hollingsworth and Byers, 1989, Niu et al., 2005, Rockmill and Roeder, 1990). Further evidence for potential involvement of Hop1 in CO formation comes from immunocytology experiments, which reveal that Hop1 and Red1 are enriched at the loci of Zip3, a marker for CO sites (Borner et al., 2008, Joshi et al., 2009). The existence of *hop1* alleles that confer a specific deficit in IH recombination products while IS recombination is unaltered or increased suggests that IH bias is lost in these mutants (Carballo et al., 2008, Niu et al., 2005).

In addition to its functions in DSB catalysis, crossover formation and SC assembly, Hop1 is also required for checkpoint. *hop1*Δ mutants progress through meiosis despite the presence of unresected breaks (*rad50S*/*sae2*Δ), hyperresected breaks (*dmc1*Δ *rad51*Δ) or synapsis defects (*zip1*Δ), producing inviable spores (Bailis et al., 2000, Carballo et al., 2008). Bypass of the delayed meiotic progression could be attributed to the severe reduction in DSB levels observed in *hop1*Δ. However, *red1-K348E HOP1* and *hop1*^{SCD} (Section 1.4.3) strains in *rad50S* or *sae2*Δ backgrounds, where DSBs are formed to levels similar to those observed in WT and cannot be repaired, also bypass arrest, indicating that Hop1 is required for checkpoint response (Carballo et al., 2008, Mao-Draayer et al., 1996, Woltering et al., 2000).

A HORMA (Hop1 Rev7 Mad2) motif, conserved in proteins involved in checkpoint response and DNA processing, is found at the N-terminus of Hop1 (Figure 1.5). It has been proposed that this motif is involved in the recognition of chromatin states that result from abnormal DNA structures, such as adducts and double-strand breaks, or from non-attachment to the spindle, acting as an adaptor for DNA repair proteins (Aravind and Koonin, 1998).

Figure 1.5 Schematic representation of Hop1

The location of the HORMA domain, SQ/TQ cluster domain (SCD), zinc finger domain (Zn) and nuclear localisation signal (NLS) within Hop1 is shown. The phosphomutant *hop1*^{SCD} was obtained through mutation of serine residues 298 and 311 and threonine residue 318 into alanine residues.
S: serine residue; T: threonine residue; A: alanine residue.
Figure adapted from (Carballo et al., 2008).

1.4.3. Regulation of Hop1 function

The first evidence that Hop1 function requires the formation of dimers or oligomers came from complementation studies of several *hop1* alleles that variably affect spore viability. These experiments found that the last 20-40 residues at the C-terminus of the protein are required for Hop1 dimerization (Ajimura et al., 1993, Friedman et al., 1994). Further *in vitro* studies showed that Hop1 forms dimers and oligomers (Kironmai et al., 1998).

Hop1 also binds AE protein Red1. Data from yeast two-hybrid experiments shows that this interaction occurs with the C-terminus of Red1 (Hollingsworth and Ponte, 1997). Binding to Red1 is required for Hop1 loading onto chromosomes, where strong co-localisation is found between the two proteins (Smith and Roeder, 1997). Also consistent with the formation of a Hop1-Red1 complex, is the fact that *RED1* overexpression rescues the spore viability of a temperature-sensitive allele of *HOP1*, *hop1-628*, which consists of a mutation that converts serine 595 to asparagine (Hollingsworth and Johnson, 1993). Overexpression of *HOP1* in *red1-K348E*, a mutant where Hop1-Red1 interaction is compromised also improves spore viability from 1% to 24.5% (Smith and Roeder, 1997, Woltering et al., 2000).

Red1 and Hop1 loading to chromosomes depends on cohesins and condensins (Klein et al., 1999, Yu and Koshland, 2003). The interaction between the two proteins is required for the recruitment of a third axial component, Mek1. The C-domain of Hop1 and formation of the Red1-Hop1-Mek1 complex are required for the dimerization and activation of Mek1 kinase (Section 1.5.3), essential for IH bias and checkpoint (Bailis and Roeder, 1998, Niu et al., 2005, Wan et al., 2004).

DSB-dependent phosphorylation of Hop1 is also essential for Mek1 recruitment and activation (Niu et al., 2005). No phosphorylated forms of Hop1 can be identified in mutants where DSB catalysis is blocked, such as *rec104*Δ and *spo11*Δ (Carballo et al., 2008, Niu et al., 2005). More recently, Hop1 was shown to be phosphorylated by Mec1/Tel1. Possessing eight SQ/TQ motifs out of a total of 605 amino acid residues, it is a typical target for Mec1/Tel1 phosphorylation (Section 1.3.1). Furthermore, three of these motifs are located in close proximity (within 20 residues), defining a SQ/TQ cluster domain (SCD) (Figure 1.5), a hallmark for Mec1/Tel1 (or ATR/ATM) phosphorylation (Carballo et al., 2008).

hop1^{SCD} is an allele where the threonine and serine residues in the SCD (T318, S298 and S311) are mutated to alanine. *hop1*^{SCD} sporulates efficiently to

generate mostly dead spores (6.3% spore viability). Analysis of DSB formation in a *rad50S* background using pulsed-field gel electrophoresis (PFGE) revealed that, unlike *hop1*Δ, *hop1*^{SCD} is proficient in DSB formation, with breaks accumulating to *HOP1* levels in this background (Carballo et al., 2008), indicating that low DSB levels are not the cause for the reduced viability.

DSB levels are, however, significantly reduced when *hop1*^{SCD} is expressed in a *dmc1*Δ background, which would normally lead to the accumulation of hyperresected breaks. Simultaneous deletion of *RAD51* (*hop1*^{SCD} *dmc1*Δ *rad51*Δ) results in the accumulation of hyperresected DSBs to levels similar to those found in *HOP1 dmc1*Δ *rad51*Δ strains. The reduction of DSBs in *hop1*^{SCD} *dmc1*Δ double mutant is, therefore, a consequence of DSB repair through IS recombination, which leads to a fast DSB turnover. When both IH and IS recombination are blocked in *dmc1*Δ *rad51*Δ background, DSBs accumulate unrepaired (Carballo et al., 2008).

This suggests that IH bias is compromised in *hop1*^{SCD}, which is confirmed through crossover analysis at the *HIS4-LEU2* artificial hotspot, where an approximate 4-fold reduction in CO levels is observed. Loss of spore viability in *hop1*^{SCD} is therefore a consequence of reduced levels of IH recombination, resulting from failure to recruit and activate Mek1. Synaptonemal complex assembly is also affected in *hop1*^{SCD}, with increased formation of polycomplexes (Carballo et al., 2008).

Phosphorylated Hop1 is also crucial for meiotic checkpoint activity. In *rad50S*, *dmc1*Δ *rad51*Δ and *zip1*Δ backgrounds, *hop1*^{SCD} mutants progress through meiosis with little or no delays, despite the presence of, respectively, unresected DSBs, hyperresected breaks or synapsis defects. Mec1/Tel1-mediated phosphorylation of Hop1 is, therefore, dispensable for DSB formation, but essential for IH bias and checkpoint functions (Carballo et al., 2008).

1.4.4. Hop1 in other organisms

Hop1 orthologues can be found in several organisms. A Hop1 protein is present in the distantly related fission yeast. The fission yeast Hop1 has been shown to localise to the linear elements (LEs), characteristic structures in *S. pombe* that are comparable to budding yeast SCs. Although the Hop1 proteins in fission and budding yeast only share homology in the C-terminus, both contain a HORMA domain and a zinc finger motif. However, in contrast to budding yeast, deletion of *HOP1* in fission yeast produces only a mild reduction in spore viability (90% of that

observed in WT), possibly due to the lesser role of IH recombination in fission yeast meiosis. As in budding yeast, the reduction of spore viability in fission yeast results from decreased levels of interchromosomal recombination events (Latypov et al., 2010, Lorenz et al., 2004).

In *C. elegans*, HIM-3 and its paralogues HTP-1, HTP-2 and HTP-3 share analogous functions to Hop1, being required for homologue pairing, recombination and synapsis. Similarly to Hop1, all four proteins contain a HORMA domain and locate to chromosome axes (Couteau et al., 2004, Zetka et al., 1999). While HIM-3 is required for homologue pairing and synaptonemal complex formation, HTP-1 is required to inhibit synapsis between nonhomologous chromosomes (Martinez-Perez and Villeneuve, 2005). Unlike Hop1, HIM-3 has also been associated with sister chromatid cohesion (Zetka et al., 1999). Like Hop1, HTP-1 is required for preventing IS recombination and is potentially involved in coordinating pairing and synapsis in *C. elegans*. At late pachytene, HIM-3 and HTP-3 remain uniformly distributed along the chromosome axes, whereas HTP-1 and HTP-2 are depleted in regions distal to the chiasma. Cohesin is protected in HTP-1/2-rich regions until MII (Martinez-Perez and Villeneuve, 2005).

Arabidopsis thaliana also encodes a *HOP1* orthologue, ASY1. Asy1 contains a HORMA domain and exhibits 51% similarity with Hop1 in the first 250 amino acids. Absence of this protein confers an asynaptic phenotype (Caryl et al., 2000). Like budding yeast Hop1, it is strongly associated with chromatin, particularly with the lateral element of the synaptonemal complex, and is required for normal synapsis and chiasma formation (Sanchez-Moran et al., 2008, Schwarzacher, 2003, Shin et al., 2010).

Two Hop1 orthologues have been detected in mice, HORMAD1 and HORMAD2, both containing HORMA domains. They associate with unsynapsed regions of chromosome axes and are required for checkpoint (Chen et al., 2005, Wojtasz et al., 2009). HORMAD1 contains several SQ/TQs and is involved in IH recombination and SC assembly, also being essential for the elimination of SC-defective oocytes (Daniel et al., 2011, Fukuda et al., 2009).

1.5. Mek1

1.5.1. Cloning

Mek1 (meiotic kinase), also known as Mre4, was first isolated, along with Red1, in a screen for mutants defective in chromosome segregation. In this screen, spores from a homothallic (*HO*) *S. cerevisiae* strain were mutagenized. Since these strains are able to switch mating type, mutagenized spores can diploidize. The resulting diploids were then induced to sporulate and mutants that sporulated efficiently but produced inviable spores were selected. These included *mek1-1*, which has a sporulation efficiency of 63%, while only 30% of the spores produced are viable (Rockmill and Roeder, 1988, Rockmill and Roeder, 1991).

The fact that spore viability of *mek1-1* is rescued to 81% by *SPO13* deletion suggested that this mutant is defective in the reductional meiotic division (Section 1.4.1). *MEK1* was cloned by complementation of the meiotic-lethal phenotype using a yeast genomic library. The gene was mapped to the right arm of chromosome XV (Ajimura et al., 1993, Leem and Ogawa, 1992, Rockmill and Roeder, 1991).

MEK1 is specifically expressed in meiosis and its deletion leads to reduced levels of spore viability (13% in *mek1*Δ compared to >95% in WT) due to a reduction in CO levels to 6-15% of wild-type. Mek1 is a 57 kDa protein constituted of 497 amino acid residues and contains a conserved sequence amongst serine/threonine protein kinases between residues 169 and 199 (Leem and Ogawa, 1992, Rockmill and Roeder, 1991).

1.5.2. Structure/function studies of Mek1

Immunocytology experiments show that Mek1 localises to meiotic chromosomes from early zygotene to pachytene in a Hop1/Red1-dependent manner (Bailis and Roeder, 1998, Burns et al., 1994). Mek1 localisation to chromosome axes is required for SC formation (Rockmill and Roeder, 1991). Mek1 interaction with the complex formed by Red1 and Hop1 has been suggested to stabilise it (de los Santos and Hollingsworth, 1999). This interaction is likely mediated by Mek1's forkhead-associated (FHA) domain (Figure 1.6), a structural motif involved in protein-protein interactions that is conserved in proteins with regulatory roles such as kinases and phosphatases (Durocher and Jackson, 2002). Mek1's FHA domain spans residues 47 to 119 and substitution of a conserved

arginine residue for an alanine residue in the Mek1 FHA domain in the mutant *mek1-R51A* results in spore viability reduction to 2% (Wan et al., 2004).

A second domain crucial for Mek1 function is the kinase domain (Figure 1.6), comprising residues 162 to 443. Mutations in residues sited within this catalytic domain confer phenotypes that resemble that of *mek1*Δ, with reduced viability (20%) and shorter SCs (Bailis and Roeder, 1998, Rockmill and Roeder, 1991). This domain is, however, dispensable for Mek1 localisation. The *mek1-D290A* mutant, which carries a mutation in a conserved residue in the kinase domain that inactivates Mek1 kinase, still localises to AEs. A Mek1-β-galactosidase fusion, containing only the first sixty three amino acids of the N-terminus of Mek1, also locates to chromosomes (Bailis and Roeder, 1998, de los Santos and Hollingsworth, 1999). The fact that reduced kinase activity is observed in the *mek1-R51A* allele, carrying a mutation in the FHA domain, suggests that Mek1 activation occurs upon recruitment (Wan et al., 2004).

Other residues in the Mek1 catalytic domain that are conserved amongst fungi species are lysine 199 and threonines 327 and 331. Mutations in these residues such as in *mek1-K199R*, *mek1-T327A* or *mek1-T331A* lead to reductions in spore viability to 1, 0.3 and 2.9%, respectively. Interestingly, T327 and T331 residues (Figure 1.6) are followed by a glutamine residue, making them potential substrates for the serine/threonine group of kinases, in which Mek1 is included. Substitution of T327 by a phosphomimetic aspartic acid in *mek1-T327D* mutant rescues spore viability to 51.9%. Furthermore, overexpression of this allele leads to an additional increase in spore viability to 68.7% (de los Santos and Hollingsworth, 1999, Niu et al., 2007, Wan et al., 2004).

Initial observations that *mek1* mutants displayed a 10-fold reduction in steady-state levels of DSBs (Goldfarb and Lichten, 2010, Leem and Ogawa, 1992, Xu et al., 1997) suggested that, like Hop1, Mek1 is required for break catalysis. However, *mek1*Δ *rad50S* double mutant accumulates the same level of DSBs as *MEK1 rad50S* (Pecina et al., 2002, Xu et al., 1997). Furthermore, *mek1*Δ single mutant is defective in interchromosomal recombination, with a 10-fold reduction in gene conversion and COs. Taken together these observations suggest that the reduced steady-state levels in DSBs are due to loss of IH bias (Leem and Ogawa, 1992, Nag et al., 1995, Rockmill and Roeder, 1991, Xu et al., 1997).

Deletion of *SPO13* in *dmc1*Δ strains containing an analogue-sensitive allele of *MEK1*, *mek1-as*, where Mek1 kinase activity can be blocked by the presence of

an inhibitor, improves spore viability from 3% to 46.7%, suggesting that reduced DSB levels are a consequence of *DMC1*-independent repair and that active Mek1 is essential for IH bias (Niu et al., 2005, Wan et al., 2004). IS recombination is, indeed, increased in *mek1* mutants, while IH recombination is decreased (Kim et al., 2010, Niu et al., 2005, Terentyev et al., 2010). Furthermore, while DSBs are repaired in *mek1*Δ *dmc1*Δ (Xu et al., 1997), this repair is blocked by the deletion of *RAD54*, which encodes an auxiliary protein that stimulates Rad51 activity, confirming that repair occurs via IS recombination (Niu et al., 2005).

A mechanism by which Mek1 imposes IH bias is through the phosphorylation of Rad54. Mek1 has been shown to phosphorylate *in vitro* a threonine residue, T132, in Rad54 that is conserved in fungi and nematodes. Mutation of this residue to a nonphosphorylatable alanine residue improves sporulation efficiency and spore viability in a *rad54-T132A dmc1*Δ mutant. Co-IP experiments indicate that the interaction between Rad51-Rad54 is reduced in a phosphomimetic allele of Rad54, *rad54-T132D* and similar to WT in *rad54-T132A*. Thus, Mek1 promotes IH bias by phosphorylating Rad54, which reduces its affinity for Rad51, down-regulating recombinase activity of the latter during meiosis (Niu et al., 2005, Niu et al., 2009).

Mek1 is also essential for checkpoint activation in meiotic prophase as *mek1*Δ mutants bypass the *zip1*Δ and *rad50S* checkpoints. In *dmc1*Δ background, deletion of *MEK1* leads to *DMC1*-independent repair of breaks and production of dead spores. Mek1 kinase activity is, once more, required for checkpoint activation, as mutations in the kinase domain of Mek1 such as *mek1-K199R*, *mek1-T327A* and *mek1-T331A* result in elevated levels of sporulation (>65%) in the *dmc1*Δ background, where only 1.3% of *MEK1 dmc1*Δ cells sporulate (Niu et al., 2007, Wan et al., 2004, Xu et al., 1997).

Figure 1.6 Schematic representation of Mek1

The location of the forkhead-associated (FHA), kinase and C-terminal (C) domains within Mek1 is shown. Phosphorylation of threonine residues 327 and 331 is essential for spore viability and arrest in *dmc1*Δ background, while phosphorylation of serine residue 320 is required for preventing *DMC1*-independent repair of DSBs. S: serine residue; T: threonine residue.
Figure adapted from (Niu et al., 2007).

1.5.3. Regulation

As described above, Mek1 localisation is dependent on Red1-Hop1 interaction. Co-IP and immunocytology experiments have demonstrated that Mek1 interacts with both proteins and that these interactions do not depend on kinase activity. Indeed, a Mek1 protein encoded by a kinase-dead allele, *mek1-D290A*, is recovered in a co-IP with Hop1 and Red1 (Bailis and Roeder, 1998). However, formation of the Red1-Hop1-Mek1 complex is required for full Mek1 activation. In *red1-K348E* mutant, where Red1-Hop1 interaction is disrupted, Mek1 activity is reduced (Niu et al., 2007, Wan et al., 2004). The N-terminus of Mek1 appears to be sufficient for interaction with Red1 and Hop1, since the *mek1-β-galactosidase* mutant (Section 1.5.2) co-IPs Red1 and Hop1 and interacts with both proteins in yeast two-hybrid experiments (Bailis and Roeder, 1998).

Dimerization of Mek1 is required for full activation of the protein and is mediated by the C-domain of Hop1. *hop1*-C-terminus mutants, such as *hop1-564*Δ, *hop1-585*Δ or *hop1-K593A*, interact with Red1 and form DSBs, but fail to synapse and produce dead spores due to reduced levels of crossovers. Introduction of a self-dimerizing GST-tagged version of *MEK1* in these mutants rescues spore viability. Furthermore, expressing *GST-MEK1* in a *hop1-K593A dmc1*Δ mutant rescues the checkpoint defect of the latter (Niu et al., 2005).

Rescue of *hop1-K593A* by *GST-MEK1* requires the ability of GST molecules to dimerize as *hop1-K593A gst-RD-MEK1* mutant, where binding of GST-tags cannot occur, fails to produce viable spores or arrest in *dmc1*Δ. Mek1 kinase activity is also required since *GST-mek1-K199R* (kinase-dead) also fails to rescue *hop1-K593A* spore viability or *dmc1*Δ arrest. These observations indicate that the C-domain of Hop1 mediates Mek1 dimerization, which is required for its roles in IH bias and checkpoint response. Additionally, the fact that no phosphorylation of the catalytic residue T327 of Mek1 can be detected in dimerization-defective or kinase-dead *mek1* mutants shows that Mek1 activity depends on establishment of Mek1-Mek1 interactions and subsequent transphosphorylation (Niu et al., 2005, Niu et al., 2007).

The latter event requires DSB-dependent Mec1/Tel1 phosphorylation of Hop1, as the *hop1*^{SCD} phosphomutant is inefficient in recruiting and activating Mek1 (Carballo et al., 2008). Mek1 transphosphorylation, as shown by the reduced spore viability observed in Mek1 phosphomutants *mek1-T327A* and *mek1-T331A*, is crucial for its roles in IH bias. Additionally, a third residue in the catalytic domain of

Mek1, serine 320 (Figure 1.6), appears to be essential and specifically required for checkpoint activation. While *mek1-S320A* mutant produces highly viable spores, when combined with *dmc1*Δ, it progresses through meiosis, generating inviable spores due to *DMC1*-independent DSB repair. Interestingly, this defect is suppressed by the expression of *GST-mek1-S320A*. Phosphorylation of S320 is proposed to stabilise Mek1 dimers, thus preventing *DMC1*-independent repair (Niu et al., 2007, Niu et al., 2005, Wan et al., 2004).

1.5.4. Mek1 in other organisms

A direct orthologue of Mek1 has only been found in *Schizosaccharomyces pombe*. As in budding yeast, fission yeast Mek1 (fyMek1) contains a FHA and a kinase domain and is required for spore viability and checkpoint. Its phosphorylation by Rad3 (the Mec1 orthologue in fission yeast) and Tel1 in response to DSB formation is required for recombination and normal meiosis progression. Upon Rad3/Tel1-mediated phosphorylation it undergoes autophosphorylation, like its budding yeast orthologue. This phosphorylation is necessary for checkpoint activation. Targets of fyMek1 include Rdh54 and Mus81 (Latypov et al., 2010, Tougan et al., 2010).

1.6. Aims of this project

As described before, Mec1/Tel1 phosphorylation of Hop1 is essential for IH bias and meiotic checkpoint (Carballo et al., 2008). The aim of this project is to better understand the molecular basis for Hop1's roles in IH bias and checkpoint through the use of *hop1* alleles that confer variable defects in spore viability and checkpoint. Specifically, I will try to determine how eliminating one particular Mec1/Tel1 phosphorylation site leads to a defect in checkpoint function and only a moderate reduction in spore viability, while disrupting phosphorylation at another site results in a *hop1*Δ-like phenotype in terms of spore viability and checkpoint response.

Chapter 2: Materials and Methods

2.1. Commonly used buffers and solutions

The composition of commonly used buffers and solutions is given in Table 2.1. All chemicals were purchased from Sigma unless otherwise indicated.

Table 2.1 Commonly used buffers and solutions

Buffer/Solution	Composition
Fixing solution	40% (v/v) ethanol, 0.1 M sorbitol
PBS (1x)	137 mM NaCl, 2.7 mM KCl, 10 mM Na_2HPO_4, 1.8 mMKH_2PO_4
PCR[a] buffer (1x)	2.25 mM $MgCl_2$, 50 mM KCl, 10 mM Tris-HCl pH 8.4
Phosphate buffer pH6.5 (1M stock)	685 mM NaH_2PO_4, 315 mM Na_2HPO_4
TAE (1x)	40 mM Tris base, 40 mM acetic acid, 1 mM EDTA
TBE (1x)	45 mM Tris base, 45 mM boric acid, 1 mM EDTA
TE (1x)	10 mM Tris-HCl pH 8.0, 1 mM EDTA[b]

[a] polymerase chain reaction (PCR)
[b] ethylenediaminetetra-acetic acid (EDTA)

2.2. Bacterial techniques

2.2.1. Bacterial strains

All bacteriological work was carried out using *Eschericia coli* (*E. coli*) strain DH5α*F' endA1 hsdR17* [$r_K^- m_K^+$] *supE44*$^-$*thi-1 recA1 gyrA* [Nal^r]*relA1* Δ[*lacZYA-argF*]*U169 deoR* [ϕ*80dlac*Δ*(lacZ)MI5*].

2.2.2. *E. coli* media and growth conditions

Luria-Bertani broth (1% [w/v] bacto-tryptone, 0.5% [w/v] yeast extract, 1% [w/v] NaCl pH 7.5) supplemented with 100 μg/ml ampicillin (LB-Amp) or 50 μg/ml kanamycin (LB-Kan) for plasmid selection was used to grow *E. coli*. Liquid cultures were grown at 37°C in a gyratory shaker at 300 rpm. 1.5% (w/v) bacto-agar was

added to LB-broth to obtain solid LB medium. *E. coli* were grown on LB-agar plates in a constant temperature incubator at 37°C. For long-term storage, 1 ml of an overnight *E. coli* culture grown in either LB-Amp or LB-Kan was added to 1 ml of 2x LB/glycerol (2x LB-broth, 50% [v/v] glycerol) and stored at -80ºC.

2.2.3. *E. coli* transformation

To obtain chemically competent *E. coli* cells for transformation, DH5α cells were grown overnight with shaking in 2 ml of LB broth (no selection) at 37°C. The next day, 100 ml of LB broth (no selection) was inoculated with 0.5 ml of the overnight culture and grown to an OD_{600} of 0.5. The culture was cooled on ice before the cells were pelleted (10,000 rpm, 1 min, 4°C). The cells were resuspended in 30 ml of filter-sterilised ice-cold buffer 1 (10 mM potassium acetate, 50 mM $MnCl_2$, 100 mM RbCl, 10 mM $CaCl_2$, 15% [v/v] glycerol, adjusted to pH 5.8 with dilute acetic acid) and left on ice for 90-120 min at 4°C. The cells were pelleted (5000 rpm, 1 min, 4°C) and gently resuspended in 4 ml of filter-sterilised ice-cold buffer 2 (10 mM MOPS, 75 mM $CaCl_2$, 10 mM RbCl, 15% [v/v] glycerol, adjusted to pH 7.0 with HCl). After addition of 60 μl of dimethyl sulphoxide (DMSO) to the cells in buffer 2, the mixture was divided into aliquots of 100 μl in pre-chilled microfuge tubes and stored at –80°C.

1-5 μl of transforming DNA was added to 50 μl of chemically competent cells for transformation. The mixture was incubated on ice for 10 minutes then heat-shocked at 42°C for 1 minute. 1 ml of LB-broth was added and the cells were incubated at 37°C in a hot-block for 1 hour to recover. Aliquots of 100 μl and 900 μl were plated onto either LB-Amp or LB-Kan agar and grown overnight at 37°C.

2.2.4. Purification of *E. coli* plasmid DNA

Plasmid DNA was extracted from a 2 ml overnight culture using a QuantumPrep Plasmid Miniprep kit [Bio-Rad] according to the manufacturer's instructions.

2.3. Yeast techniques

2.3.1. Yeast media and growth conditions

Details of the yeast media used in this study are described in Table 2.2.

Table 2.2 Yeast growth and sporulation media

Medium	Composition
YEP	1% (w/v) yeast extract, 2% (w/v) bacto-peptone
YPD	1% (w/v) yeast extract, 2% (w/v) bacto-peptone, 2% (w/v) glucose
YPG agar	1% (w/v) yeast extract, 2% (w/v) bacto-peptone, 3% (v/v) glycerol, 2% (w/v) bacto-agar
SD	0.67% (w/v) yeast nitrogen base, with either appropriate amino acid supplements at 40 µg/ml or 0.8 g/L amino acid dropout mix, 2% (w/v) glucose
Amino acid dropout mix	800 mg adenine, 800 mg arginine, 800 mg histidine, 2400 mg leucine, 1200 mg lysine, 800 mg methionine, 2000 mg phenylalanine, 8000 mg threonine, 800 mg tryptophan, 1200 mg tyrosine, 800 mg uracil (with the appropriate amino acid dropped out)
SPM agar	1% (w/v) potassium acetate, 2% (w/v) bacto-agar
YPA	1% potassium acetate, 2% bacto-peptone, 1% yeast extract
BYTA	1% yeast extract, 2% tryptone, 1% potassium acetate, 50 mM potassium phtalate
liquid SPM	0.3% potassium acetate, 0.02% raffinose

Yeast strains were grown either in YPD rich medium or, for auxotrophic selection, in synthetic dextrose (SD) medium (Table 2.2). SD medium supplemented with all the amino acids listed in the dropout mix in Table 2.2 (i.e. with no amino acid dropped out) is referred to as synthetic complete (SC) medium. Liquid cultures were incubated in a gyratory shaker [New Brunswick] at 175 rpm. For growth on solid media 2% (w/v) bacto-agar was added to the media. Yeast strains were incubated at 30ºC on agar plates in a constant temperature incubator.

Overnight growth on YPG agar (Table 2.2) was used to select against petite mutants. To select for drug resistance, 200 µg/ml G-418 [GIBCO] or 300 µg/ml Hygromycin B [Sigma] was added to YPD agar.

For long-term storage, freshly grown yeast cells were removed from agar plates and inoculated into 1.8 ml of 25% (v/v) glycerol. The strain stocks were then stored at -80°C.

2.3.2. Mating yeast strains

To obtain diploid strains, two haploid strains of opposite mating types were mixed in a patch on a YPD agar plate and incubated overnight at 30°C.

Where possible, diploids were isolated by auxotrophic selection. If auxotrophic selection was not possible, cells from the mating patch were streaked for single colonies on a YPD agar plate and diploids were selected by microscopic screening (Section 2.3.10, Figure 2.1) and their ability to sporulate, as only diploid strains will undergo meiosis.

2.3.3. Tetrad dissection

Diploid strains were incubated on minimal sporulation medium (SPM agar; Table 2.2) at 30°C for 24 hours. The walls of the asci were digested for 30 minutes with 50 μl of 5 mg/ml Zymolyase-20T [ICN Biomedicals] in SCE buffer (1 M sorbitol, 100 mM sodium citrate, 60 mM EDTA) at 37°C. Tetrads were dissected on YPD agar plates using a Singer MSM micromanipulator.

In order to determine the genotype of the haploid strains resulting from tetrad dissection, YPD plates were replica plated onto the appropriate SD-dropout or drug selection media.

The mating type of the resulting haploid strains after tetrad dissection was determined by their ability to mate with mating type tester strains (RCY313 and RCY314; Table 2.8) to produce a prototrophic diploid. When haploids were prototrophic, mating with the mating type testers was assessed by microscopic screening (Section 2.3.10, Figure 2.1) and their ability to undergo meiosis.

A

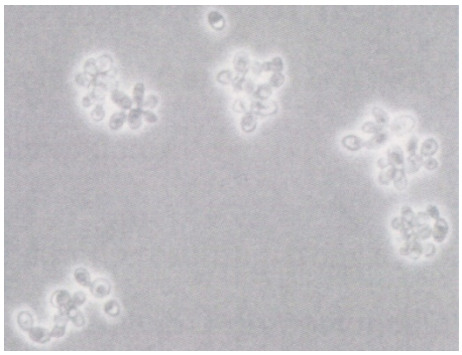

B

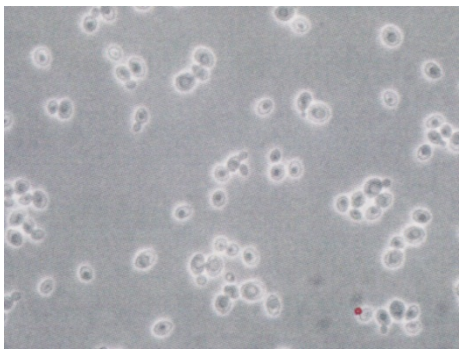

Figure 2.1 Haploid and diploid SK1 *S. cerevisiae* cells

Phase contrast microscope images of SK1 haploid (RCY1047) **(A)** and diploid (RCY2464) **(B)** cells grown overnight on YPD agar. SK1 haploid cells are more flocculent than diploid cells.
Images collected by Dr. Nadia Hashash.

2.3.4. Determination of spore viability

To address the effect of temperature on spore viability of diploid strains, cells were incubated on SPM agar (Table 2.2) for 24 hours at 30, 33 or 36ºC or for 48 hours at 18 or 23ºC. After incubation, cells were treated and tetrads dissected as described above (Section 2.3.3). Spore viability was expressed as the fraction of spores that germinate and produce visible colonies out of the total number of spores dissected after 48 hours of incubation in YPD at 30ºC.

For determination of spore viability in liquid medium, cells were incubated at 30ºC in YPD liquid medium for 24 hours, when $1/10^{th}$ of the obtained saturated culture was transferred to BYTA medium (Table 2.2) and grown overnight at 30ºC. On the following day cells were pelleted (12,000 rpm, 2 min), inoculated into liquid SPM medium (Table 2.2) and left to sporulate for 48 hours at the desired temperature, upon which 500 µl of the cell culture was spun down and treated as described for cultures sporulated on solid SPM medium.

2.3.5. Determination of sporulation efficiency

In order to determine sporulation efficiency, cells were induced to sporulate at the desired temperature as described above (Section 2.3.4), fixed using 300 µl of fixing solution (Table 2.1) and the fraction of cells containing two or more spores out of the total number of cells scored was determined by microscopic screening (Section 2.3.10).

For determination of sporulation efficiency in liquid medium, cells were prepared as described above (Section 2.3.4). After 48 hours incubation, 1 ml of cell culture was collected and resuspended in 300 µl of fixing solution (Table 2.1). Sporulation efficiency was assessed as for cultures sporulated on solid SPM medium.

2.3.6. Determination of cell density

The cell density of yeast cultures was determined by the optical density at 600 nm (OD_{600}). This was measured in a CO8000 cell density meter [WPA], using a cuvette [Fisherbrand] containing 1 ml of liquid culture (diluted up to 10x if necessary).

2.3.7. Synchronization of meiotic cultures

Synchronous meiosis was induced using two previously established protocols, the YPA method, described in (Padmore et al., 1991), or the BYTA method, described in (Falk et al., 2010).

For the YPA method, cultures were grown in YPD liquid medium (Table 2.2) for 1 day and then transferred to YPA medium (Table 2.2) at an OD_{600} of approximately 0.2 and incubated for 13.5 hours at 30°C in a gyratory incubator at 200 rpm. On the following day, after 2 washes in sterile distilled water (warmed up to the temperature at which meiosis was to be induced), liquid SPM (also pre-warmed to the desired temperature; Table 2.2) was inoculated to an OD_{600} of 1.2-1.4. Cultures were incubated at the desired temperature in a gyratory incubator at 250 rpm and samples were collected at various time points.

The protocol for the BYTA method differs from the YPA method in that pre-growth is carried out in BYTA medium (instead of YPA medium; Table 2.2), which is inoculated to an OD_{600} of 0.3 and incubated at 30ºC for 16h. After incubation, liquid SPM is inoculated to an OD_{600} of 1.9.

The BYTA method provides better synchrony and quicker meiotic progression. Unless otherwise stated, this was the method used for synchronization of meiotic cultures.

2.3.8. Yeast transformation

Yeast strains were transformed by a standard lithium acetate method as described in (Gietz and Woods, 2002). To prepare competent cells, a 50 ml culture was grown to mid-log phase. The cells were pelleted (3000 rpm, 2 min) and washed once with 25 ml sterile H_2O. The cells were resuspended at a concentration of 10^9 cells/ml in sterile H_2O and 100 μl of this cell suspension was used per transformation. The cells were pelleted (13,000 rpm, 1 min) and resuspended in 360 μl of transformation mix (30% [w/v] polyethylene glycol $(PEG)_{3350}$, 100 mM lithium acetate, 100 μg single-stranded carrier DNA, 1-10 μg of transforming DNA). The cells were incubated in the transformation mixture at 42°C for 40 minutes.

For auxotrophic selection, cells were pelleted (6000 rpm, 1 min) after the heat shock treatment and resuspended in 500 μl sterile H_2O. Aliquots of 200 μl were plated directly onto SD-dropout agar plates. To select for drug resistance, the cells were pelleted (6000 rpm, 1 min) after the heat shock treatment, resuspended in 1 ml

YPD rich medium and allowed to recover for 2-3 hours before plating onto selective media as above.

2.3.9. Isolation of yeast genomic DNA

Cells from a 2 ml overnight culture were pelleted (13,000 rpm, 1 min), washed with 500 μl H_2O, and resuspended in 100 μl breakage buffer (50 mM Tris-HCl pH 7.6, 20 mM EDTA, 1% [w/v] sodium dodecyl sulphate [SDS]). Glass beads (0.5 mm) [BioSpec Products] were added to the level of the liquid and the cells were lysed by two 10 second pulses at speed setting 4 in a RiboLyser [Hybaid] with 1 minute on ice between pulses. The lysate was collected by piercing the bottom of the tube with a red-hot needle, placing this tube inside a clean 1.5 ml tube supported by a 15 ml tube, and centrifuging for 30 seconds at 3000 rpm. The lysate was then incubated for 10 minutes at 70°C in a hot block. After mixing briefly using a vortex mixer, 200 μl of 5 M potassium acetate and 150 μl of 5 M NaCl were added to the lysate and the mixture was incubated on ice for 20 minutes. The cell debris were removed by centrifugation (13,000 rpm, 20 min, 4°C). The supernatant was transferred to a new 1.5 ml tube and 150 μl 30% (w/v) PEG_{6000} was added. The mixture was incubated on ice for 10 minutes and then the DNA was recovered by centrifugation (13,000 rpm, 10 min, 4°C). The supernatant was removed and the DNA pellet resuspended in 40 μl of nuclease-free H_2O.

2.3.10. Microscopy

An Eclipse E200 phase-contrast microscope [Nikon] with a 40x objective was used to routinely view yeast cultures.

2.4. DNA manipulation

2.4.1. Agarose gel electrophoresis

Routine agarose gel electrophoresis was carried out in 1% (w/v) agarose gels (electrophoresis grade) [Invitrogen] with TBE electrophoresis buffer (Table 2.1). When the DNA fragments were to be purified, low melting point (LMP) agarose [Invitrogen] and TAE electrophoresis buffer (Table 2.1) were used.

DNA was loaded with 1/6 volume 6x DNA loading buffer (0.2% [w/v] bromophenol blue, 30% [v/v] glycerol) and run with a constant voltage of 75 volts. 0.05% (w/v) ethidium bromide [GIBCO] was used to stain DNA. It was added directly to the molten agarose before pouring the gel and visualised under short

wave ultra-violet radiation using a BioDoc-It System transilluminator [UVP]. The size of DNA fragments was estimated by comparison to the DNA markers in a 1 kilo base pair (kb) DNA ladder [Invitrogen].

2.4.2. Recovery of DNA fragments from agarose gels

DNA fragments were extracted from TAE agarose gels using a Wizard PCR Preps DNA purification system [Promega] according to the manufacturer's instructions.

2.4.3. Pulsed-field gel electrophoresis (PFGE)

To prepare agarose plugs containing chromosome-sized DNA, cell pellets were collected and stored in 1 ml 50 mM EDTA. The number of plugs that could be prepared from each cell pellet was determined by the weight of the dry pellet. For each plug 0.1 g of cells was used. To the cell pellet, 25 μl of solution I (1 M sorbitol, 100 mM sodium citrate, 60 mM EDTA, 5% [v/v] β-mercaptoethanol, 5 mg/ml zymolyase-20T) per plug (i.e. per 0.1 g cells) was added and mixed into the cell pellet. 75 μl of melted 1.5% (w/v) LMP agarose [Invitrogen] was then added per plug and mixed into the cell pellet. The mixture was placed into plug moulds and left to set at 4ºC for 10 minutes. Plugs were dispensed from the mould into a 2 ml plastic tube.

The plugs were treated with 2 ml of solution II (0.45 M EDTA, 10 mM Tris-HCl pH 7, 7.5% [v/v] β-mercaptoethanol, 10 μg/ml RNaseA) for a minimum of 6 hours at 37°C. The tube was then cooled on ice for 10 minutes before replacing solution II with 2 ml solution III (0.25 M EDTA, 10 mM Tris-HCl pH 7, 1% [w/v] sarkosyl, 1 mg/ml Proteinase K [Roche]). The plugs were incubated overnight in solution III at 37°C. The next day the tube was chilled on ice for 10 minutes, before removing solution III and replacing it with 1 ml storage solution (50 mM EDTA, 50% [v/v] glycerol). The prepared agarose plugs were stored at –20°C.

Electrophoresis was performed using 1/3 plug per lane in a Bio-Rad CHEF Mapper according to the parameters listed in Table 2.3.

Table 2.3 Parameters for pulsed-field gel electrophoresis

Parameters	Chromosome III
Voltage gradient	6 V/cm^2
Switch times	5- 30sec
Run time	24 hours
Temperature	14^{o}C
% Agarose[a]	1% (w/v)
TBE (Table 2.1)	0.5X

[a]Pulsed Field Certified Agarose [Bio-Rad]

2.4.4. Southern blot analysis

The agarose gel to be blotted was rinsed in water for 10 minutes, followed by depurination in 0.25 M HCl for 20 minutes. Next, the gel was rinsed again in water and denatured in 0.4 M NaOH for 30 minutes. The gel was blotted overnight in 0.4 M NaOH onto Hybond-N+ positively charged nylon transfer membrane [GE Healthcare].

The blotted membrane was neutralised with 50 mM sodium phosphate buffer pH 6.5 for 15 minutes. The membrane was then placed in a hybridisation tube [Hybaid] with 15 ml of prehybridisation buffer (7% [w/v] SDS, 0.5 M sodium phosphate buffer pH 6.5, 1 mM EDTA) rotating at 65°C for a minimum of 10 minutes. The DNA probe used, *CHA1*, was obtained by *Hind*III/*Kpn*I digestion (Section 2.4.5) of plasmid pRSC38 (Table 2.7). The DNA probe was labelled with ^{32}P-dCTP [GE Healthcare] using a Prime-It RmT Random Primer Labeling kit [Stratagene] according to the manufacturer's instructions. The ^{32}P-labelled probe was denatured by incubation in a hot block at 95˚C for 5 minutes before being added to a fresh 15 ml of prehybridisation buffer. The resulting solution was then transferred to the hybridisation tube with the membrane. The membrane was incubated at 65°C with the ^{32}P-labelled probe overnight.

To remove non-specific signal the membrane was washed twice for 20 minutes in ~500 ml wash buffer (1% [w/v] SDS, 40 mM sodium phosphate buffer, 1 mM EDTA) before being wrapped in Saran wrap and exposed to a storage phosphor screen [Kodak] for 1-3 days.

The screen was scanned using a Storm 860 Phosphorimager and band intensity was quantified with ImageJ software [NIH].

2.4.5. Restriction endonuclease digestions

DNA was incubated with the required restriction endonuclease enzyme(s) [New England Biolabs or Roche] in the appropriate restriction endonuclease buffer according to the manufacturer's instructions at 37°C for a minimum of 2 hours.

2.4.6. DNA ligation

Following restriction enzyme digestion (Section 2.4.5), plasmid vector DNA to be used for ligation was incubated with 1 U calf intestine alkaline phosphatase [Roche] at 37°C for 1 hour.

Ligation of DNA fragments was carried out in a 20 μl reaction mixture containing 1x T4 DNA ligase buffer [Promega], 1.5 U T4 DNA ligase [Promega] and a 1:3 molar ratio of vector:insert DNA (roughly estimated from an ethidium bromide stained agarose gel). A control reaction without any insert DNA was carried out alongside. Ligation reactions were incubated overnight at 18°C and 5 μl of the reaction mix was transformed into competent *E. coli* cells (Section 2.2.3) the following day.

2.4.7. Polymerase chain reaction (PCR)

Polymerase chain reactions were carried out in a Biometra T3 thermocycler [Thistle Scientific].

DNA fragments for genomic modifications were generated by PCR as described in (Longtine et al., 1998) in a 100 μl reaction containing 1x PCR buffer, 1 μM of each primer, 200 μM dNTPs [GE healthcare], 5 U Taq polymerase [Abgene] and 100 ng template plasmid DNA. The PCR program was an initial denaturation at 94°C for 3 minutes, followed by 30 cycles of 94°C (1 min), 55°C (1 min), 72°C (1 min), and a final elongation step at 72°C for 7 minutes.

Diagnostic colony PCR was carried out in 40 μl reactions containing 1x PCR buffer, 1 μM of each primer, 100 μM dNTPs, 2.5 U Taq polymerase. The yeast colony was picked and added to 15 μl of sterile distilled water and heated to 95ºC for 10 minutes, before being added to the reaction mixture. The colony PCR program was an initial denaturation at 94°C for 3 minutes, followed by 35 cycles of 94°C (1 min), 55°C (1 min), 72°C (1 min), and a final elongation step at 72°C for 7 minutes.

Details of the primers [Eurogentec] used in this study are shown in Table 2.4. All primers were supplied desalted.

Table 2.4 Primers used in this study

Name	Sequence 5'-3'	Source
MFP	ATG TGA TCT TTG GTC TTT GGG	This study
MRP	AGA CCC GGG AGC AGG ATT ATC GGA TGT ACG	This study
HFP	AGA CAA TTG CCA GAT CTG TTT AGC TTG CC	This study
HRP2	AAG CAA TTG AAT ACG ACT CAC TAT AGG GAG	This study
AFP3	AGC AGC TAC GTT AGA GCA ACG	This study
ARP3	AGG GAA CAA AAG CTG GTA CCG	This study

2.5. Protein techniques

2.5.1. Preparation of yeast TCA extracts

Approximately 10^7-10^8 Yeast cells were pelleted (3000 rpm, 2 min) and resuspended in 1 ml 20% (w/v) trichloroacetic acid (TCA) [Fisher Scientific]. Cells were transferred to a 2 ml tube, pelleted (13,000 rpm, 1 min) and resuspended in 200 μl 20% (w/v) TCA. Glass beads (0.5 mm) [BioSpec Products] were added up to the level of the liquid and mixed vigorously in four cycles of 10 s at 4.0 m/s using a FastPrep®-24 homogeneizer (MPbio™) with 1 minute cooling on ice between cycles. Next, 400 μl of 5% (w/v) TCA was added to the tube and the whole aqueous extract removed to a new 2 ml tube. The precipitated proteins were pelleted (3000 rpm, 10 min, 4°C) and the supernatant discarded. To the protein pellet, 100 μl of 3x Laemmli buffer (150 mM Tris-HCl pH 6.8, 6% [w/v] SDS, 30% [v/v] glycerol, 0.3% [w/v] bromophenol blue, 15% [v/v] β-mercaptoethanol) and 50 μl of Tris-HCl pH 9.4 were added and mixed using a vortex for 10 seconds. The protein extract was incubated at 95°C in a hot block for 5 minutes. Insoluble material was pelleted (3000 rpm, 10 min, 4°C) and the soluble supernatant removed to a clean tube for storage at -20°C.

2.5.2. SDS polyacrylamide gel electrophoresis

Proteins were separated by denaturing sodium-dodecyl-sulphate polyacrylamide gel electrophoresis (SDS-PAGE). Polyacrylamide gels (7 x 9 cm) were assembled in a Hoefer Dual Gel Caster vertical apparatus [Amersham Biosciences]. The resolving gel (% acrylamide [Protogel] as indicated, 0.04% [w/v] SDS, 375 mM Tris-HCl pH 8.8, polymerised with 0.1% [w/v] ammonium persulphate [APS] [Bio-Rad] and 0.05% [v/v] N,N,N',N'-tetramethyl-ethylenediamine [TEMED] [Bio-Rad]) was overlaid with stacking gel (5% [w/v] acrylamide, 0.04% [w/v] SDS, 375 mM Tris-HCl pH 6.8, polymerised as before) and left at room temperature to set with a well-forming comb in place. Protein samples were heated up to 95ºC for 5 minutes in a hot block prior to loading on the gel. 5-10 μl of a TCA protein extract was loaded per lane. Electrophoresis was performed at a constant current of 35 mA in electrophoresis running buffer (365 mM glycine, 50 mM Tris base, 0.1% [w/v] SDS) until the bromophenol blue dye reached the bottom of the resolving gel. Proteins on the gel were detected by Western blot analysis (Section 2.5.3). The molecular weight of proteins was estimated by comparison with full-range rainbow molecular weight markers (5 μl per gel lane) [Amersham Biosciences].

When indicated, Phos-tag reagent (AAL-107; NARD Institute, Amagasaki, Japan) (Hidetaka, 2009) was used to improve separation of phosphorylated forms of the relevant protein. For this, Phos-tag and $MnCl_2$ were added to the resolving gel to a final concentration of 4 μM and 200 μM, respectively.

2.5.3. Western blot analysis

The proteins separated by SDS-PAGE (Section 2.5.2) were transferred to a Protran nitrocellulose membrane [Schleicher & Schnell]. The V10-SDB semi-dry electroblotter apparatus [BDH] was assembled using Whatman 3MMChr filter paper, the membrane and the gel according to the manufacturer's instructions. The filter paper, membrane and gel were all pre-incubated in transfer buffer (40 mM glycine, 48.5 mM Tris base, 0.04% [w/v] SDS, 20% [v/v] methanol) for at least 10 minutes. The transfer was performed at 2-5 mA/cm^2 of gel area for 2 hours.

When Phos-tag was added to the resolving gel, the gel was incubated for 10 minutes at room temperature with gentle agitation in the transfer buffer solution supplemented with 1 mM EDTA, followed by 10 minutes incubation with standard

transfer buffer. The proteins were then transferred to a Hybond-P PVDF membrane [GE Healthcare]. The Mini Trans-Blot® electrophoretic transfer cell [Bio-Rad] was assembled using Whatman 3MMChr filter paper, the membrane and the gel according to the manufacturer's instructions. The filter paper, membrane and gel were all pre-incubated in transfer buffer (40 mM glycine, 48.5 mM Tris base, 0.04% [w/v] SDS, 20% [v/v] methanol) for at least 10 minutes. The transfer was performed overnight at 30 V and 90 mA.

After transfer, the membrane was incubated with blocking buffer (phosphate-buffered-saline [PBS; Table 2.1] containing 0.2% [v/v] Tween-20 [PBS-T], 5% [w/v] dried milk [Marvel]) for 1 hour at room temperature. Then the membrane was probed with the indicated primary antibody (Table 2.5) at the appropriate dilution in blocking buffer, gently shaking overnight at 4°C. The next day it was washed in PSB-T (3 x 20 min), and then incubated with the appropriate horseradish peroxidase- or alkaline phosphatase-conjugated secondary antibody [Sigma] at a 1:10,000 dilution in blocking buffer for 1 hour. The membrane was washed (3 x 10 min) in PBS and the signal visualised by enhanced chemiluminescence (ECL) [GE healthcare] or Alkaline Phosphatase Magenta™ [Sigma-Aldrich].

The two ECL reagents were mixed in a 1:1 ratio and the membrane was incubated with a total volume of 3 ml of the ECL reagents for 1 minute at room temperature. The excess liquid was drained off the membrane, which was then wrapped in Saran wrap and exposed to autoradiography film [Kodak] in the dark in an exposure cassette. The time of exposure varied depending on the intensity of the signal. Films were developed in an X150 X-ray film processor [X-ograph Imaging Systems]. Developed films were scanned and the images were saved as TIFF files.

Alternatively, a tablet of alkaline phosphatase substrate was dissolved into 10 ml of distilled water. The membrane was then incubated with this solution until the signal from degradation of the substrate could be detected by the naked eye. Membranes were scanned at various time points during incubation and the images were saved as TIFF files.

Table 2.5 Antibodies used for Western blot analysis in this study

Antibody	Type	Dilution for Western blot	Source
α-HA (12CA5)	mouse monoclonal	1:1000	NIMR, London
α-Hop1	rabbit polyclonal	1:1000	Franz Klein, MFPL, Austria
α-phospho-S298[a]	guinea pig polyclonal	1:200	Eurogentec
α-phospho-T318[a]	rabbit polyclonal	1:1000	Cambridge Research Biochemicals

[a] Section 2.5.4

2.5.4. Phospho-specific antibodies

Antibodies were generated against phosphorylated amino acid residues T318 and S298 of Hop1.

The α-pT318 polyclonal antibody [Cambridge Research Biochemicals] was obtained by immunising two rabbits with the antigenic peptide [C]-Ahx-ASIQP-[pT]-QFVSN, where C represents the C-terminus of the peptide, Ahx is aminohexanoic acid and pT is a phosphorylated threonine residue. Upon bleeding, antibodies were purified through two affinity columns (each followed by a purification pass), the first adsorbing antibodies that bind to nonphosphorylated peptides and the second adsorbing the phospho-specific antibodies to pT318. The specificity of the antibody was tested using ELISA (enzyme-linked immunosorbent assay) analysis.

The polyclonal phospho-specific antibody against phosphorylated serine residue 298 [Eurogentec] was obtained by immunising four guinea pigs with the antigenic peptide [C]-PQNFVT-[pS]-QTTNV, where C represents the C-terminus of the peptide and pS is a phosphorylated serine residue. The α-pS298 antibody was purified in a similar manner to the α-pT318 antibody.

2.6. Fluorescence microscopy

2.6.1. Assessment of meiotic progression

Progression through meiosis was assessed by staining whole cells with a solution of 1 μg/ml of 4,6-diamino-2-phenylimide (DAPI). For this, 1 ml samples of synchronous meiotic cultures were resuspended in 300 µl of fixing solution (Table 2.1). 2 µl of this suspension were mixed with 2 µl of DAPI solution on a microscope

slide and covered with a cover slip. The fraction of cells that had progressed through one or both meiotic divisions (MI+) was determined as the ratio between the number of cells where 2 or more DAPI staining bodies were detected and the total number of cells scored.

An Olympus BX41 microscope with a 40x objective equipped for fluorescent microscopy was used to view DAPI-stained cells.

2.6.2. Preparation of immunostained nuclear spreads

Meiotic spreads were prepared as previously described (Dresser and Giroux, 1988). Immunostaining was carried out following an established protocol (Gasior et al., 1998). The primary antibodies used for immunostaining are listed in Table 2.6. Secondary antibodies used were: chicken anti-mouse Alexa-488, chicken anti-rabbit Alexa-594 and goat anti-guinea pig Alexa-594 [Invitrogen], used at 1:500 dilution. A solution of 1 μg/ml of DAPI was used for chromosomal DNA staining.

Table 2.6 Antibodies used for immunostaining in this study

Antibody	Type	Dilution for immunostaining	Source
α-HA (12CA5)	mouse monoclonal	1:100	Steve Ley, NIMR, London
α-Hop1	rabbit polyclonal	1:300	Franz Klein, MFPL, Austria
α-phospho-S298[a]	guinea pig polyclonal	1:50	Eurogentec
α-phospho-T318[a]	rabbit polyclonal	1:100	Cambridge Research Biochemicals
α-Zip1	rabbit polyclonal	1:300	Valentin Börner, Cleveland State Universtity, USA

[a] Section 2.5.4

2.6.3. Imaging meiotic spreads

Meiotic spreads were analysed and photographed on a Deltavision Spectris system containing a photometrics CH350L liquid cooled charge-coupled device camera and an Olympus IX70 inverted microscope with a 100x objective equipped with Deltavision data collection system [Applied Precision].

For each image, 5 images (0.1 μm apart) were acquired. Images were processed using SoftWoRx image processing suite [Applied Precision] and PhotoShop version CS [Adobe] software. Out of focus images were discarded prior to projecting the stack of images onto one plane. Exposure times varied and were dependent upon the intensity of the observed fluorescence.

2.7. Plasmid construction

2.7.1. Details of plasmids used in this study

The plasmids used in this study are summarised in Table 2.7. Details of the plasmids constructed in this study are given in Section 2.7.2.

Table 2.7 Plasmids used in this study

Plasmid Name	Details	Reference/Source
pAG32	PCR template for gene manipulation (pFA6a-hphMX4)	(Goldstein and McCusker, 1999)
pAP1-MEK1	pLP37-*MEK1::hphMX*	this study
pAP1-S320A	pLP37-*mek1-S320A::hphMX*	this study
pAP1-S320D	pLP37-*mek1-S320A::hphMX*	this study
pLP37-MEK1	*ura3::MEK1::URA3*	(de los Santos and Hollingsworth, 1999)
pLP37-S320A	*ura3::mek1-S320A::URA3*	(de los Santos and Hollingsworth, 1999)
pLP37-S320D	*ura3::mek1-S320D::URA3*	(de los Santos and Hollingsworth, 1999)
pLT11-S298D	*ura3::hop1-S298D::URA3*	Cha lab
pRSC38	pUC19-*CHA1*	Cha lab

2.7.2. pAP1

Plasmids pAP1-MEK1, -S320A and -S320D were derived from previously described plasmids pLP37-MEK1, -S320A and -S320D, respectively (Table 2.7) (de los Santos and Hollingsworth, 1999). A 3' sequence downstream of genomic *MEK1* was amplified by PCR (Section 2.4.7) using the 3' primer MFP and the 5' primer MRP (Table 2.4). After *Hpa*I and *Xma*I restriction enzyme digestion (Section 2.4.5), the 3' sequence of *MEK1* was inserted into the pLP37 plasmids, producing pLP37-MEK1+3',

-S320A+3' and -S320D+3' plasmids. These plasmids were sequenced using the 3' primer AFP3 and the 5' primer ARP3 in order to verify correct integration of the *MEK1* downstream sequence.

A hygromycin-resistance gene marker was amplified from plasmid pAG32 (Table 2.7) using the 3' primer HFP and the 5' primer HRP2. The resultant PCR product was purified, digested with the restriction enzyme *Mfe*I and inserted into the pLP37+3' plasmids produced above. The plasmids obtained in this way, pAP1-MEK1, -S320A and -S320D were checked by restriction enzyme digestion.

2.8. Yeast strain construction

2.8.1. Details of yeast strains used in this study

Details of all the strains used in this study are given in Table 2.8. All strains are of the SK1 strain background. Strains constructed in this study by genomic modification are described below in Sections 2.8.2 and 2.8.3.

Strains constructed in this study by standard yeast methods (mating [Section 2.3.2], tetrad dissection [Section 2.3.3] and transformation [Section 2.3.8]) are listed in Table 2.8.

Table 2.8 Yeast strains used in this study

Name	Genotype	Reference/Source
Cha Lab Stocks		
JCY190	*MAT**a**/MAT**α**, ho::LYS2/", lys2/", ura3/", leu2::hisG/", zip1Δ::LEU2/"*	(Carballo et al., 2008)
JCY448	*MAT**a**/MAT**α**, ho::LYS2/", lys2/", ura3/", leu2::hisG/", hop1Δ::LEU2/"*	(Carballo et al., 2008)
JCY553-554	*MAT**a**/MAT**α**, ho::LYS2/", lys2/", ura3/", leu2::hisG/", hop1Δ::LEU2/", ura3::hop1-T318A::URA3/"*	(Carballo et al., 2008)
JCY555-556	*MAT**a**/MAT**α**, ho::LYS2/", lys2/", ura3/", leu2::hisG/", hop1Δ::LEU2/", ura3:: hop1^{SCD}::URA3/"*	(Carballo et al., 2008)
JCY559-560	*MAT**a**/MAT**α**, ho::LYS2/", lys2/", ura3/", leu2::hisG/", hop1Δ::LEU2/", ura3::hop1-S298A::URA3/"*	(Carballo et al., 2008)
JCY573	*MAT**a**/MAT**α**, ho::hisG/", lys2/", ura3/", leu2::hisG/", ade2/ADE2, hop1Δ::LEU2/", ura3::hop1-T318A::URA3/", MEK1-3HA::URA3/", dmc1Δ::KanMX4/"*	(Carballo et al., 2008)
JCY591-592	*MAT**a**/MAT**α**, ho::hisG/", lys2/", ura3/", leu2::hisG/", hop1Δ::LEU2/", ura3::hop1-S298A::URA3/", dmc1Δ::kanMX4/"*	(Carballo et al., 2008)
JCY593-594	*MAT**a**/MAT**α**, ho::hisG/", lys2/", ura3/", leu2::hisG/", hop1Δ::LEU2/", ura3::HOP1::URA3/", dmc1Δ::kanMX4/"*	(Carballo et al., 2008)
JCY604/610	*MAT**a**/MAT**α**, ho::LYS2/", lys2/", ura3/", leu2::hisG/", hop1Δ::LEU2/", ura3::hop1-S311A::URA3/"*	(Carballo et al., 2008)
JCY623	*MAT**a**/MAT**α**, ho::LYS2/", lys2/", leu2::hisG/", ura3/", hop1Δ::LEU2/", ura3::HOP1::URA3/", rad50S::URA3/"*	(Carballo et al., 2008)

Name	Genotype	Reference/Source
JCY634	*MAT**a**/MAT**α**, ho::LYS2/", lys2/", ura3/", leu2::hisG/", arg4N/ARG4N, his4X/HIS4, mek1∆::URA3/"*	
RCY313	*MAT**a**, ade8*	
RCY314	*MAT**α**, ade8*	
Tsubouchi Lab Stocks		
HTY2091	*MAT**a**/MAT**α**, ho::hisG/", leu2::hisG/" ura3(delta Sma-Pst)/", HIS4::LEU2-(NBam)/his4X::LEU2-(NBam)-URA3, hed1∆::hphMX/"*	(Tsubouchi and Roeder, 2006)
HTY2092	*MAT**a**/MAT**α**, ho::hisG/", leu2::hisG/" ura3(delta Sma-Pst)/", HIS4::LEU2-(NBam)/his4X::LEU2-(NBam)-URA3, dmc1Δ::KanMX4/", hed1Δ::hphMX/"*	(Tsubouchi and Roeder, 2006)
Strains constructed in this study		
APY1-2	*MAT**a**/MAT**α**, ho::LYS2/", lys2/", leu2::hisG/", hop1∆::LEU2/", ura3::HOP1::URA3/"*	
APY25-26	*MAT**a**/MAT**α**, ho::hisG/", hop1Δ::LEU2/", ura3::hop1-S298A::URA3/", zip1Δ::LEU2/"*	
APY32-33	*MAT**a**/MAT**α**, ho::hisG/", lys2/", leu2::hisG/", hop1Δ::LEU2/", ura3::hop1-S298A::URA3/", dmc1Δ::KanMX/", MEK1-3HA::URA/"*	
APY50-51	*MAT**a**/MAT**α**, ho::hisG/", lys2/", rad50S::URA/", ura3::hop1-S298A::URA3/", hop1Δ::LEU2/"*	
APY67	*MAT**a**/MAT**α**, ho::hisG/", lys2/", leu2::hisG/", hop1Δ::LEU2/", ura3::hop1-S298A::URA3/", hed1∆::hphMX/", dmc1∆::kanMX4/"*	

Name	Genotype	Reference/Source
APY68 & 70	*MAT**a**/MAT**α**, ho::hisG/", lys2/", leu2::hisG/", hop1Δ::LEU2/", ura3::hop1-S298A::URA3/", hed1∆::hphMX/"*	
APY83	*MAT**a**/MAT**α**, ho::hisG/", lys2/", ura3::HOP1::URA3/", hop1Δ::LEU2/", MEK1-3HA::URA3/"*	
APY85	*MAT**a**/MAT**α**, ho::hisG/ho::LYS2, lys2/", leu2/", hop1Δ::LEU2/", ura3::hop1-S298A::URA3/", MEK1-3HA::URA3/"*	
APY90-91	*MAT**a**/MAT**α**, ho::LYS2/", lys2/", leu2::hisG/", hop1∆::LEU2/", ura3::hop1-S298D::URA3/"*	
APY134	*MAT**a**/MAT**α**, ho::hisG/", lys2/", leu2::hisG/", hop1∆::LEU2/", ura3::HOP1::URA3/", MEK1-3HA::URA/", dmc1∆::KanMX4/"*	
APY172-173	*MAT**a**/MAT**α**, ho::LYS2/", lys2/", leu2::hisG/", hop1∆::LEU2/", ura3::hop1-S298A::URA3x2/"*	
APY199	*MAT**a**/MAT**α**, ho::LYS2/", lys2/", leu2::hisG/", hop1∆::LEU2/", ura3::hop1-S298D::URA3/", arg4B/", dmc1∆::kanMX4/"*	
APY200 & APY237	*MAT**a**/MAT**α**, ho::LYS2/ho::hisG, lys2/", leu2::hisG/", hop1∆::LEU2/", ura3::hop1-S298D::URA3/", arg4B/ARG4, dmc1∆::kanMX4/"*	
APY209	*MAT**a**/MAT**α**, ho::hisG/", lys2/", leu2::hisG/", hop1∆::LEU2/", ura3::hop1-S298A::URA3x2/", dmc1∆::kanMX4/"*	
APY210	*MAT**a**/MAT**α**, ho::LYS2/ho::hisG, lys2/", leu2::hisG/", hop1∆::LEU2/", ura3::hop1-298D::URA3x2/", arg4B/ARG4, dmc1∆::kanMX4/"*	
APY214-215	*MAT**a**/MAT**α**, ho::LYS2/", lys2/", leu2::hisG/", hop1∆::LEU2/", ura3::hop1-S298D::URA3/", his4X/+*	

Name	Genotype	Reference/Source
APY217	*MAT**a**/MAT**α**, ho::LYS2/", lys2/", leu2::hisG/", hop1∆::LEU2/", ura3::hop1-S298D::URA3/ura3, his4X/HIS4*	
APY218	*MAT**a**/MAT**α**, ho::LYS2/ho::hisG, lys2/", leu2::hisG/", hop1Δ::LEU2/", ura3::hop1-S298A::URA3/ ura3::HOP1::URA3, his4X/HIS4*	
APY219	*MAT**a**/MAT**α**, ho::LYS2/", lys2/", leu2::hisG/", hop1∆::LEU2/", ura3::hop1-S298A::URA3x2/ura3*	
APY220	*MAT**a**/MAT**α**, ho::LYS2/", lys2/", ura3::HOP1::URA3/ura3::hop1-S298A::URA3x2, leu2::hisG/", his4X/HIS4, arg4N/ARG4, hop1Δ::LEU2/"*	
APY221	*MAT**a**/MAT**α**, ho::LYS2/ho::hisG, lys2/", ura3::HOP1::URA3/ ura3::hop1-S298D::URA3, leu2::hisG/", HIS4/his4X, hop1Δ::LEU2/"*	
APY222	*MAT**a**/MAT**α**, ho::LYS2/", lys2/", ura3::HOP1::URA3/ura3, leu2::hisG/", his4X/HIS4, hop1Δ::LEU2/"*	
APY223	*MAT**a**/MAT**α**, ho::LYS2/ho::hisG, lys2/", leu2::hisG/", hop1∆::LEU2/", ura3::HOP1::URA3/ura3::hop1-S298D::URA3, arg4B/", dmc1∆::kanMX4/"*	
APY224	*MAT**a**/MAT**α**, ho::LYS2/", lys2/", leu2::hisG/", hop1Δ::LEU2/", ura3::hop1-S298A::URA3/ura3*	
APY233	*MAT**a**/MAT**α**, ho::hisG/", lys2/", leu2::hisG/", hop1∆::LEU2/", ura3::hop1-S298A::URA3x2/ ura3::HOP1::URA3, dmc1∆::kanMX4/"*	
APY234	*MAT**a**/MAT**α**, ho::hisG/", lys2/", leu2::hisG/", arg4/ARG4, hop1∆::LEU2/", ura3::HOP1::URA3/ura3::hop1-S298A::URA3, dmc1∆::KanMX4/"*	
APY239	*MAT**a**/MAT**α**, ho::LYS2/ho::hisG, lys2/", leu2::hisG/", arg4B/", hop1∆::LEU2/", ura3::HOP1::URA3/ura3, dmc1∆::KanMX4/"*	

Name	Genotype	Reference/Source
APY240	*MAT**a**/MAT**α**, ho::LYS2/ho::hisG, lys2/", leu2::hisG/", hop1∆::LEU2/", ura3::hop1-S298D::URA3/ura3, dmc1∆::KanMX4/"*	
APY241	*MAT**a**/MAT**α**, ho::LYS2/ho::hisG, lys2/", leu2::hisG/", hop1∆::LEU2/", ura3::hop1-S298A::URA3x2/ura3, arg4B/ARG4, dmc1∆::kanMX4/"*	
APY242	*MAT**a**/MAT**α**, ho::hisG/", lys2/", ura3, leu2::hisG/", hop1∆::LEU2/", hop1-S298A::URA3/ura3, dmc1∆::KanMX4/"*	
APY257	*MAT**a**/MAT**α**, ho::LYS2/", lys2/", ura3/", leu2::hisG/", mek1-S320A::hphMX4/", his4X/HIS4, arg4N/ARG4*	
APY258	*MAT**a**/MAT**α**, ho::LYS2/", lys2/", leu2::hisG/", arg4N/ARG4, ura3/", mek1-S320A::hphMX4/"*	
APY259	*MAT**a**/MAT**α**, ho::LYS2/", lys2/", ura3/", mek1-S320D::hphMX4/", leu2::hisG/", his4X/HIS4, arg4N/ARG4*	
APY260	*MAT**a**/MAT**α**, ho::LYS2/", lys2/", ura3/", mek1-S320D::hphMX4/", leu2::hisG/", arg4N/"*	
APY305-306	*MAT**a**/MAT**α**, ho::LYS2/", lys2/", leu2::hisG/", arg4/", hop1Δ::LEU2/", ura3::hop1-S298A::URA3/", mek1-S320A::hphMX/", dmc1Δ::kanMX4/"*	
APY307-308	*MAT**a**/MAT**α**, ho::LYS2/", lys2/", leu2::hisG/", arg4/", hop1Δ::LEU2/", ura3::hop1-S298A::URA3/", mek1-S320A::hphMX4/"*	
APY309	*MAT**a**/MAT**α**, ho::LYS2/", lys2/", leu2::hisG/", arg4/", hop1Δ::LEU2/", ura3::hop1-S298A::URA3/", mek1-S320D::hphMX/", dmc1Δ::kanMX4/"*	
APY310	*MAT**a**/MAT**α**, ho::hisG/ho::LYS2, lys2/", leu2::hisG/", ARG4/arg4, hop1Δ::LEU2/", ura3::hop1-S298A::URA3/", mek1-S320D::hphMX/", dmc1Δ::kanMX4/"*	

Name	Genotype	Reference/Source
APY311	*MAT**a**/MAT**α**, ho::hisG/", lys2/", leu2::hisG/", hop1Δ::LEU2/", ura3::hop1-S298A::URA3/", mek1-S320D::hphMX4/"*	
APY312	*MAT**a**/MAT**α**, ho::hisG/ho::LYS2, lys2/", leu2::hisG/", ARG4/arg4, hop1Δ::LEU2/", ura3::hop1-S298A::URA3/", mek1-S320D::hphMX4/"*	
APY315-316	*MAT**a**/MAT**α**, ho::LYS2/", lys2/", HIS4/", arg4/", ura3/", leu2::hisG/", mek1-S320A::hphMX/", dmc1Δ::kanMX4/"*	
APY317-318	*MAT**a**/MAT**α**, ho::LYS2/", lys2/", ura3/", leu2::hisG/", mek1-S320D::hphMX/", dmc1Δ::kanMX4/"*	
APY355	*MAT**a**/MAT**α**, ho::LYS2/ho::hisG, lys2/", arg4B/ARG4, leu2::hisG/", hop1Δ::LEU2/", ura3::hop1-S298D::URA3/", mek1-S320A::hphMX/"*	
APY356	*MAT**a**/MAT**α**, ho::LYS2/", lys2/", arg4B/", leu2::hisG/", hop1Δ::LEU2/", ura3::hop1-S298D::URA3/", mek1-S320A::hphMX/"*	
APY357	*MAT**a**/MAT**α**, ho::LYS2/ho::hisG, lys2/", arg4B/", leu2::hisG/", hop1Δ::LEU2/", ura3::hop1-S298D::URA3/", mek1-S320A::hphMX/", dmc1Δ::kanMX4/"*	
APY358	*MAT**a**/MAT**α**, ho::LYS2/ho::hisG, lys2/", arg4B/ARG4, his4X/HIS4, leu2::hisG/", hop1Δ::LEU2/", ura3::hop1-S298D::URA3/", mek1-S320A::hphMX/", dmc1Δ::kanMX4/"*	
APY359-360	*MAT**a**/MAT**α**, ho::LYS2/ho::hisG, lys2/", arg4B/ARG4, leu2::hisG/", hop1Δ::LEU2/", ura3::hop1-S298D::URA3/", mek1-S320D::hphMX/"*	
APY361-362	*M/MAT**α**, ho::LYS2/ho::hisG, lys2/", arg4B/+, HIS4/", leu2::hisG/", hop1Δ::LEU2/",ura3::hop1-S298D::URA3/", mek1-S320D::hphMX/", dmc1Δ::kanMX4/"*	

Name	Genotype	Reference/Source
APY370-371	*MAT**a**/MAT**α**, ho::hisG/", lys2/", leu2::hisG/", hop1Δ::LEU2/", ura3::hop1-T318A::URA3/", MEK1-3HA::URA3/", arg4N/", his4X/HIS4*	

2.8.2. Integration of a *hop1-S298D* containing plasmid

A *hop1*Δ diploid strain (JCY448) (Table 2.8) was transformed with the integrative plasmid pLT11-S298D (Table 2.7; Section 2.3.8). Stable transformants were selected on SD medium supplemented with a dropout mix lacking uracil and induced to sporulate. The tetrads produced were dissected and haploids prototrophic for uracil were selected and crossed to obtain homozygous diploids.

2.8.3. Integration of pAP1 plasmids

The integrative plasmids pAP1-MEK1, -S320A and -S320D (Table 2.7; Section 2.7.2) were linearised by restriction enzyme digestion with *Hpa*I and *Xma*I and transformed into a diploid *mek1*Δ strain (JCY634) where *MEK1* deletion is marked with *URA3*. Stable integrants were selected on YPD-Hyg medium and induced to sporulate. Viable spore colonies with a pattern of mutually exclusive 2:2 segregation on URA^- and YPD-Hyg plates were selected and crossed to obtain homozygous diploid strains expressing *MEK1*, *mek1-S320A* or *mek1-S320D* alleles at the *MEK1* locus.

Chapter 3: *hop1-S298A* confers a temperature- and dose-dependent loss of spore viability

3.1. Introduction

Hop1 is an essential meiotic protein with roles in double-strand break (DSB) formation, inter-homologue (IH) bias and checkpoint. Deletion of *HOP1* leads to high spore lethality and absence of checkpoint. Both phenotypes are linked to reduced levels of DSBs and defects in IH recombination. *hop1*^{SCD}, an allele of *HOP1* where the Mec1/Tel1 phosphorylation sites at S298, S311 and T318 are eliminated, confers *hop1*Δ-like levels of spore viability. Further analysis has shown that *hop1*^{SCD} strains are proficient in break catalysis, but defective in IH bias and checkpoint functions, demonstrating that Mec1/Tel1 phosphorylation at the three S/T residues in the SQ/TQ cluster domain (SCD) is essential for the latter two functions of Hop1 (Section 1.4) (Carballo and Cha, 2007, Carballo et al., 2008).

In addition to *hop1*^{SCD}, several other phosphomutants were tested for spore viability and sporulation efficiency in *dmc1*Δ. Of all the mutants studied, most show either of two phenotypes: full spore viability and checkpoint proficiency (*hop1-S22A*, *hop1-S69A*, *hop1-S311A*, *hop1-S454A*, *hop1-T547A*) or high spore lethality and absence of *dmc1*Δ arrest (*hop1*^{SCD}, *hop1-5A*, *hop1-T318A*, *hop1-T181A*). One of the alleles tested, *hop1-S298A*, however, shows high sporulation efficiency in a *dmc1*Δ background, but only moderately compromised spore viability (Carballo et al., 2008).

This phenotype makes *hop1-S298A* a potentially useful allele in the study of Hop1 functions. Specifically, moderate level of spore viability (51.3%) (Carballo et al., 2008) suggests that IH bias is at least partly conserved, yet sporulation efficiency in a *dmc1*Δ background is comparable to *hop1*^{SCD} or *hop1*Δ mutants (58.8% in *hop1-S298A*, 62.5% in *hop1*^{SCD} and 70.0% in *hop1*Δ) (Carballo et al., 2008). The latter suggested that two Hop1 functions, IH bias and checkpoint regulation, might be uncoupled in *hop1-S298A*. We reasoned that characterisation

of this allele might provide insights into the molecular mechanisms underlying these two Hop1 functions. Additionally, I chose to characterise *hop1-T318A*, a phenocopy of *hop1^{SCD}* with regard to spore viability and *dmc1*Δ arrest. Comparison of the phenotypes conferred by individual mutations within the SCD could provide insight on how Mec1/Tel1 phosphorylation regulates the IH bias and checkpoint functions of Hop1.

Since the impact of inactivating several genes involved in meiotic recombination is affected by temperature (Baudrimont et al., 2011, Borner et al., 2004, Cha and Kleckner, 2002, Henderson et al., 2000, Zimmering, 1963), I began a basic characterisation of *hop1-S298A* and *hop1-T318A* by assessing spore viability at different temperatures.

3.2. Results

3.2.1. Effect of temperature on spore viability of *hop1* phosphomutants

In order to determine spore viability dependence on temperature, the relevant strains were incubated in solid sporulation medium (SPM) at the specified temperature for 24h (for temperatures of 30ºC or above) or 48h (for temperatures below 30ºC). At least 40 tetrads (160 spores) were dissected onto YPD for each strain and viable spores were scored after two days of incubation at 30ºC. Spore viability is calculated as the fraction of viable spores in the total number of spores dissected.

HOP1, *hop1-S298A*, *hop1-S311A*, *hop1-T318A* and *hop1^{SCD}* strains were tested. As expected, *HOP1* cells show consistently high spore viability. Like wild-type (WT), *hop1-S311A* mutants produce highly viable spores at the three temperatures tested. In contrast, *hop1^{SCD}* and *hop1-T318A* produce dead spores at 18, 30 and 36ºC (Figure 3.1A).

Notably, at 18ºC most of *hop1-S298A* spores are viable. As the temperature of sporulation is increased to 30ºC, the spore viability is moderately compromised as published (Carballo et al., 2008) At the highest temperature tested, 36ºC, few spores are viable (Figure 3.1A).

To better characterise the temperature-dependence of this strain, two independently derived *hop1-S298A* strains were sporulated at two additional temperatures: 23 and 33ºC. Results show that spore viability is not significantly

affected when temperature is increased from 18 to 23ºC (96.5 and 95.6% spore viability, respectively). In contrast, a notable reduction is observed when temperature is increased from 30 to 33ºC (from 53.2 to 15.0%) (Figure 3.1B). Taken together, these observations reveal that the spore viability of *hop1-S298A* is temperature-sensitive.

3.2.2. Impact of temperature on *hop1-S298A* sporulation efficiency

Next, the effect of temperature on *hop1-S298A* sporulation efficiency was assessed. For this, WT and *hop1-S298A* cells were induced to sporulate on solid sporulation medium (SPM) at 18, 30 and 36ºC for either 24h (30 and 36ºC) or 48h (18ºC). After incubation, sporulation efficiency was determined (Figure 3.2).

As shown in Figure 3.2, *HOP1* sporulates efficiently at the three temperatures tested, with minor differences observed with temperature changes. A small reduction in *hop1-S298A* sporulation efficiency is observed as the temperature increases. Nevertheless, the impact of *hop1-S298A* on sporulation efficiency is considerably milder than its impact on spore viability (Figure 3.1).

A

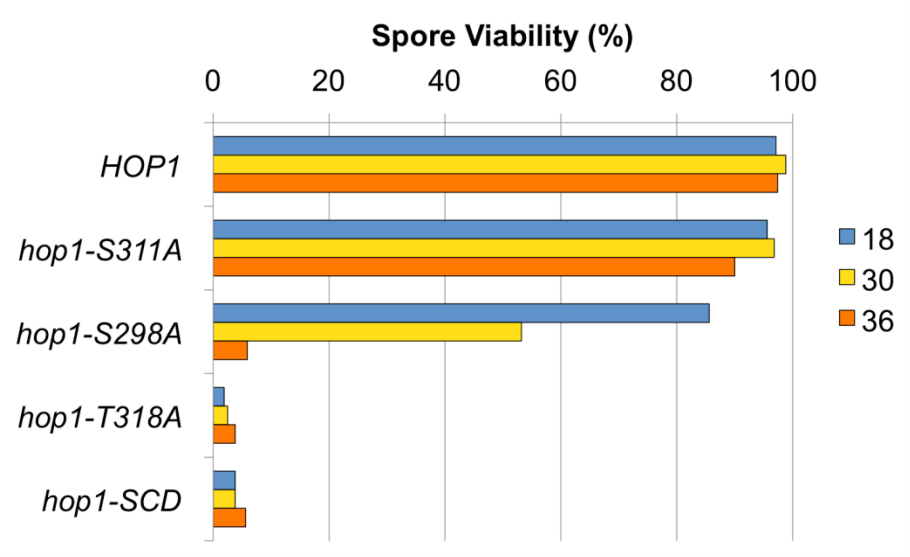

B

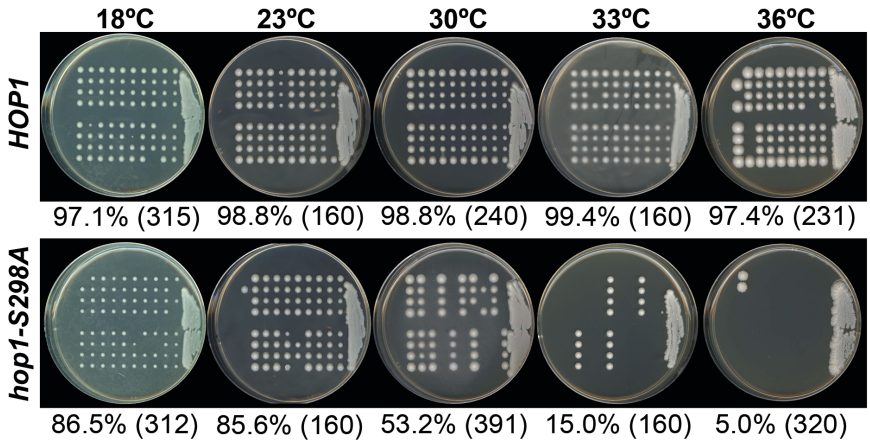

Figure 3.1 Effect of temperature on spore viability of *hop1* phosphomutants

(A) Homozygous diploids of indicated genotypes were incubated on SPM plates at 18, 30, and 36ºC for one (T≥30º) or two days (T<30ºC). Tetrads were dissected on YPD plates and incubated at 30ºC for 2 days. Spore viability is calculated as the number of visible spore colonies (e.g., Figure 3.1B) over the total number of spores dissected. For each strain, at least 40 tetrads (160 spores) were analysed.

(B) Representative images of tetrad analysis. Indicated strains were incubated on SPM plates at the specified temperatures for one (T≥30º) or two days (T<30ºC). Tetrads were dissected on YPD and incubated at 30ºC. The images were taken following 2 days incubation. The percentage corresponds to the number of visible colonies among the total number of spores analysed (shown in brackets).

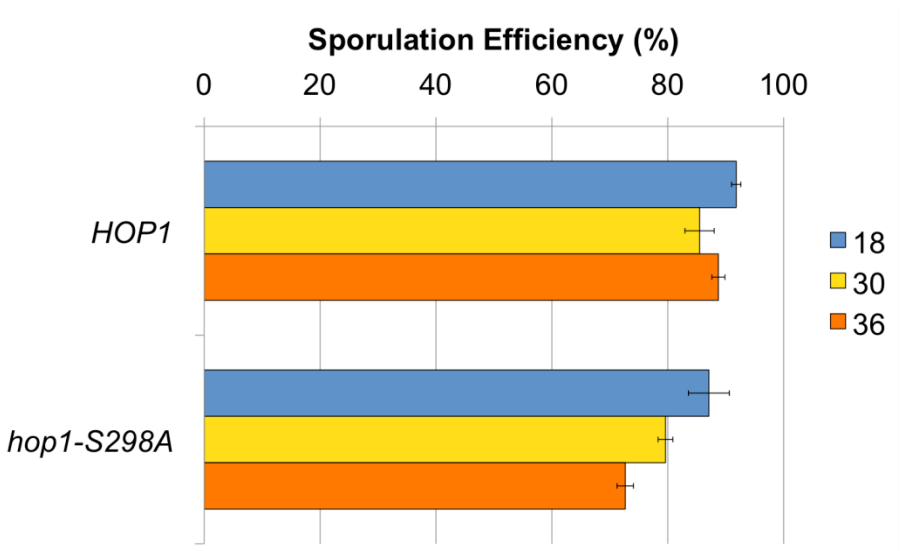

Figure 3.2 Impact of temperature on *hop1-S298A* sporulation efficiency

Two independent homozygous diploid strains of the indicated genotypes were incubated on SPM plates at 18, 30, and 36ºC for one (T≥30º) or two days (T<30ºC). Sporulation efficiency is assessed as the fraction of cells containing two or more spores out of the total number of cells scored. For each condition, 200 or more cells were scored in two independent experiments. Error bars represent the standard deviation from the mean.

3.2.3. *hop1-S298A* overexpression improves spore viability

Next, a strain overexpressing *hop1-S298A* (*hop1-S298Ax2*) was tested for spore viability at 18, 30 and 36ºC as described above (Section 3.2.1).

It was observed that spore viability is rescued in *hop1-S298Ax2* (Figure 3.3A), indicating that higher levels of the mutant protein can improve its function. At 18 and 30ºC, spore viability in *hop1-S298Ax2* strains is comparable to WT. Spore viability at 36ºC is not fully restored, but is comparable to that observed in the single-copy allele at 30ºC.

3.2.4. Spore viability is fully restored in *hop1-S298D*

I then examined whether the expression of a negatively charged amino acid at position 298 in Hop1 would restore the wild-type phenotype. A mutant where the serine residue at this position was replaced by an aspartic acid residue, *hop1-S298D*, was generated (Section 2.8.2).

Results show that spore viability is fully restored to WT levels in *hop1-S298D* at 18, 30 and 36ºC (Figure 3.3A), indicating that the presence of a negative charge at this position is sufficient for full spore viability.

3.2.5. Dose-dependent loss of spore viability in *hop1-S298* alleles

The impact of *hop1-S298Ax2* on spore viability suggests that *hop1-S298A* phenotype is dose- as well as temperature-dependent. To further investigate this, different heterozygous and hemizygous diploid mutants were obtained. These contained the relevant allele of *HOP1* (*HOP1*, *hop1-S298A*, *hop1-S298Ax2* or *hop1-S298D*) and *HOP1* or *hop1*Δ in the allelic locus (Table 2.8).

Spore viability was determined in liquid medium culture. For this, two to four independent strains of each genotype were taken through the standard procedure for preparing meiotic cultures as described in Chapter 2 (Section 2.3.4). Following 48h of incubation at 23ºC in liquid SPM, 40 tetrads or more were dissected from each culture. Spore viability was calculated as described (Section 3.2.1).

The results show that one copy of *HOP1* is sufficient to confer a wild-type phenotype in terms of spore viability (Figure 3.3B). When a single copy of the mutant protein Hop1^{S298A} is present (*hop1-S298A/hop1*Δ), spore viability is reduced to 6.4%. As expected, the presence of a single allele of *hop1-S298Ax2* (*hop1-*

*S298Ax2/hop1*Δ) leads to a phenotype identical to that of *hop1-S298A* homozygous (Figure 3.3B). Notably, *hop1-S298D/hop1*Δ spore viability at 23ºC is reduced, indicating that the replacement of S298 by an aspartic acid residue does not lead to a fully wild-type phenotype.

A

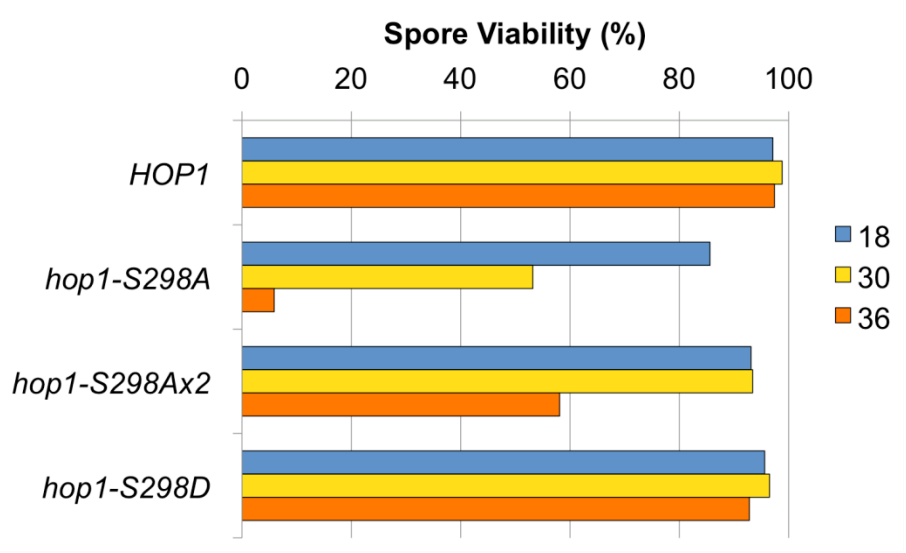

B

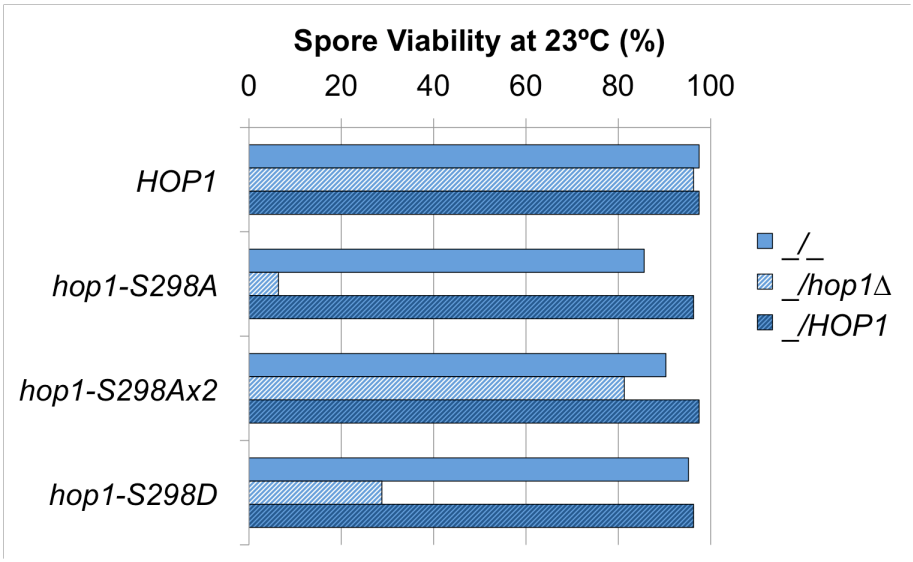

Figure 3.3 Temperature- and dose-effects on the spore viability of *hop1-S298* alleles

(A) Homozygous diploids of indicated genotypes were incubated on SPM plates at 18, 30, and 36ºC for one (T≥30º) or two days (T<30ºC). Tetrads were dissected on YPD plates and incubated at 30ºC for 2 days. Spore viability is calculated as the number of visible spore colonies (e.g., Figure 3.1B) over the total number of spores dissected. For each strain, at least 40 tetrads (160 spores) were analysed.

(B) Spore viability of indicated *HOP1* alleles as homozygous (*_/_*), hemizygous (*_/hop1Δ*), or heterozygous (*_/HOP1*) diploids. Each strain was incubated at 23ºC in liquid SPM medium for 2 days and spore viability was determined as in (A).

3.3. Discussion

3.3.1. Hints from *hop1-S298A* alleles

Increased temperature can affect protein-protein and protein-DNA interactions in two manners: producing alterations in protein structure and inducing faster dynamics of cellular processes. As shown in this chapter, *hop1-S298A* confers a temperature-sensitive defect in spore viability (Figure 3.1). This suggests that Mec1/Tel1 phosphorylation of Hop1 at serine 298 is probably stabilising interaction of Hop1 with either chromosomal DNA or other protein(s). Since the mutant protein encoded by *hop1*^{SCD} loads efficiently to chromosomes, it is more likely that it is the interaction between the Hop1^{S298A} mutant and other protein or a complex that is disrupted at higher temperatures.

The defects in spore viability conferred by the *hop1-S*298A allele are dose-dependent (Figure 3.3). Overexpression of mutant alleles can rescue protein functions when the mutant protein is inefficient in a particular process, such as binding other proteins and complexes, but not when the mutant protein is completely defective in such process. The fact that overexpression of *hop1-S298A* rescues spore viability suggests that the defects conferred by *hop1-S298A* result from inefficient interaction of the mutant protein with one (or more) of its partners.

Conversely, reducing expression of a defective mutant allele is likely to exacerbate its phenotype by compromising further the processes in which the mutant protein is inefficient. Results show that *hop1-S298A/hop1*Δ hemizygous diploids produce considerably fewer viable spores at 18ºC than *hop1-S298A/hop1-S298A* homozygous diploids (Figure 3.3B). This supports the hypothesis that Hop1^{S298A} is inefficient in a particular process.

Taken together, these observations suggest that the mutant protein Hop1^{S298A} may be partially defective in the formation of maintenance of a complex or complexes containing Hop1. This defect or defects are exacerbated at high temperature, due to increased dynamics and/or alteration in protein conformation. Reducing the levels of the mutant protein would further compromise these functions.

3.3.2. The phenotype of *hop1-S298D*

Expression of the phosphomimetic allele *hop1-S298D* rescues spore viability at all temperatures tested (Figure 3.3A). The presence of a negatively charged amino acid residue at a position where phosphorylation should occur can mimic the

phosphorylated protein shape and thus restore its functions. However, the structural resemblance conferred by phosphomimetic alleles may be limited. Additionally, the constitutive presence of a negative charge differs from phosphorylation in that it cannot be regulated in response to cellular processes.

The mutant protein Hop1^{S298D} restores Hop1's function, possibly because it resembles Hop1 phosphorylated at serine 298, thus allowing interaction with Hop1's partner protein(s). However, rescue of Hop1 function requires the presence of two copies of the phosphomimetic allele (Figure 3.3B), indicating that Hop1^{S298D} does not fully simulate phosphorylation at Hop1-S298, either due to structural or regulatory differences.

Chapter 4: Genetic interaction between *hop1-S298A* and genes involved in meiotic recombination

4.1. Introduction

As described above (Section 1.4.3), *hop1*^{SCD} is proficient in DSB formation, but deficient in IH bias and checkpoint. Hence, the loss of spore viability in this mutant stems from insufficient IH recombination events rather than from reduced DSB levels (Carballo et al., 2008). It is thus highly unlikely that spore viability defects in *hop1-S298A*, a mutant for an individual residue within the Hop1 SCD, will result from reduced DSB levels. The defects in spore viability detected in *hop1-S298A* are then most probably a consequence of a defect in processing of DSBs. In order to investigate this, genetic interactions between this *HOP1* allele and various genes involved in inter-homologue recombination was assessed.

4.2. Results

4.2.1. *hop1-S298A* is defective in *dmc1Δ* arrest

Previous data obtained at 30ºC indicates that *hop1-S298A* mutants are defective in mediating *dmc1*Δ-dependent prophase arrest (Carballo et al., 2008). In order to test whether temperature had any effects on this mutant's *dmc1Δ* checkpoint proficiency, *HOP1 dmc1*Δ and *hop1S298A dmc1*Δ strains were incubated in solid sporulation medium (SPM) at 30 and 36ºC for 24h and at 18ºC for 48h. After incubation, cells were collected for sporulation efficiency analysis.

As expected, the *HOP1 dmc1*Δ control did not sporulate at any of the temperatures tested (Figure 4.1A) (Bishop et al., 1992). In contrast, *hop1-S298A* produces spores in a *dmc1*Δ background at all three temperatures. There seems to be a slight trend to the increase of the sporulation efficiency, i.e., reduction in checkpoint proficiency, of this mutant when temperature is risen, but the differences in the values obtained are statistically insignificant (Figure 4.1A).

4.2.2. Overexpression of *hop1-S298A* restores *dmc1Δ* arrest

Given that overexpression of *hop1-S298A* improves spore viability (Section 3.2.3), it was decided to determine whether the *hop1-S298Ax2* allele would also rescue *dmc1*Δ arrest. *hop1-S298Ax2 dmc1*Δ double mutant was then obtained and tested for sporulation efficiency along with *hop1-S298A dmc1*Δ and *HOP1 dmc1*Δ in the manner described above (Section 4.2.1).

The results obtained show that *dmc1*Δ arrest is restored in *hop1-S298Ax2* (Figure 4.1A). Notably, overexpression of *hop1-S298A* can restore *dmc1*Δ arrest even at 36ºC, when spore viability was still moderately compromised in *DMC1* background (Figure 3.3A).

4.2.3. *dmc1Δ* arrest is fully restored in *hop1-S298D*

The expression of a negatively charged residue at position 298 of Hop1 was sufficient to restore full levels of spore viability (Section 3.2.4). This allele, *hop1-S298D*, was then introduced into a *dmc1*Δ background and sporulation efficiency determined at 18, 30 and 36ºC as described in Section 4.2.1.

The data obtained reveals that *dmc1*Δ checkpoint, like spore viability (Figure 3.3A), is fully restored in *hop1-S298D* homozygous diploids at the three temperatures tested (Figure 4.1A), indicating that the presence of a negative charge at this position is sufficient for full spore viability and *dmc1*Δ arrest.

A

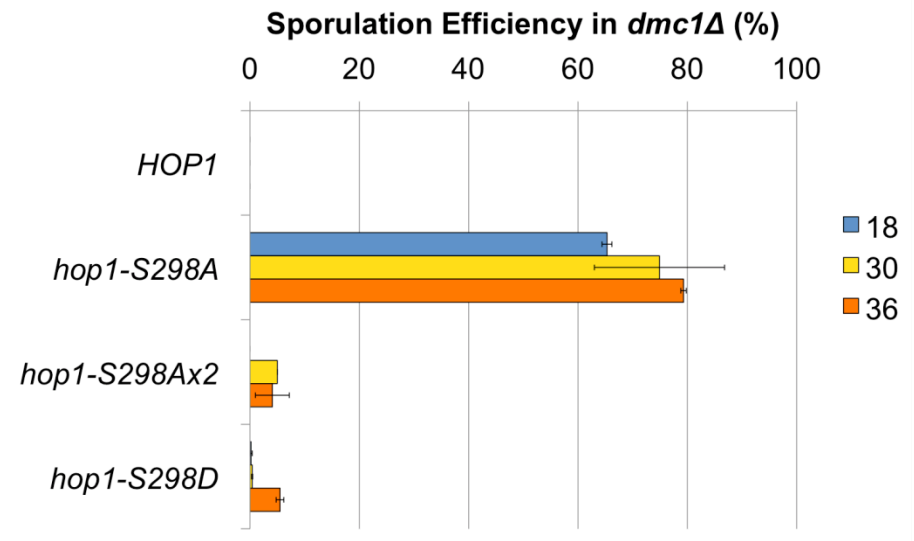

B

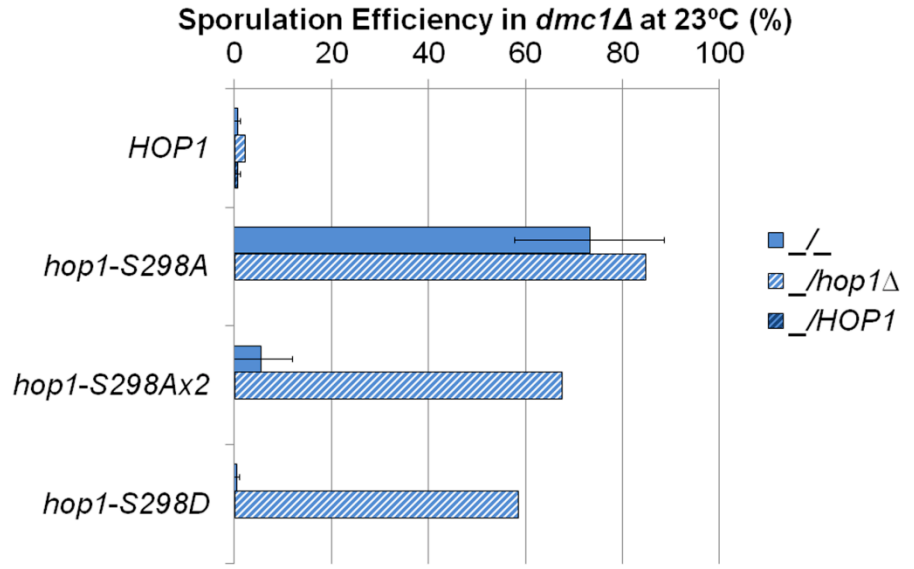

Figure 4.1 Temperature and dose effects on the sporulation efficiency of *hop1-S298* alleles in *dmc1*Δ background

(A) Homozygous diploids of indicated genotypes were incubated on SPM plates at 18, 30, and 36ºC for one (T≥30º) or two days (T<30ºC). Sporulation efficiency is assessed as the fraction of cells containing two or more spores. For each condition, 200 or more cells were scored in two independent experiments. Error bars represent the standard deviation from the mean.

(B) Sporulation efficiency in *dmc1*Δ of indicated *HOP1* alleles as homozygous (*_/_*), hemizygous (*_/hop1*Δ), or heterozygous (*_/HOP1*) diploids. Each strain was incubated at 23ºC in liquid SPM medium for 2 days and sporulation efficiency was assessed as in (A).

4.2.4. Dose-dependent *dmc1Δ* arrest in *hop1-S298* alleles

In the previous chapter (Section 3.2.5), spore viability defects of *hop1-S298* alleles were found to be dependent on the copy number. Hence, it was relevant to address if the same effects could be detected for sporulation efficiency in *dmc1*Δ background. *HOP1*, *hop1-S298A*, *hop1-S298Ax2* and *hop1-S298D* alleles were then combined with *HOP1* in heterozygous diploids or *hop1*Δ in hemizygous diploids in the *dmc1*Δ background.

Two independent strains of each genotype were taken through the standard procedure for preparing meiotic cultures as described in Chapter 2 (Section 2.3.4). Samples were collected after 48h incubation at 23ºC and sporulation efficiency was determined as the fraction of cells containing 2-4 spores out of the total number of cells scored (over 200 per sample).

Similarly to the observations for spore viability in *DMC1* background, the presence of a single copy of *HOP1* is sufficient to promote arrest in *dmc1*Δ (Figure 4.1B). When only one copy of the mutant allele *hop1-S298A* is present (*hop1-S298A/hop1*Δ), sporulation in *dmc1*Δ is increased relatively to the homozygous mutant (*hop1-S298A/hop1-S298A*).

As expected, the presence of a single allele of *hop1-S298Ax2* (*hop1-S298Ax2/hop1*Δ) confers identical sporulation efficiency to that of homozygous *hop1-S298A* mutants. Like spore viability in *DMC1* background, sporulation efficiency of *hop1-S298D/hop1*Δ *dmc1*Δ strains does not confer the *HOP1* phenotype, confirming that although *hop1-S298D* resembles *HOP1* in spore viability and *dmc1*Δ arrest, the phenotype conferred by this allele is not fully WT (Figure 4.1B).

4.2.5. DSBs are repaired in *hop1-S298A dmc1Δ*

Like *hop1-S298A*, *hop1*^{SCD} produces spores in *dmc1*Δ background. However, it has been shown that this is due to incorrect repair of DSBs via IS recombination rather than a lack of checkpoint response. In order to assess whether DSBs are repaired in *hop1-S298A dmc1*Δ, DSB levels were determined by pulsed-field gel electrophoresis (PFGE) (Section 2.4.3).

For this, *HOP1 dmc1*Δ and *hop1-S298A dmc1*Δ strains were taken through synchronous meiosis as described (Section 2.3.7). Samples were collected at various time points during the 12h incubation at 23ºC and DNA plugs prepared for

PFGE analysis (Sections 2.4.3 and 2.4.4). The pulsed-field gel obtained was probed with *CHA1* probe, which hybridises to the sub-telomeric region of Chromosome III (Figure 4.2A).

As expected, DSBs accumulate in *HOP1 dmc1*Δ cells and get hyperresected, producing the characteristic smear at later time points caused by the presence hyperresected DNA tails (Figure 4.2B). Contrastingly, in *hop1-S298A dmc1*Δ, no accumulation of DSBs can be detected, suggesting that *DMC1*-independent repair of breaks occurs in this mutant.

A

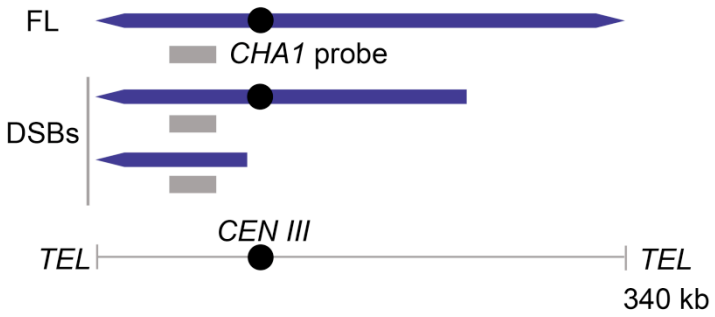

B

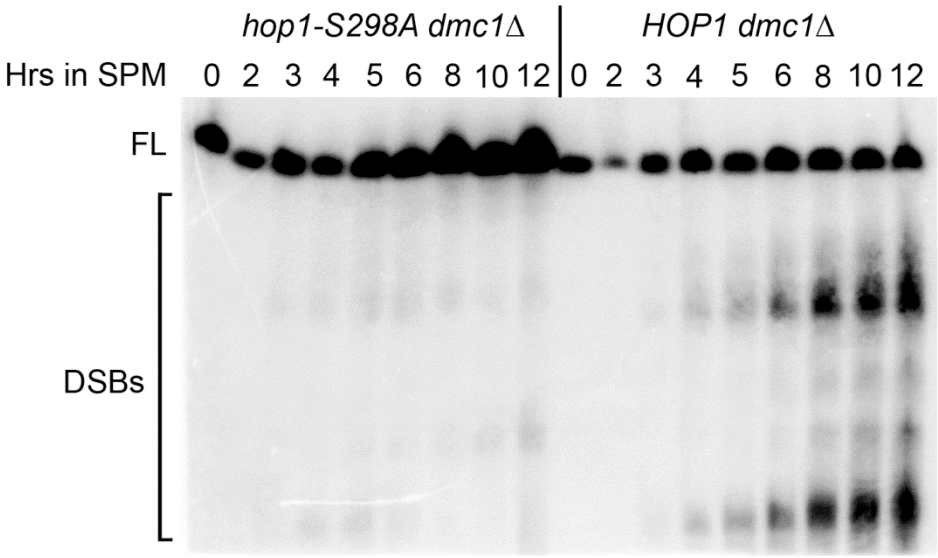

Figure 4.2 DSBs are repaired in *hop1-S298A dmc1*Δ

(A) Chromosome III species revealed by PFGE followed by hybridization with radiolabelled *CHA1* probe. Full-length linear chromosome (FL) and chromosome fragment species extending from the labelled end to the site of DSBs are shown.

(B) Synchronous meiotic cultures of homozygous diploids from indicated genotypes were obtained (YPA method; Section 2.3.7) and samples were collected at various time points up to 12h into meiosis at 23ºC for PFGE/Southern analysis of Chromosome III. Positions of FL and DSBs are as indicated.

The PFGE/Southern analysis was carried out by Dr. Rita Cha.

4.2.6. *hed1Δ* does not rescue spore viability of *hop1-S298A dmc1Δ*

As in *hop1*^{SCD} *dmc1*Δ, bypass of *dmc1*Δ arrest in *hop1-S298A dmc1*Δ is a consequence of *DMC1*-independent repair of DSBs (Section 4.2.5), which is normally a result of defects in IH bias. However, since spore viability of *hop1-S298A*, contrastingly to that of *hop1*^{SCD}, is comparable to WT at low temperature (Figure 3.1A), IH bias appears to be maintained to some extent in this mutant. A genetic approach was taken to assess the strength of IH bias in *hop1-S298A*.

As described above (Section 1.2.3.2), Dmc1 is a meiotic protein essential for IH recombination. Deletion of *DMC1* triggers a delay or complete arrest (depending on strain background) at meiotic prophase I. *dmc1*Δ mutants that sporulate generate inviable spores as DSBs are repaired via IS recombination (Bishop et al., 1992, Shinohara et al., 1997a). Deletion of the meiosis-specific gene *HED1* in *dmc1*Δ strains leads to a significant rescue of spore viability. Indeed, *dmc1*Δ *hed1*Δ double mutants produce about 65% of viable spores at 30ºC (Tsubouchi and Roeder, 2006). This is due to the effect of Hed1 on Rad51 activity. Specifically, Hed1 has been to shown to bind the latter, inhibiting its activity during meiosis, thus favouring *DMC1*-dependent repair of DSBs (Busygina et al., 2008, Tsubouchi and Roeder, 2006).

In *dmc1*Δ mutants, the deletion of *HED1* leads to improved spore viability because, by relieving Hed1-inhibition, Rad51 can now carry out repair of DSBs. However, unlike Dmc1, which mainly uses the homologous chromosome as the repair template, Rad51 will often use the sister chromatid to carry out homologous recombination. This preference leads to a reduction in crossover levels which accounts for the mild reduction in spore viability observed in *dmc1*Δ *hed1*Δ (~65%) double mutants comparatively to WT (~100%) (Busygina et al., 2008, Tsubouchi and Roeder, 2006).

If IH bias is intact in *hop1-S298A*, deletion of *HED1* in a *dmc1*Δ background would rescue viability as observed in wild-type. However, if IH bias is compromised, increased activity of Rad51 would lead to more IS events in *hop1-S298A dmc1*Δ *hed1*Δ than in *HOP1 dmc1*Δ *hed1*Δ cells and the improvement in spore viability would be less significant.

To address this, the relevant strains were obtained and incubated for 48h in solid sporulation medium at 18ºC, the temperature at which the spores produced by

hop1-S298A are most viable. At least 80 spores (20 tetrads) of each strain were dissected and spore viability was scored as described (Section 3.2.1). Spore viability was not determined for *HOP1 dmc1*Δ as checkpoint is triggered in this mutant and, consequently, it produces no spores to be analysed.

The results obtained (Figure 4.3) show that spore viability is not rescued in *hop1-S298A dmc1*Δ *hed1*Δ triple mutant at 18ºC. Moreover, *HED1* deletion reduces *hop1-S298A* spore viability at this temperature, whilst WT viability is not affected as predicted from previous work on *hed1*Δ (Tsubouchi and Roeder, 2006). It was also noted that spore viability for the *HOP1 dmc1*Δ *hed1*Δ mutant was lower at 18ºC than the value reported for 30ºC (29.6 versus ~65%) (Tsubouchi and Roeder, 2006).

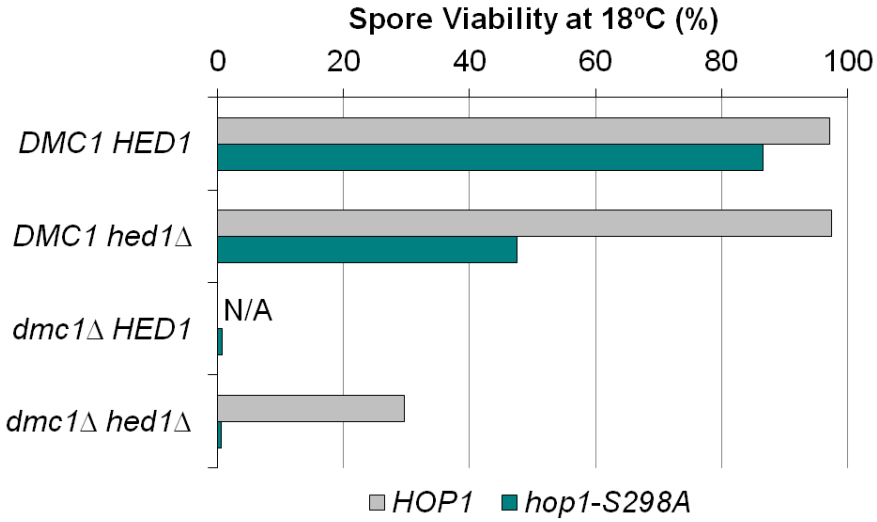

Figure 4.3 Effect of *HED1* deletion on *HOP1* and *hop1-S298A* spore viability in *DMC1* and *dmc1*Δ backgrounds at 18ºC

Homozygous diploids of indicated genotypes were incubated on SPM plates at 18ºC for 2 days. Tetrads were dissected on YPD plates and incubated at 30ºC for 2 days. Spore viability is calculated as the number of visible spore colonies (e.g., Figure 3.1B) over the total number of spores dissected. For each strain, at least 20 tetrads (80 spores) were analysed.

4.2.7. *HED1* deletion affects *hop1-S298A* spore viability differently to wild-type

Next, the impact of *HED1* deletion on temperature-sensitivity of *hop1-S298A* was assessed. For this, *HOP1 hed1*Δ and *hop1-S298A hed1*Δ mutants were sporulated at 18, 30 and 36ºC (48h incubation for 18ºC and 24h for higher temperatures) and their spore viability was determined as before (Section 3.2.1).

*HOP1 hed1*Δ spore viability is constitutively high (≥ 86.0%) at the three tested temperatures. Contrastingly the spore viability of *hop1-S298A hed1*Δ is reduced to approximately 50% of *hop1-S298A HED1* at 18 and 30ºC (Figure 4.4A).

4.2.8. *hed1Δ dmc1Δ* is cold-sensitive for spore viability

The results obtained in Section 4.2.6 suggested that simultaneous deletion of *HED1* and *DMC1* might confer a cold-sensitive phenotype in terms of spore viability. In order to verify if this was the case, *HOP1 dmc1*Δ *hed1*Δ and *hop1-S298A dmc1*Δ *hed1*Δ strains were sporulated at 18, 30 and 36ºC and spore viability was determined as described above (Section 3.2.1).

It was confirmed that spore viability of *dmc1*Δ *hed1*Δ is cold-sensitive. At 30ºC, it is in agreement with the published value (71.3 observed versus ~65% reported) (Tsubouchi and Roeder, 2006) and it reaches its maximum at 36ºC (77.5%) (Figure 4.4B). In *hop1-S298A dmc1*Δ *hed1*Δ triple mutant, spore viability is constitutively low, confirming that *hed1*Δ does not rescue viability in the context of *hop1-S298A dmc1*Δ.

A

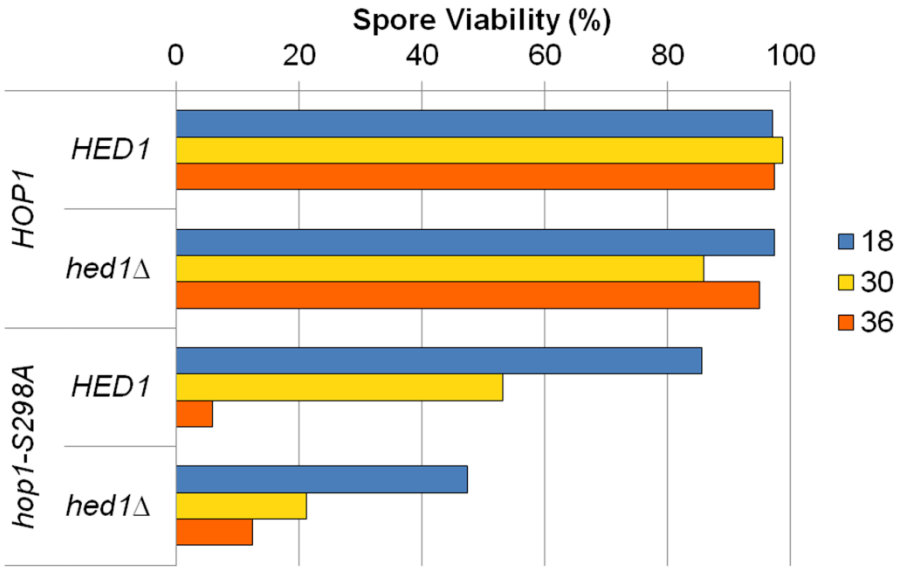

B

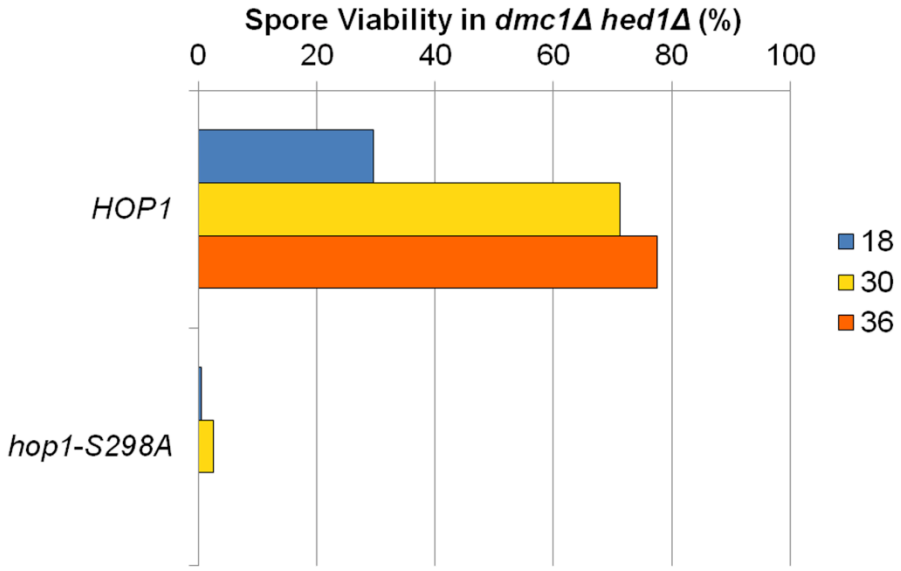

Figure 4.4 Effects of temperature and *HED1* deletion on the spore viability of *HOP1* and *hop1-S298A* alleles in *DMC1* and *dmc1*Δ backgrounds

Homozygous diploids of indicated genotypes in *HED1*, *hed1*Δ **(A)** or *dmc1*Δ *hed1*Δ **(B)** backgrounds were incubated on SPM plates for 2 days at 18ºC or 1 day at 30 and 36ºC. Tetrads were dissected on YPD plates and incubated at 30ºC for 2 days. Spore viability is calculated as the number of visible spore colonies (e.g., Figure 3.1B) over the total number of spores dissected. For each strain, at least 20 tetrads (80 spores) were analysed.

4.2.9. *hop1-S298A* confers a modest defect in *rad50S* background

The results obtained in this chapter indicate that IH bias is compromised in *hop1-S298A*. Indeed, it is shown that, as in *hop1*^{SCD}, the absence of *dmc1*Δ arrest is a result of incorrect DSB repair rather than lack of checkpoint function (Figure 4.2). In order to assess whether checkpoint response is maintained in this mutant, meiosis progression was analysed in a *rad50S* background, where DSBs cannot be processed.

Synchronous meiotic cultures of *HOP1 rad50S* and *hop1-S298A rad50S* strains were prepared as described (Section 2.3.7). Samples were collected at various time points and the fraction of cells that had undergone MI or MII (MI+) at each time point was determined based on DAPI staining analysis of at least 200 cells (Section 2.6.1).

Results show a 2-fold increase in the fraction of cells that progress through meiosis in *hop1-S298A rad50S* compared to *HOP1 rad50S* (36.5 versus 17.5%, respectively) (Figure 4.5), suggesting that checkpoint function is compromised in *hop1-S298A*.

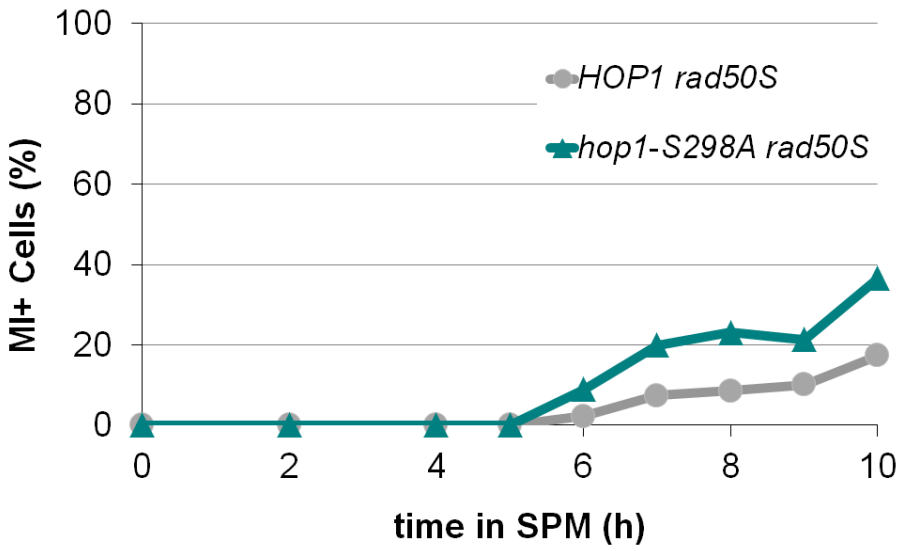

Figure 4.5 Meiotic progression in *rad50S* background at 23ºC

Synchronous meiotic cultures of homozygous diploids from indicated genotypes were obtained (YPA method; Section 2.3.7) and samples were collected at various time points up to 10h into meiosis at 23ºC for DAPI staining. The fraction of MI+ cells corresponds to the ratio of cells with 2-4 DAPI staining bodies to the total number of cells scored (over 200 per sample).

4.2.10. *hop1-S298A* is defective in *zip1Δ* checkpoint

Deletion of *ZIP1*, the major component of the central element of the synaptonemal complex also triggers a delay in meiosis progression (Section 1.3.5) (Sym et al., 1993). In order to further confirm that *hop1-S298A* is defective in checkpoint response, sporulation efficiency was determined in *HOP1 zip1*Δ and *hop1-S298A zip1*Δ mutants at 18, 30 and 36ºC as described above (Section 4.2.1).

HOP1 zip1Δ cells exhibit approximately 10-30% sporulation efficiency depending on temperature (Figure 4.6A), compared to over 97% in *ZIP1* background (Figure 3.1A). The fraction of cells producing spores in *hop1-S298A zip1Δ* at 18°C (~30-50%; Figure 4.6A) was also reduced when compared to *hop1-S298A ZIP1* (~87.1%; Figure 3.2), although higher than in *HOP1 zip1*Δ. Taken together, these observations suggest that *hop1-S298A* may confer a partial defect in *zip1Δ* arrest at 18ºC. At higher temperatures the variations observed in sporulation efficiency on solid medium in *zip1*Δ background (Figure 4.6A) preclude definite conclusions.

It has been noted in previous reports (Borner et al., 2004) that the phenotype conferred by *ZIP1* deletion can be affected by several experimental conditions, such as temperature or concentration of potassium acetate in the sporulation medium. In order to better evaluate if *hop1-S298A zip1*Δ cells exhibit any delay or arrest in meiosis, sporulation efficiency was assessed using liquid medium cultures so that experimental conditions were more uniform. This experiment was carried out at 30ºC, the temperature at which sporulation efficiency of *HOP1* and *hop1-S298A* strains in *zip1*Δ background appears most similar.

Cultures were synchronised as described above (Section 2.3.7) and samples were collected at various time points up to 10h following meiosis induction. Progression through meiosis was determined using the fraction of cells that has undergone MI or MII (MI+; Section 2.6.1).

The results clearly show the impact of *hop-S298A* in *zip1*Δ meiosis (Figure 4.6B). In contrast to *HOP1 zip1*Δ cells, where very few cells undergo meiosis, over 60% of *hop1-S298A zip1*Δ cells have done so by 10h, demonstrating that checkpoint is compromised in *hop1-S298A*.

Next, the impact of *hop1-S298A* on *zip1*Δ spore viability was assessed. For this, *HOP1* and *hop1-S298A* strains in *zip1*Δ background were induced to sporulate on solid SPM plates for 2 days at 18ºC or 1 day at 30 and 36ºC. At least 40 tetrads

(160 spores) were dissected per condition and spore viability was determined (Section 2.3.4).

Spore viability of *HOP1 zip1Δ* tends to increase slightly with temperature (Figure 4.7). Spore viability of *hop1-S298A zip1*Δ is uniformly reduced at all temperatures tested. The impact was greater at 30ºC where the spore viability of the *hop1-S298A* single mutant is already compromised (Figure 3.1).

A

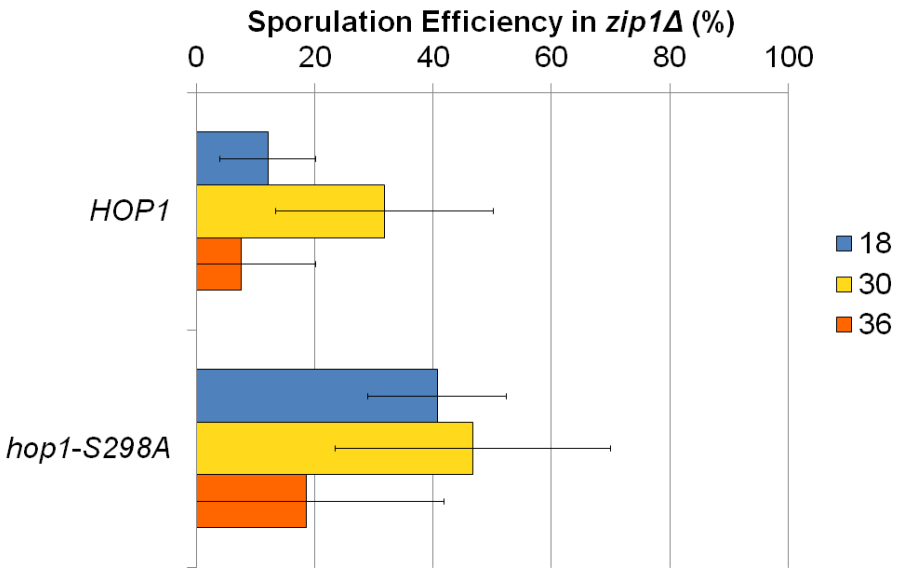

B

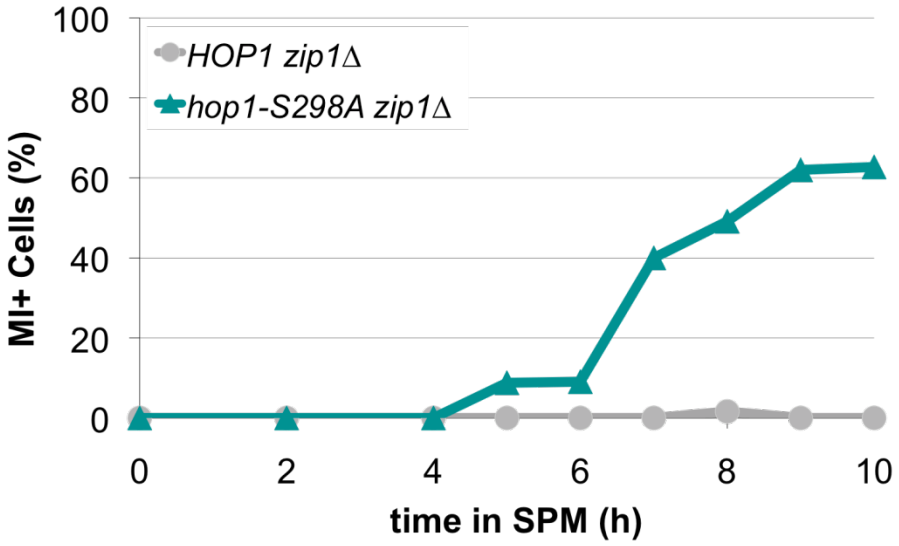

Figure 4.6 Meiosis in *zip1*Δ background

(A) Homozygous diploids of indicated genotypes in *zip1*Δ background were incubated on SPM plates at 18, 30, and 36ºC for one (T≥30º) or two days (T<30ºC). Sporulation efficiency is assessed as the fraction of cells containing two or more spores. For each condition, 200 or more cells were scored in two independent experiments. Error bars represent the standard deviation from the mean.

(B) Synchronous meiotic cultures of homozygous diploids from indicated genotypes were obtained (YPA method; Section 2.3.7) and samples were collected at various time points up to 10h into meiosis at 30ºC for DAPI staining. The fraction of MI+ cells corresponds to the ratio of cells with 2-4 DAPI staining bodies to the total number of cells scored (over 200 per sample).

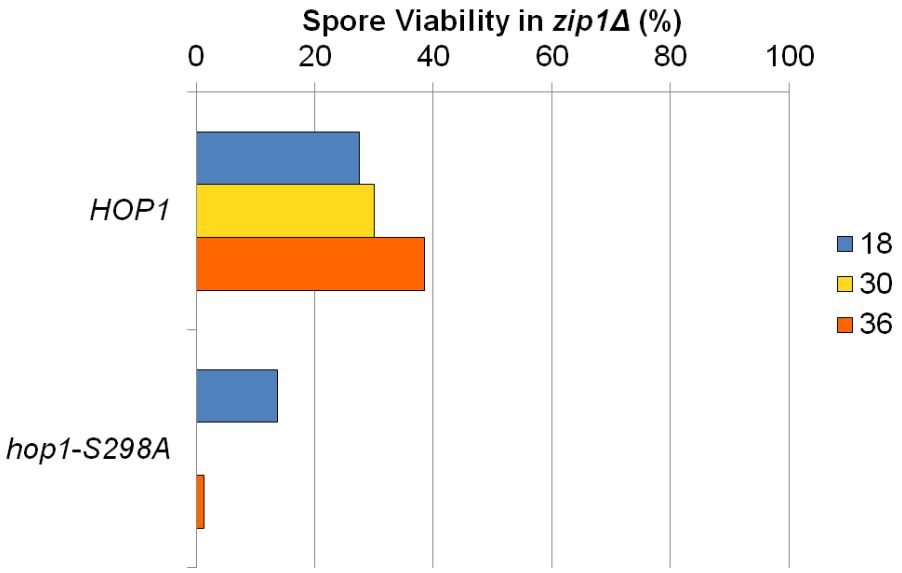

Figure 4.7 Effect of temperature on the spore viability of *HOP1* and *hop1-S298A* in *zip1*Δ background

Homozygous diploids of indicated genotypes in *zip1*Δ background were incubated on SPM plates at 18, 30, and 36ºC for one (T≥30º) or two days (T<30ºC). Tetrads were dissected on YPD plates and incubated at 30ºC for 2 days. Spore viability is calculated as the number of visible spore colonies (e.g., Figure 3.1B) over the total number of spores dissected. For each strain, at least 40 tetrads (160 spores) were analysed.

4.3. Discussion

4.3.1. IH bias is compromised in *hop1-S298A*

hop1-S298A sporulates efficiently in *dmc1*Δ background at all temperatures tested (Figure 4.1A). This could be explained in two ways: (i) elimination of the checkpoint trigger due to repair of DSBs in a *DMC1*-independent manner or (ii) absence of checkpoint response. The first explanation is supported by the observation that DSBs are repaired in *hop1-S298A dmc1*Δ (Figure 4.2). This observation also suggests that phosphorylation of serine residue 298 of Hop1 is required for preventing *DMC1*-independent repair of breaks.

Expression of the phosphomimetic allele *hop1-S298D* rescues the *dmc1*Δ arrest defect, indicating that the presence of a negative charge at the amino acid residue 298 of Hop1 can mimic Hop1 phosphorylation at S298. This probably allows the formation of Hop1-containing complexes, required for preventing *DMC1*-independent repair. When only one copy of *hop1-S298D* is expressed (in *hop1-S298D/hop1*Δ hemizygous diploids), *dmc1*Δ arrest is not restored, indicating that the phenotype conferred by this allele is not fully WT.

Observations that the *hop1-S298A* allele confers a dose-dependent defect in *dmc1*Δ arrest (Figure 4.1) suggest that IH bias is more robust when more copies of *hop1-S298A* are expressed (e.g., *hop1-S298Ax2/hop1-S298Ax2* homozygous diploid; Figure 4.1A and B) and weakened when a single copy is present (e.g., *hop1-S298A/hop1*Δ hemizygous diploid; Figure 4.1B). This is consistent with the earlier hypothesis (Section 3.3.1) that phosphorylation at S298 of Hop1 is required for efficient interaction with other proteins or complexes involved in the establishment of IH bias.

It is likely that the rescue of spore viability in *dmc1*Δ background by *HED1* deletion requires a robust IH bias. If IH bias was not maintained, the increase in Rad51 activity resultant from *HED1* deletion would lead to IS rather than IH recombination. Given that the spores produced at low temperature by *hop1-S298A dmc1*Δ *hed1*Δ are inviable, unlike those generated by *HOP1 dmc1*Δ *hed1*Δ, this suggests that IH bias is compromised in *hop1-S298A*.

It has been previously reported that *HED1* deletion leads to slightly reduced levels of COs (Tsubouchi and Roeder, 2006), suggesting that IH recombination events occur less frequently in *hed1*Δ. In Chapters 3 and 4, I have shown that the phosphomutant allele *hop1-S298A* confers temperature- and dose-dependent

effects on spore viability (Figure 3.3) and that DSBs are repaired in *hop1-S298A dmc1*Δ (Figure 4.2). These observations suggest that IH bias is compromised in *hop1-S298A*. The *hop1-S298A hed1*Δ double mutant produces fewer viable spores than either of the single mutants (Figure 4.4A), suggesting that the two alleles might act synergistically to reduce IH recombination.

Taken together, these results show that IH bias is inefficiently established in *hop1-S298A*. It is sufficient to ensure the formation of the obligatory COs during unchallenged meiosis (e.g., lower temperatures and no further compromises to IH bias), but not to prevent IS recombination in challenged meiosis (e.g., higher temperature, *hed1*Δ, *dmc1*Δ or reduction in copy number).

4.3.2. Checkpoint bypass in *hop1-S298A*

hop1-S298A progresses through meiosis in *rad50S* or *zip1*Δ backgrounds (Figure 4.5 and 4.6B), suggesting that, as well as IH bias, checkpoint function is compromised in this mutant.

Furthermore, introduction of the *hop1-S298A* allele into a *zip1*Δ background exacerbates the loss of spore viability observed in *HOP1 zip1*Δ strains (Figure 4.7), possibly due to cumulative defects in synapsis conferred by *hop1-S298A* and *zip1*Δ. If IH recombination is compromised in *hop1-S298A*, this may lead to defects in synapsis, which are worsened in a *zip1*Δ background.

Chapter 5: Impact of Hop1 phosphorylation on Hop1-Mek1 interaction

5.1. Introduction

Analysis thus far indicates that Mec1/Tel1 phosphorylation at serine 298 and threonine 318 of Hop1 is essential for its functions in IH bias and checkpoint. Previous characterisation of the phosphomutant *hop1*^{SCD} has demonstrated that Mec1/Tel1 phosphorylation of Hop1 is not necessary for DSB formation or Red1 and Hop1 loading onto chromosomes. However, failure in the phosphorylation of the SCD residues leads to defects in Mek1 recruitment and activation, which in turn, lead to loss of IH bias, *DMC1*-independent repair of DSBs in *dmc1*Δ background and lack of *rad50S* and *zip1*Δ checkpoint responses (Carballo et al., 2008).

Mek1 is a meiosis-specific kinase essential for IH bias and checkpoint (Section 1.5). Its loading onto the chromosomes requires Red1 and phosphorylated Hop1 (Bailis and Roeder, 1998, Carballo et al., 2008). Upon recruitment, Mek1 dimerization is mediated by the C-domain of Hop1, an essential step for Mek1 activation. The proximity between Mek1 molecules induced by dimerization of the protein allows transphosphorylation and full activation of the catalytic domain of Mek1 (Niu et al., 2005, Niu et al., 2007, Wan et al., 2004).

Three phosphorylation sites have been identified in the activation loop of Mek1 kinase domain. Two of them, threonines 327 and 331 are essential for the establishment of IH bias, spore viability and checkpoint response. A third residue, serine 320, is specifically phosphorylated during *dmc1*Δ meiosis and is required for *dmc1*Δ arrest (de los Santos and Hollingsworth, 1999, Niu et al., 2007, Niu et al., 2005, Wan et al., 2004).

In this chapter, Hop1 and Mek1 recruitment to chromosomes and their phosphorylation in *hop1-S298A* and *hop1-T318A* are assessed. As described above (Chapter 3) (Carballo et al., 2008), loss of phosphorylation at either site exerts a differential impact on spore viability and *dmc1*Δ arrest. While both phosphomutants are deficient in *dmc1*Δ arrest (Carballo et al., 2008), spore viability is differentially affected in each (Figure 3.1A). This difference is greatest at low temperature, when

spore viability in *hop1-S298A* mutant is comparable to WT, while *hop1-T318A* produces mostly dead spores. To improve the possibility of detecting potential distinctive effects resulting from mutating each residue, all the experiments in this chapter were carried out at 23ºC.

5.2. Results

5.2.1. Meiotic progression in *hop1-S298A* and *hop1-T381A*

To evaluate the impact of *hop1-S298A* and *hop1-T318A* on meiotic progression, synchronous meiotic cultures of the two mutants were obtained and the kinetics of meiotic progression was assessed (Sections 2.3.7 and 2.6.1).

The results show no statistically significant difference in meiotic progression between WT and either phosphomutant (Figure 5.1). The current observation is expected given the lack of impact of $hop1^{SCD}$ on meiotic progression (Carballo et al., 2008).

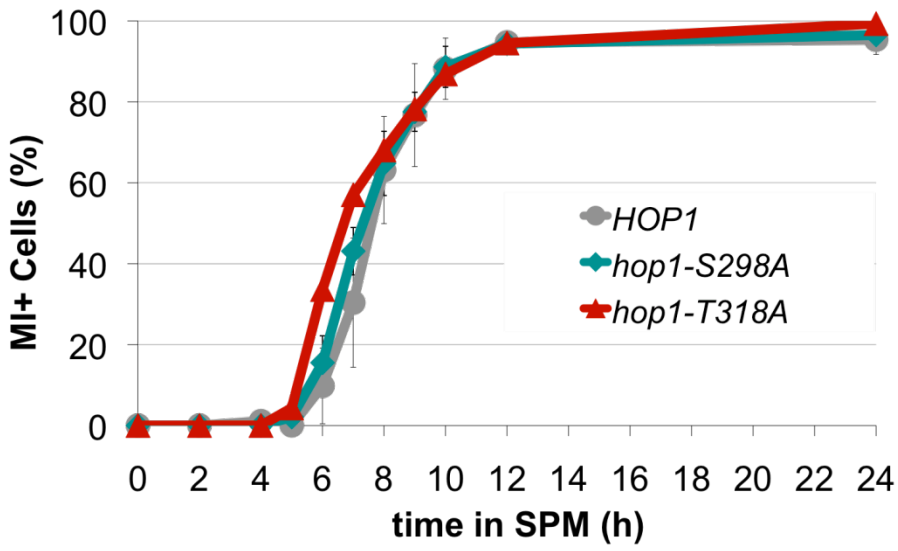

Figure 5.1 Meiotic progression of *hop1* phosphomutants at 23ºC

Homozygous diploids of indicated genotypes were taken through synchronous meiosis at 23ºC. Samples were collected at various time points for DAPI staining. The fraction of MI+ cells corresponds to the ratio of cells with 2-4 DAPI staining bodies to the total number of cells scored (over 200 cells per sample). Error bars represent the standard deviation from the mean.

5.2.2. Validation of phospho-specific antibodies for cytology

To achieve a more direct assessment of Hop1 phosphorylation at serine 298 and threonine 318, phospho-specific antibodies were generated against each phospho-peptide (Section 2.5.4).

The antibody against pS298 (phosphorylated serine 298) was obtained in guinea pig, allowing for simultaneous detection of Hop1 protein (rabbit polyclonal antibody) and phospho-S298. To verify the specificity of α-pS298 antibody, samples were collected at 5h from *HOP1* and *hop1-S298A* synchronous meiotic cultures. The selection of the 5h time point was based on the observation that it corresponds to maximal levels of Hop1 at chromosomes (e.g., Figures 5.3 and 5.4). Meiotic nuclear spreads were prepared and immunostained using α-Hop1 and α-pS298 antibodies. As shown in Figure 5.2, wild-type cells are positive for α-pS298 antibody, while *hop1-S298A* cells show no staining, confirming the antibody's specificity.

A similar approach was taken to verify the specificity of α-pT318 antibody. However, this antibody has been generated in rabbit, similarly to α-Hop1 antibody, thus not allowing for comparison of phospho-specific antibody with whole Hop1 staining as above. In the current case, cells from *HOP1* and *hop1-T318A* cultures, obtained as in the previous experiment, were stained using α-pS298 and α-pT318 antibodies. As expected, signals of both antibodies are observed in WT, while no α-pT318 staining is detected in *hop1-T318A* (Figure 5.2).

These observations demonstrate that both antibodies are specific for the phosphorylated residue they are intended to detect and therefore suitable for detection of specific Mec1/Tel1 phosphorylation events.

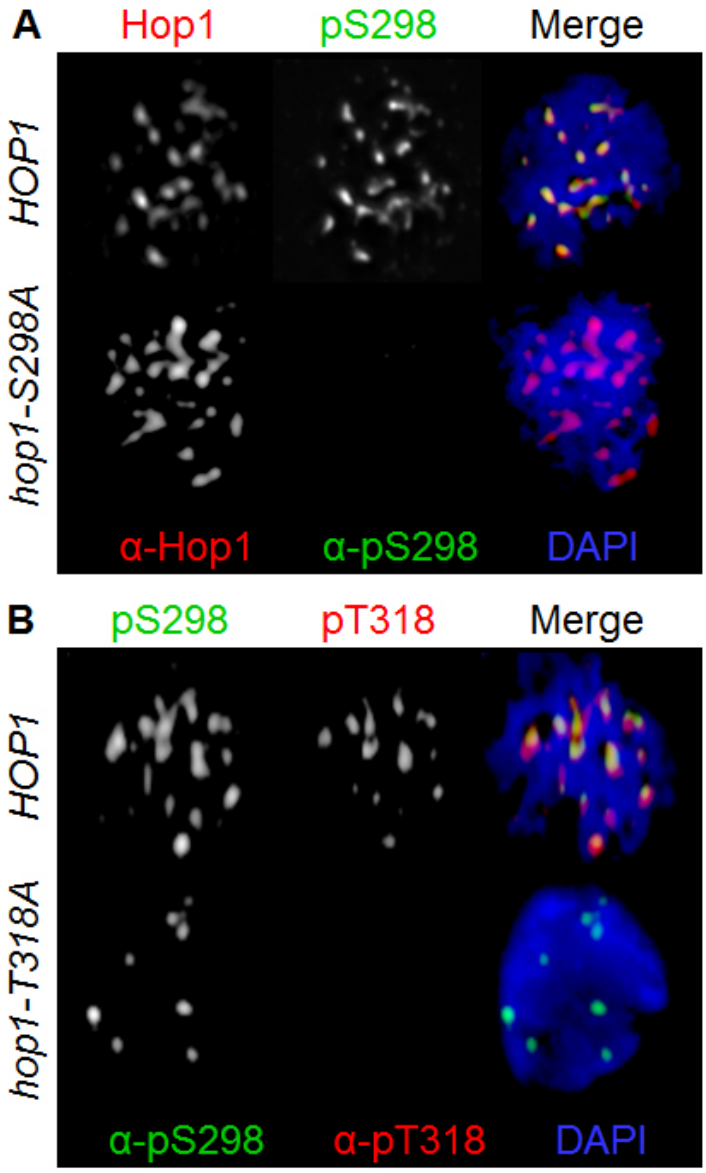

Figure 5.2 Validation of phospho-specific antibodies

Synchronous meiotic cultures of homozygous diploids from indicated genotypes were obtained and samples were collected 5h into meiosis at 23ºC. Meiotic nuclear spreads were prepared and immunostained with α-Hop1 and α-pS298 antibodies **(A)** or α-pS298 and α-pT318 antibodies **(B)**.

5.2.3. Hop1 recruitment to chromosomes is comparable in wild-type and *hop1* phosphomutants

In order to determine whether Hop1^{S298A} and Hop1^{T318A} mutant proteins are efficiently recruited to chromosomes, meiotic spreads were prepared at different time points of synchronous meiotic cultures of *HOP1*, *hop1-S298A* and *hop1-T318A* in *MEK1-3HA* background. The spreads were immunostained using a polyclonal anti-Hop1 antibody and a monoclonal anti-HA antibody (Section 5.2.4) and appropriate secondary antibodies (Section 2.6.2). DNA was stained using DAPI. Analysis of these spreads was then carried out in at least 100 cells per sample.

To investigate the extent of Hop1 recruitment, cells were categorised according to the number of Hop1 foci/patches per cell in the following manner:

(i) Between 10 and 20 signals;
(ii) More than 20 signals.

The fraction of cells in each category was calculated by dividing the number of cells in each category by the total number of cells stained with DAPI. Cells containing less than 10 foci/patches were difficult to distinguish as real signal and thus not included in the analysis.

The results (Figures 5.3 and 5.4A, panel i) failed to show an obvious difference between the total cells stained with α-Hop1 antibody in wild-type and mutant cells. In *hop1-T318A*, however, removal of Hop1 from chromosomes appears to be faster than in *HOP1* or *hop1-S298A* strains. For example, at 5h into meiosis, 80.2% of cells stain for Hop1 in *HOP1* and *hop1-S298A* and 62.8% in *hop1-T318A* (Figure 5.4A, panel i).

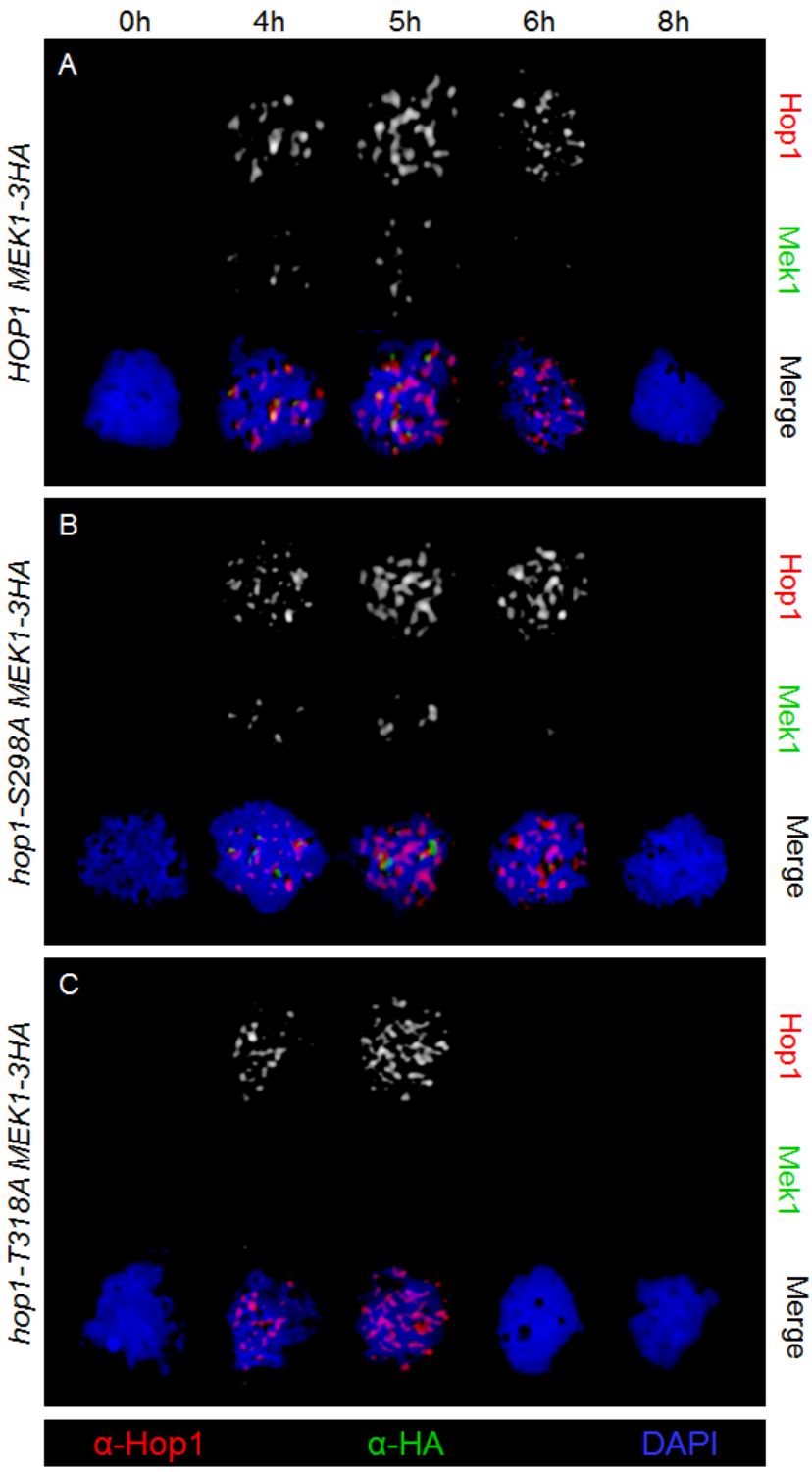

Figure 5.3 Hop1 and Mek1 recruitment to chromosomes in *hop1* phosphomutants

Homozygous diploids of indicated genotypes were taken through synchronous meiosis at 23ºC. Samples were collected at indicated time points for further analysis. Meiotic nuclear spreads for *HOP1* **(A)**, *hop1-S298A* **(B)** and *hop1-T318A* **(C)** strains in *MEK1-3HA* background were immunostained with α-Hop1 and α-HA (Mek1-3HA) antibodies.

Figure 5.4 Impact of *hop1* phosphomutants on Hop1 loading/ phosphorylation and Mek1 recruitment

Homozygous diploids of indicated genotypes were taken through synchronous meiosis at 23ºC. Samples were collected at indicated time points. Meiotic nuclear spreads for *HOP1*, *hop1-S298A* and *hop1-T318A* strains in *MEK1-3HA* background were immunostained with α-Hop1, α-pS298, α-pT318 and α-HA (Mek1-3HA) antibodies. The fraction of cells where ten or more signals of each antibody were detected is plotted for each antibody **(A)** or genotype **(B)**. Over 100 cells were scored per sample. Error bars represent high and low intervals of 95% confidence assuming a binomial distribution.

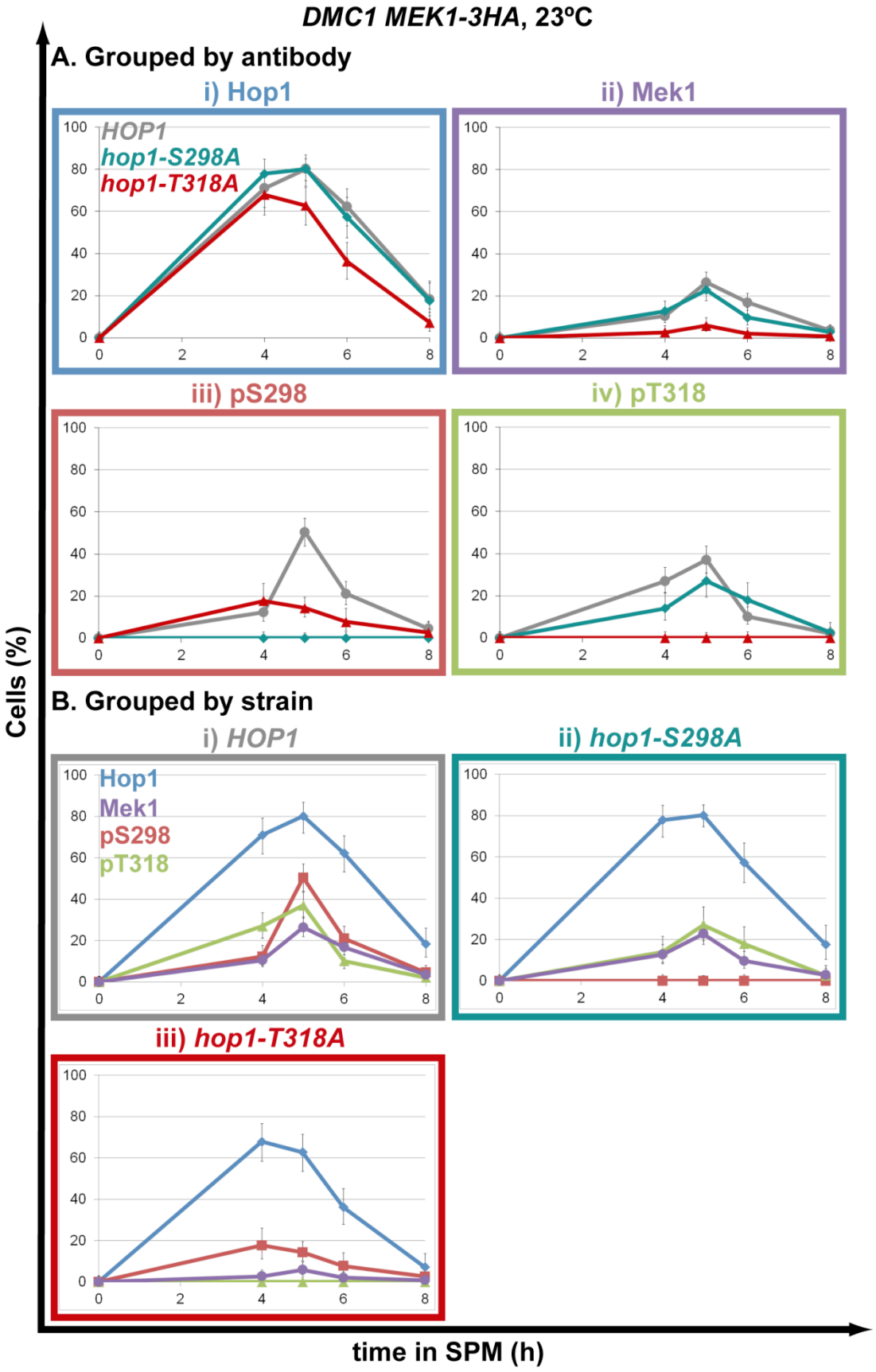
DMC1 MEK1-3HA, 23ºC
A. Grouped by antibody
i) Hop1
ii) Mek1
iii) pS298
iv) pT318
HOP1
hop1-S298A
hop1-T318A
B. Grouped by strain
i) HOP1
ii) hop1-S298A
iii) hop1-T318A
Hop1
Mek1
pS298
pT318
Cells (%)
time in SPM (h)

5.2.4. Mek1 recruitment is compromised specifically in *hop1-T318A*

Previous results have shown that in Mec1/Tel1 phosphorylation of Hop1 is required for the chromosomal recruitment of Mek1 (Carballo et al., 2008). Therefore, it was relevant to determine whether *hop1-S298A* and *hop1-T318A* mutants are proficient in Mek1 recruitment.

The same set of spreads analysed for Hop1 localisation (Section 5.2.3) was analysed for efficiency in Mek1 recruitment. A primary anti-HA antibody was used as all the strains were obtained in a *MEK1-3HA* background. Upon staining with the appropriate secondary antibody (Section 2.6.2), cells were categorised as described for Hop1 loading analysis (Section 5.2.3).

Results show that the levels of Mek1 are similar in WT and *hop1-S298A* (Figures 5.3 and 5.4A, panel ii). The kinetics of Mek1 recruitment and removal from chromosomes are also comparable in these strains. The levels of Mek1 are reduced in *hop1-T318A*, with few cells showing significant Mek1 staining, suggesting that phosphorylation at threonine residue 318 of Hop1 is required for efficient Mek1 recruitment.

5.2.5. Hop1-Mek1 co-localisation is reduced in both phosphomutants

Mek1 interacts with both Red1 and Hop1 at chromosomes and the interaction with the latter is required for its functions in IH bias and checkpoint (Niu et al., 2005). To address how phosphorylation of S298 and T318 of Hop1 affects Hop1-Mek1 interaction, co-localisation between the two proteins in *HOP1*, *hop1-S298A* and *hop1-T318A* strains in *MEK1-3HA* background was examined. For this, the same set of spreads examined for Hop1 and Mek1 localisation were used (Sections 5.2.3 and 5.2.4). The categories defined for co-localisation analysis were:

(i) Minimal, where little or no overlap between Hop1 and Mek1 is observed (Figure 5.5, panel i);

(ii) Partial, where there is some overlap between Hop1 and Mek1 (Figure 5.5, panel ii);

(iii) Significant, where major overlap between Hop1 and Mek1 is detected (Figure 5.5, panel iii).

The fraction of cells in each category was determined as before (Section 5.2.3).

In wild-type, most Mek1 signals are associated with Hop1 (Figure 5.3A). However, in *hop1-S298A*, despite similar levels to *HOP1* of each of the proteins (Figure 5.4A, panels i and ii), co-localisation is reduced (Figure 5.6A, panel i). In *hop1-T318A*, where few foci of Mek1 are detected (Figures 5.3C and 5.4A, panel ii), the co-localisation with Hop1 is minimal as well (Figure 5.6A, panel i).

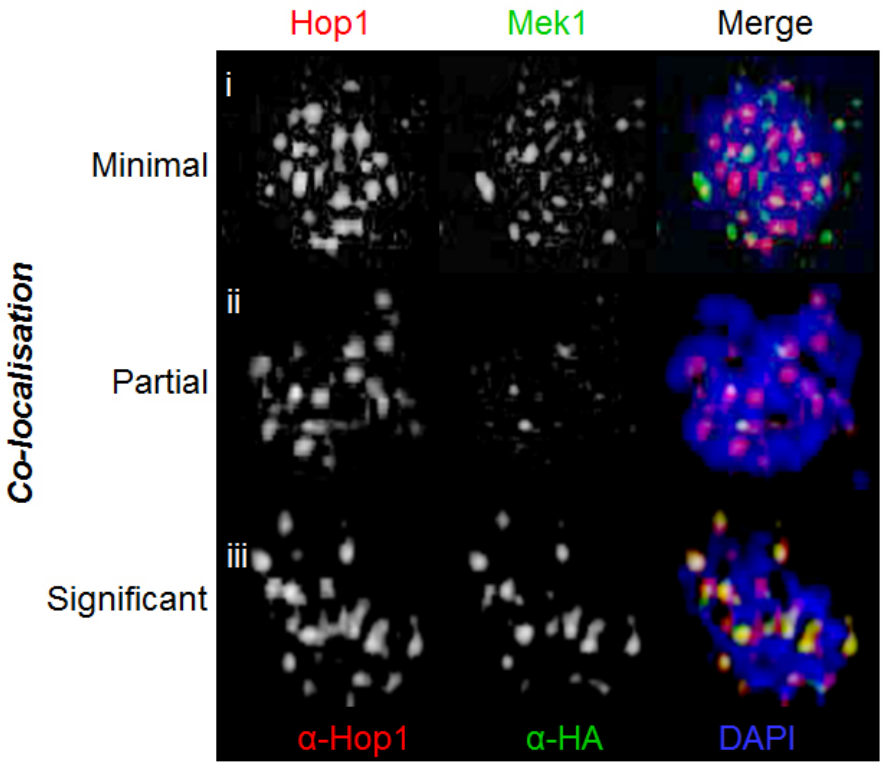

Figure 5.5 Categories defined for analysis of co-localisation between Hop1 and Mek1

Nuclear spreads were prepared from synchronous meiotic cultures and stained with DAPI and the antibodies against the two proteins for which co-localisation was to be analysed (e.g., Hop1 and Mek1). Photographs were taken of the microscope images obtained in each channel and superimposed. Each cell was classified in one of the following categories:

- **(i)** Minimal, where little or no overlap of signals between the two antibodies is observed;
- **(ii)** Partial, where there is some overlap of signals between the two antibodies;
- **(iii)** Significant, where major overlap of signals between the two antibodies is detected.

Figure 5.6 Impact of *hop1* phosphomutants on Hop1-Mek1 co-localisation

Homozygous diploids of indicated genotypes were taken through synchronous meiosis at 23ºC. Samples were collected at indicated time points for further analysis. Meiotic nuclear spreads for *HOP1*, *hop1-S298A* and *hop1-T318A* strains in *MEK1-3HA* background were immunostained with α-Hop1, α-pS298, α-pT318 and α-HA (Mek1-3HA) antibodies. The fraction of cells where partial or significant co-localisation of each antibody pair (e.g., Figure 5.5) was observed was determined and plotted for each combination of antibodies **(A)** or genotype **(B)**. Over 100 cells were analysed per sample. Error bars represent high and low intervals of 95% confidence assuming a binomial distribution.

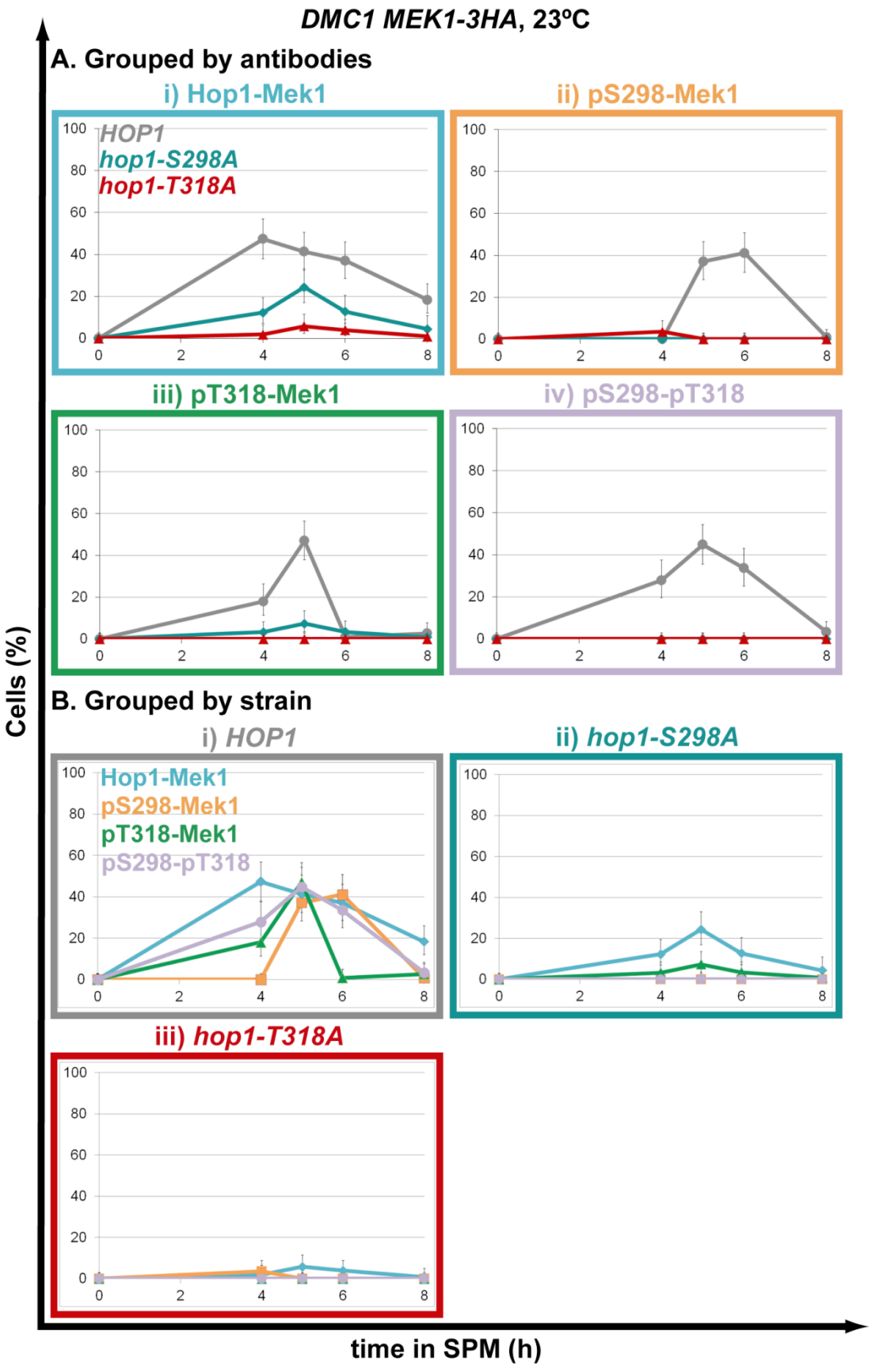
DMC1 MEK1-3HA, 23ºC
A. Grouped by antibodies
i) Hop1-Mek1
ii) pS298-Mek1
iii) pT318-Mek1
iv) pS298-pT318
HOP1
hop1-S298A
hop1-T318A
B. Grouped by strain
i) HOP1
ii) hop1-S298A
iii) hop1-T318A
Hop1-Mek1
pS298-Mek1
pT318-Mek1
pS298-pT318
Cells (%)
time in SPM (h)

5.2.6. Presence of Mek1 at the chromosomes correlates with the status of Hop1 phosphorylation

Next, the impact of Hop1 phosphorylation on Mek1 recruitment to chromosomes was examined. Samples from synchronous meiotic cultures of *HOP1*, *hop1-S298A* and *hop1-T318A* strains in *MEK1-3HA* background were collected at various time points and meiotic nuclear spreads were prepared. These spreads were then immunostained with either of the phospho-specific antibodies and α-HA antibody (Figure 5.6) and analysed as described above (Sections 5.2.3 and 5.2.5; Figure 5.5).

Results show that in *HOP1*, the highest level of Mek1 at chromosomes is detected at 5h, when the greatest number of signals from α-pS298 and α-pT318 antibodies is also observed (Figure 5.4B, panel i). Notably, co-localisation between α-pT318 and α-HA antibodies (Mek1-3HA) appears to be maximal at 5h, while that between α-pS298 and α-HA antibodies remains at its highest between 5 and 6h (Figure 5.6B, panel i).

In *hop1-S298A*, Mek1 recruitment correlates with phosphorylation at threonine 318, with a comparable number of signals of α-HA (Mek1-3HA) and α-pT318 antibodies observed at all the time points studied (e.g., 27.0% of cells staining for α-pT318 and 22.8% for α-HA at 5h; Figure 5.4B, panel ii). In *hop1-T318A*, while 17.7% of the cells show more than 10 signals of α-pS298 antibody at 4h, only 2.8% stain for α-HA antibody (Figure 5.4B, panel iii). This is consistent with the notion that phosphorylation of threonine residue 318 of Hop1 is essential for Mek1 recruitment to chromosomes (Section 5.2.4).

Notably, phosphorylation at S298 is reduced in *hop1-T318A*, with 50.4% of *HOP1* cells staining with α-pS298 antibody at 5h, compared to 14.3% in *hop1-T318A* (Figure 5.4A, panel iii). A milder reduction in phosphorylation at T318 is observed in *hop1-S298A*, with 37.0% of *HOP1* and 27.0% of *hop1-S298A* cells staining with α-pT318 at 5h (Figure 5.4A, panel iv). These observations suggest that Hop1-T318 phosphorylation may affect phosphorylation at S298.

5.2.7. Synaptonemal complex formation is compromised in *hop1-S298A*

hop1-S298A shows Mek1 recruitment that is comparable to *HOP1*, but reduced Hop1-Mek1 co-localisation. This suggests that Mek1 presence at

chromosomes is more transient in this mutant. Given that Mek1 is required for the formation of mature SCs (Rockmill and Roeder, 1991), it was decided to examine the status of SC formation in *hop1-S298A*. For this, nuclear spreads were prepared (Section 2.6.2) from 5 and 7h samples of *HOP1* and *hop1-S298A* strains undergoing synchronous meiosis. Zip1 was detected using a polyclonal anti-Zip1 antibody and DNA stained using DAPI. The spreads were then analysed and each cell was classified according to the status of SC polymerisation into one of the following categories:

(i) Minimal: most Zip1 signals appear as foci (Figure 5.7A, panel i);
(ii) Partial: Zip1 signals appear as a mixture of foci and lines (Figure 5.7A, panel ii);
(iii) Extensive: most Zip1 signals appear as lines (Figure 5.7A, panel iii);
(iv) Polycomplex (PC): Zip1 forms unstructured aggregates (Figure 5.7A, panel iv).

Total cells staining for Zip1 (Total Zip1) were calculated as a sum of the cells classified in (i-iv) and all categories were expressed as a fraction of total DAPI stained cells (at least 60 nuclei scored per sample; Figure 5.7B and C).

Overall, the total number of cells showing Zip1 staining (Total Zip1) and the fraction of PCs in WT and *hop1-S298A* were comparable at 5 and 7 hours (Figure 5.7B and C). However, a notable difference is observed in the fraction of cells exhibiting extensive Zip1 polymerisation at 5h: whilst 39.1% of *HOP1* cells form a complete SC by this time, only 3.5% of *hop1-S298A* cells do so. The fraction of cells showing minimal SC polymerisation is increased at this time point from 15.6% in *HOP1* to 41.5% in *hop1-S298A* (Figure 5.7B).

Similarly, 8.3% of *HOP1* and 18.7% of *hop1-S298A* cells show minimal SC polymerisation 7h into meiosis induction. The fraction of cells where extensive polymerisation of Zip1 is observed is also reduced in *hop1-S298A* at this time point (7.3% in *hop1-S298A* and 21.7% in *HOP1*) (Figure 5.7C). Taken together, these observations suggest that SC polymerisation is compromised in *hop1-S298A*.

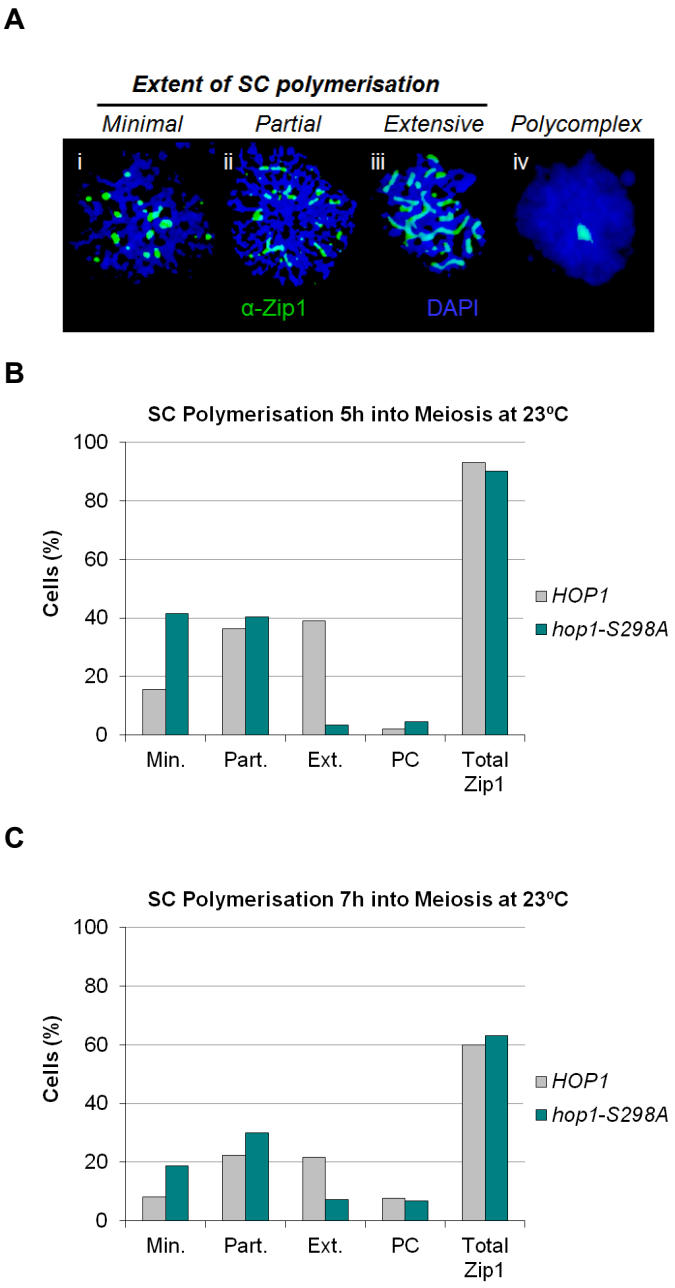

Figure 5.7 Extent of SC polymerisation in *HOP1* and *hop1-S298A*

Homozygous diploids of indicated genotypes were taken through synchronous meiosis at 23ºC (YPA method; Section 2.3.7). Nuclear spreads were prepared from samples collected at 5 **(B)** and 7h **(C)** into meiosis and immunostained with α-Zip1 antibody. At least 60 cells per sample were classified into four categories of SC polymerisation (panel **A**):

(i) Minimal: most Zip1 signals appear as foci;
(ii) Partial: Zip1 signals appear as a mixture of foci and lines;
(iii) Extensive: most Zip1 signals appear as lines;
(iv) Polycomplex (PC): Zip1 forms unstructured aggregates.

5.2.8. Hop1 levels and the extent of phosphorylation in *hop1-S298A* and *hop1-T318A*

Western blot analysis of Hop1, Hop1^{S298A} and Hop1^{T318A} during synchronous meiosis at 23ºC was then used to assess Hop1 levels and phosphorylation status in *HOP1*, *hop1-S298A* and *hop1-T318A*. Samples were collected at various time points during a synchronous meiotic time course and Western blot analysis was performed using α-Hop1, α-pS298 and α-pT318 antibodies (Figure 5.8).

No major differences can be detected between protein levels in WT and the mutants. When α-Hop1 antibody is used, the shift corresponding to slow migrating phosphorylated Hop1 (P-Hop1) can be observed in *HOP1* as well as *hop1-S298A* and *hop1-T318A* strains, indicating that eliminating phosphorylation at one of the two residues does not significantly impair other phosphorylation events in Hop1 (Figure 5.8). It appears, however, that in WT cells slow-migrating bands are stronger than in either mutant, which could be due to the absence of phosphorylation at S298 or T318 in the respective phosphomutants.

The steady-state levels of Hop1 and its phosphorylation occur with comparable kinetics in *HOP1* and *hop1-S298A* (Figure 5.8). The protein is detectable by 2h and exhibits significant phosphorylation between 4 and 6h into meiosis. At 8h P-Hop1 is significantly reduced and lower levels of Hop1 are detected at 10h. In both strains, the protein is no longer detected at 12h.

In *hop1-T318A*, although Hop1 is also first detected at 2h, its maximum phosphorylation is only detected from 4 to 5h. Most P-Hop1 forms are no longer detected at 6h. Some protein is still detected at 10h, but no longer at 12h. This suggests that although Hop1 production may occur with similar kinetics to WT, phosphorylation events might be more transient in this mutant (Figure 5.8). This result is consistent with the observations from immunocytology experiments, where turnover of Hop1 at chromosomes appears to be faster in *hop1-T318A* than in *HOP1* or *hop1-S298A* (Section 5.2.3).

Detection of phosphorylation of S298 and T318 using the phospho-specific antibodies α-pS298 and α-pT318 confirms that they are specific for the residue intended (no bands are detected in *hop1-S298A* using α-pS298 or in *hop1-T318A* using α-pT318). In WT both phosphorylations are detected at the times corresponding to maximum overall phosphorylation (Figure 5.8).

Reduced levels of S298 phosphorylation can be detected in *hop1-T318A* and some T318 phosphorylation is observed in *hop1-S298A*. In both cases, the signals were considerably lower than in WT (Figure 5.8). Notably, this contrasts with the cytology results previously described (Section 5.2.6), where phosphorylation at threonine 318 appears to be only slightly reduced in *hop1-S298A* cells. It is possible that difference in immunocytology and Western blot data may stem from the different sensitivities of the antibody when used in each technique.

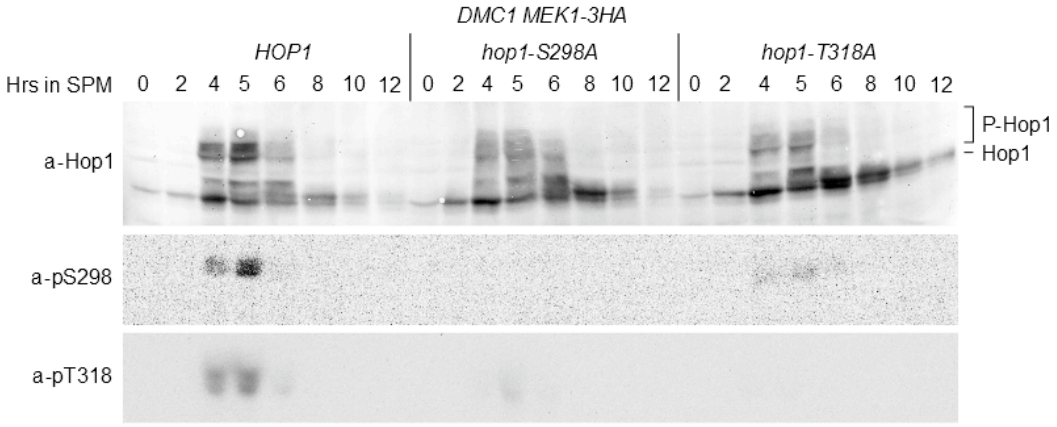

Figure 5.8 Hop1 phosphorylation in *hop1* phosphomutants

Homozygous diploids of indicated genotypes were taken through synchronous meiosis at 23ºC. Samples were collected at indicated time points for further analysis. Crude protein extracts were prepared using the TCA method and run on a 10% polyacrylamide gel. Following blotting onto a nitrocellulose membrane, this was probed with α-Hop1, α-pS298 and α-pT318 antibodies.

5.2.9. Mek1 levels and phosphorylation in *hop1-S298A* and *hop1-T318A*

Mek1 recruitment/co-localisation with Hop1 is affected in both *hop1* phosphomutants (Sections 5.2.4 and 5.2.5). Next, the extent of Mek1 phosphorylation was assessed in *HOP1*, *hop1-S298A* and *hop1-T318A* in a *MEK1-3HA* background by Western blot using a monoclonal anti-HA antibody.

The results obtained indicate that Mek1-3HA levels in the three cultures are similar (Figure 5.9). Mek1 phosphorylation is detected in *HOP1* and *hop1-S298A* strains. It appears that the mobility shift detected at 4h in *HOP1* may be higher than in *hop1-S298A*. This could be due to a delay in Mek1 phosphorylation or partial phosphorylation of Mek1 in *hop1-S298A*. In *hop1-T318A*, no Mek1 phosphorylation is observed. This suggests that phosphorylation at threonine 318, but not at serine 298, of Hop1 is required for Mek1 activation.

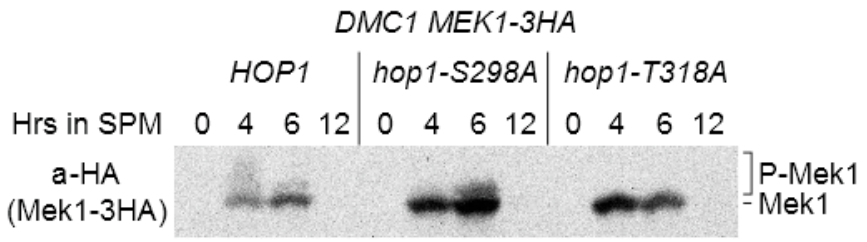

Figure 5.9 Mek1 phosphorylation in *hop1* phosphomutants

Homozygous diploids of indicated genotypes were taken through synchronous meiosis at 23ºC. Samples were collected at indicated time points for further analysis. Crude protein extracts were prepared using the TCA method and run on a 7.5% polyacrylamide gel containing 4 µM Phos-tag. Following blotting onto a PVDF membrane, this was probed with α-HA (Mek1-3HA) antibody.

5.3. Discussion

5.3.1. Impact of Hop1 phosphorylation on Mek1 recruitment and activation

Chromosomal levels of Mek1 are comparable in *HOP1* and *hop1-S298A*, but reduced in *hop1-T318A* (Figure 5.4A, panel ii). This suggests that Hop1-T318 phosphorylation is essential for Mek1 recruitment to chromosomes. Co-localisation between Hop1 and Mek1 is compromised in *hop1-S298A* (Figure 5.6A, panel i), suggesting that phosphorylation at serine residue 298 of Hop1 is required for enhancement or stabilisation of Hop1-Mek1 interaction.

The *hop1-S298A* allele confers a defect in the formation of mature SCs (Figure 5.7). This could be a downstream effect of more transient interactions between Hop1 and Mek1 in *hop1-S298A*, as it has been reported that deletion of *MEK1* leads to the formation of shorter SCs (Rockmill and Roeder, 1991).

Mek1 phosphorylation can be detected in *hop1-S298A*, but is absent in *hop1-T318A* (Figure 5.9). Activation of Mek1 requires its recruitment to chromosomes through interaction with the complex formed by Red1 and Hop1 (Bailis and Roeder, 1998, Wan et al., 2004). Given that this interaction is disrupted in *hop1-T318A*, no phosphorylation of Mek1 is observed in this mutant. In *hop1-S298A*, Mek1 activation occurs and is sufficient for ensuring IH recombination at low temperature.

These observations suggest that phosphorylation at threonine residue 318 of Hop1 ensures recruitment and activation of Mek1, while phosphorylation of Hop1 at serine residue 298 stabilises Hop1-Mek1 interaction. The latter becomes important when other alleles that compromise IH recombination are present (e.g., *dmc1*Δ, *hed1*Δ) or when higher temperatures further disrupt protein-protein interactions.

Chapter 6: Impact of Hop1 phosphorylation on Mek1 activation

6.1. Introduction

Mec1/Tel1 phosphorylation of Hop1 is required for preventing *DMC1*-independent repair of DSBs (Carballo et al., 2008). *hop1*^{SCD} mutants do not arrest in a *dmc1*Δ background due to the deficient recruitment and activation of Mek1. Similarly, *hop1-S298A* strains do not arrest in *dmc1*Δ, repairing DSBs in a *DMC1*-independent manner (Figure 4.2). However, most spores produced by *hop1-S298A* are viable at lower temperature (approximately 96% spore viability at 18 and 23ºC; Figure 3.1), suggesting that IH bias is not abolished in this mutant. Furthermore, phosphorylation of Mek1 occurs in *hop1-S298A* (Figure 5.9). This raises the possibility that phosphorylation at serine residue 298 of Hop1 is essential during challenged meiosis but dispensable in unchallenged meiosis.

In contrast, *hop1-T318A*, like *hop1*^{SCD}, shows consistently low spore viability (≤3.8%; Figure 3.1A) and defects in Mek1 recruitment and activation (Figures 5.4 and 5.9), consistent with the notion that phosphorylation at threonine residue 318 of Hop1 is essential for Hop1 function.

hop1-S298A and *hop1-T318A* meiosis in a *dmc1*Δ background was characterised and contrasted at 23ºC in order to determine why *hop1-S298A* is deficient in *dmc1*Δ arrest, despite the fact that phosphorylation at S298 appears to be dispensable for the generation of viable spores at this temperature.

6.2. Results

6.2.1. Meiotic divisions in *dmc1Δ*

First, meiotic progression in *HOP1*, *hop1-S298A* and *hop1-T318A* strains in a *dmc1*Δ *MEK1-3HA* background was assessed. For this, synchronous meiotic cultures were obtained and samples collected at various time points up to 24h after meiosis induction. Meiotic progression was determined by DAPI scoring as described above (Sections 2.3.7 and 2.6.1).

As expected in the context of *dmc1*Δ, *HOP1* strains undergo a strong arrest due to the presence of hyperresected DSBs (~5% of MI+ cells 24h after meiosis induction). In contrast, over 90% of cells in both *hop1* phosphomutants have gone through meiosis at 24h (Figure 6.1). However, kinetics of meiotic divisions in these mutants is different. While in *DMC1* background, *hop1-S298A* and *hop1-T318A* went through meiosis with similar kinetics (Figure 5.1), in *dmc1*Δ background, meiotic divisions occur later in *hop1-S298A* than in *hop1-T318A* (Figure 6.1). Approximately 50% of *hop1-T318A* cells have undergone at least one meiotic division (MI+) at 6h. In *hop1-S298A* the fraction of MI+ cells reaches 50% approximately 9h after meiosis induction.

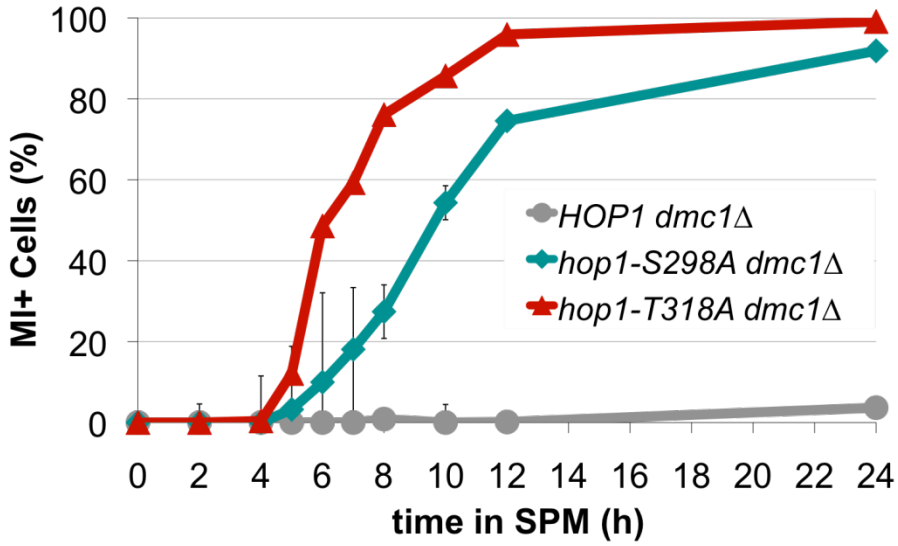

Figure 6.1 Meiotic progression of *hop1* phosphomutants in *dmc1*Δ background at 23ºC

Homozygous diploids of indicated genotypes were taken through synchronous meiosis at 23ºC. Samples were collected at indicated time points for DAPI staining. The fraction of MI+ cells corresponds to the ratio of cells with 2-4 DAPI staining bodies to the total number of cells scored (over 200 cells per sample). Error bars represent the standard deviation from the mean.

6.2.2. Hop1 recruitment to chromosomes in *dmc1Δ* background

The recruitment of Hop1 WT and mutant proteins was assessed in *dmc1*Δ background as before in *DMC1* background (Section 5.2.3). Meiotic nuclear spreads were prepared from synchronous cultures of *HOP1*, *hop1-S298A* and *hop1-T318A* in *dmc1*Δ *MEK1-3HA* background. These spreads were immunostained using α-Hop1 and α-HA antibodies as described above (Section 2.6.2) and classified in terms of number of antibody signals detected per cell.

As shown before (Carballo et al., 2008), Hop1 accumulates at the chromosomes in *HOP1 dmc1*Δ due to the activation of checkpoint (Figures 6.2 and 6.3A, panel i). Unlike in *HOP1* strains, in both phosphomutants the protein is absent from the majority of cells by 8h after meiosis induction. The removal of Hop1 from chromosomes is faster in *hop1-T318A* than in *hop1-S298A*, consistent with the quicker progression through meiotic divisions in the first (Figure 6.1).

Chromosomal levels of Hop1 are greatest at 4h into meiosis in *hop1-T318A dmc1*Δ, with significant levels of Hop1 being detected in 82.9% of cells. The fraction of cells staining for Hop1 in this mutant is reduced to 44.7% at 5h. In *hop1-S298A dmc1*Δ, maximal levels of Hop1 are detected an hour later than in *hop1-T318A dmc1*Δ, 5h into meiosis, with 73.3% of cells staining for α-Hop1 antibody. The chromosomal levels of the protein then decrease more gradually than in *hop1-T318A dmc1*Δ, with significant levels of Hop1 still being detected in 36.8% of *hop1-S298A dmc1*Δ cells at the 8h time point (in contrast to 7.5% of cells in *hop1-T318A dmc1*Δ). Notably, the maximal level of Hop1 loading in the three strains is comparable at approximately 80%, although occurring at different times into meiosis (8h in *HOP1 dmc1*Δ, 5h in *hop1-S298A dmc1*Δ and 4h in *hop1-T318A dmc1*Δ) (Figure 6.3A, panel i).

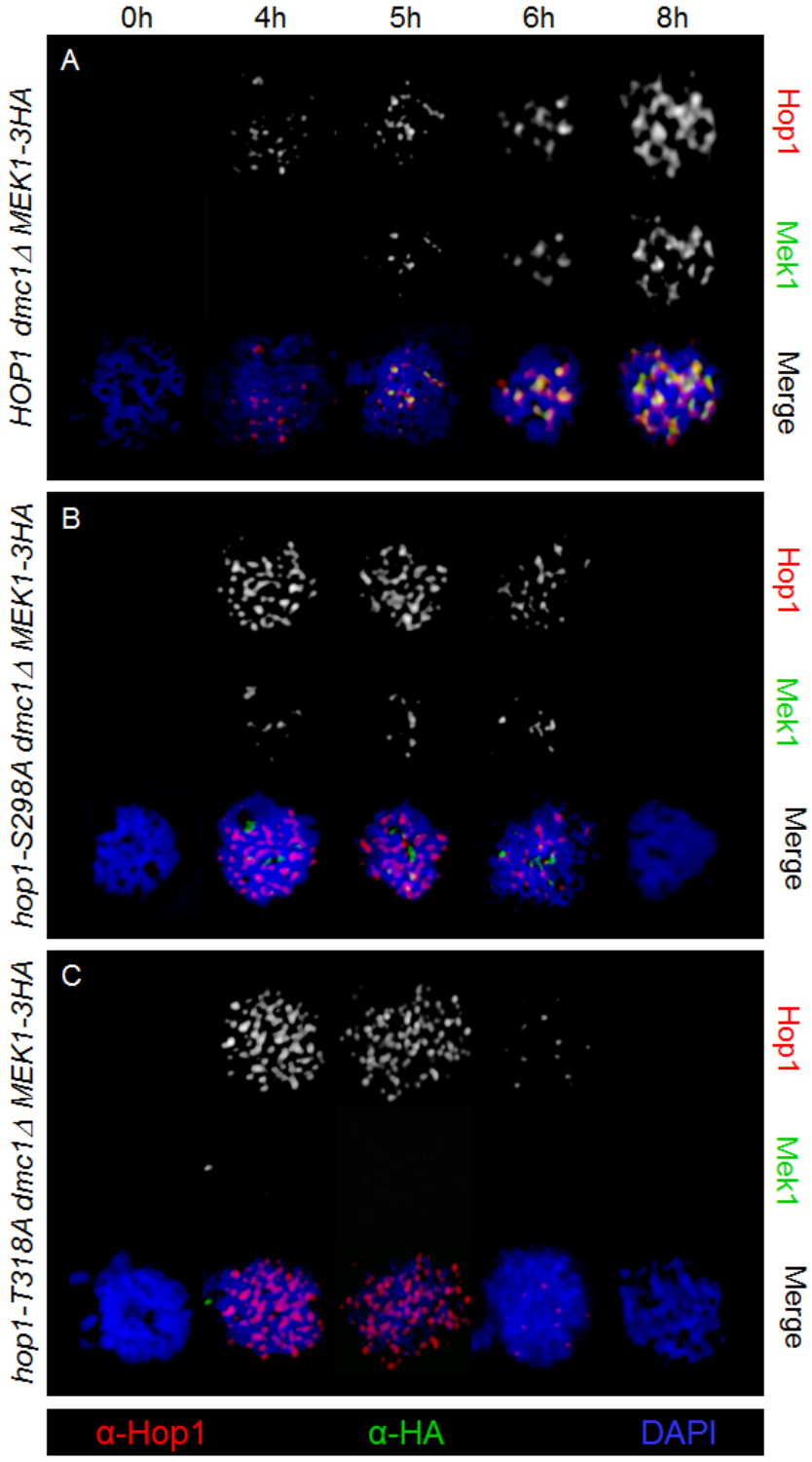

Figure 6.2 Hop1 and Mek1 recruitment to chromosomes in *hop1* phosphomutants in *dmc1*Δ background

Homozygous diploids of indicated genotypes were taken through synchronous meiosis at 23ºC. Samples were collected at indicated time points for further analysis. Meiotic nuclear spreads for *HOP1* **(A)**, *hop1-S298A* **(B)** and *hop1-T318A* **(C)** strains in *dmc1*Δ *MEK1-3HA* background were immunostained with α-Hop1 and α-HA (Mek1-3HA) antibodies.

Figure 6.3 Impact of *hop1* phosphomutants on Hop1 loading, phosphorylation and Mek1 recruitment in *dmc1*Δ background

Homozygous diploids of indicated genotypes were taken through synchronous meiosis at 23ºC. Samples were collected at indicated time points. Meiotic nuclear spreads for *HOP1*, *hop1-S298A* and *hop1-T318A* strains in *dmc1*Δ *MEK1-3HA* background were immunostained with α-Hop1, α-pS298, α-pT318 and α-HA (Mek1-3HA) antibodies. The fraction of cells where ten or more signals of each antibody were detected is plotted for each antibody **(A)** or genotype **(B)**. Over 100 cells were scored per sample. Error bars represent high and low intervals of 95% confidence assuming a binomial distribution.

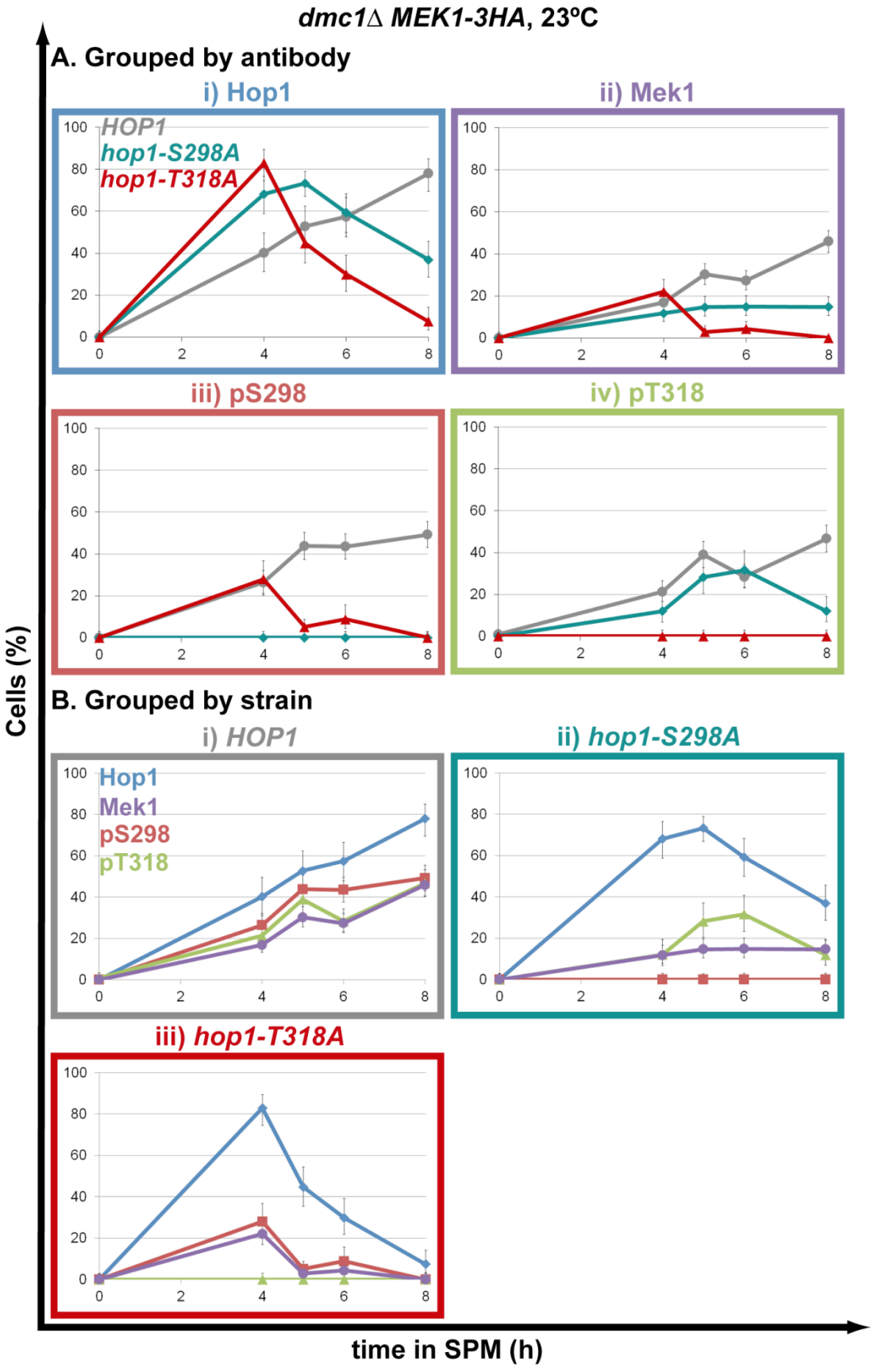
dmc1Δ MEK1-3HA, 23ºC
A. Grouped by antibody
i) Hop1
ii) Mek1
iii) pS298
iv) pT318
HOP1
hop1-S298A
hop1-T318A
B. Grouped by strain
i) HOP1
ii) hop1-S298A
iii) hop1-T318A
Hop1
Mek1
pS298
pT318
Cells (%)
time in SPM (h)

6.2.3. Mek1 recruitment in *dmc1Δ*

Next, Mek1 chromosomal recruitment in *HOP1 dmc1*Δ, *hop1-S298A dmc1*Δ and *hop1-T318A dmc1*Δ strains carrying a Mek1-3HA tagged protein was evaluated as in *DMC1* background (Section 5.2.4). The same set of meiotic nuclear spreads used for analysis of Hop1 chromosomal recruitment in *dmc1*Δ background (Section 6.2.2) was used for analysis of Mek1 recruitment.

Like Hop1, Mek1 accumulates at chromosomes in *HOP1 dmc1*Δ, with maximal levels being detected at the last time point for which nuclear spreads were prepared, 8h. In *hop1-S298A dmc1*Δ, Mek1 is seen at chromosomes at levels comparable to those observed in *DMC1* background at 4 and 5h into meiosis (e.g., 22.8% of *hop1-S298A DMC1* cells and 15.0% of *hop1-S298A dmc1*Δ cells stain for Mek1 5h into meiosis; Figure 6.3A, panel ii).

Chromosomal levels of Mek1 appear to remain constant in *hop1-S298A dmc1*Δ from 4 to 8h after meiosis induction, with approximately 15% of cells showing more than ten foci of Mek1 (Figure 6.3A, panel ii). This was not observed in *DMC1* background, where only 2.8% of *hop1-S298A* cells stain for Mek1 at 8h (Figure 5.4A, panel ii). In *hop1-T318A dmc1*Δ, Mek1 recruitment is compromised, with 22.7% of cells recruiting Mek1 at 4h into meiosis, but few cells showing significant number of Mek1 signals at any of the remaining time points (Figures 6.2 and 6.3A, panel ii).

6.2.4. Hop1-Mek1 co-localisation

The impact of *DMC1* deletion in the co-localisation of Hop1 and Mek1 was assessed as in Section 5.2.5 using the set of meiotic nuclear spreads analysed above (Sections 6.2.2 and 6.2.3).

As in *DMC1* background, results show that Hop1 and Mek1 co-localise significantly in *HOP1 dmc1*Δ*,* whilst the interaction between the two proteins is reduced in *hop1-S298A dmc1*Δ and *hop1-T318A dmc1*Δ*.* The highest fraction of cells showing partial or significant co-localisation between Mek1 and Hop1 in *hop1-S298A dmc1*Δ is 23.7% at 6h, compared to 81.4% maximal co-localisation in *HOP1 dmc1*Δ at 8h. In *hop1-T318A dmc1*Δ, Hop1-Mek1 co-localisation is reduced to 14.9% at 5h (Figures 6.2 and 6.4A, panel i).

Figure 6.4 Impact of *hop1* phosphomutants on Hop1-Mek1 co-localisation in *dmc1*Δ background

Homozygous diploids of indicated genotypes were taken through synchronous meiosis at 23ºC. Samples were collected at indicated time points for further analysis. Meiotic nuclear spreads for *HOP1*, *hop1-S298A* and *hop1-T318A* strains in *dmc1*Δ *MEK1-3HA* background were immunostained with α-Hop1, α-pS298, α-pT318 and α-HA (Mek1-3HA) antibodies. The fraction of cells where partial or significant co-localisation of each antibody pair (e.g., Figure 5.5) was observed was determined and plotted for each combination of antibodies **(A)** or genotype **(B)**. Over 100 cells were analysed per sample. Error bars represent high and low intervals of 95% confidence assuming a binomial distribution.

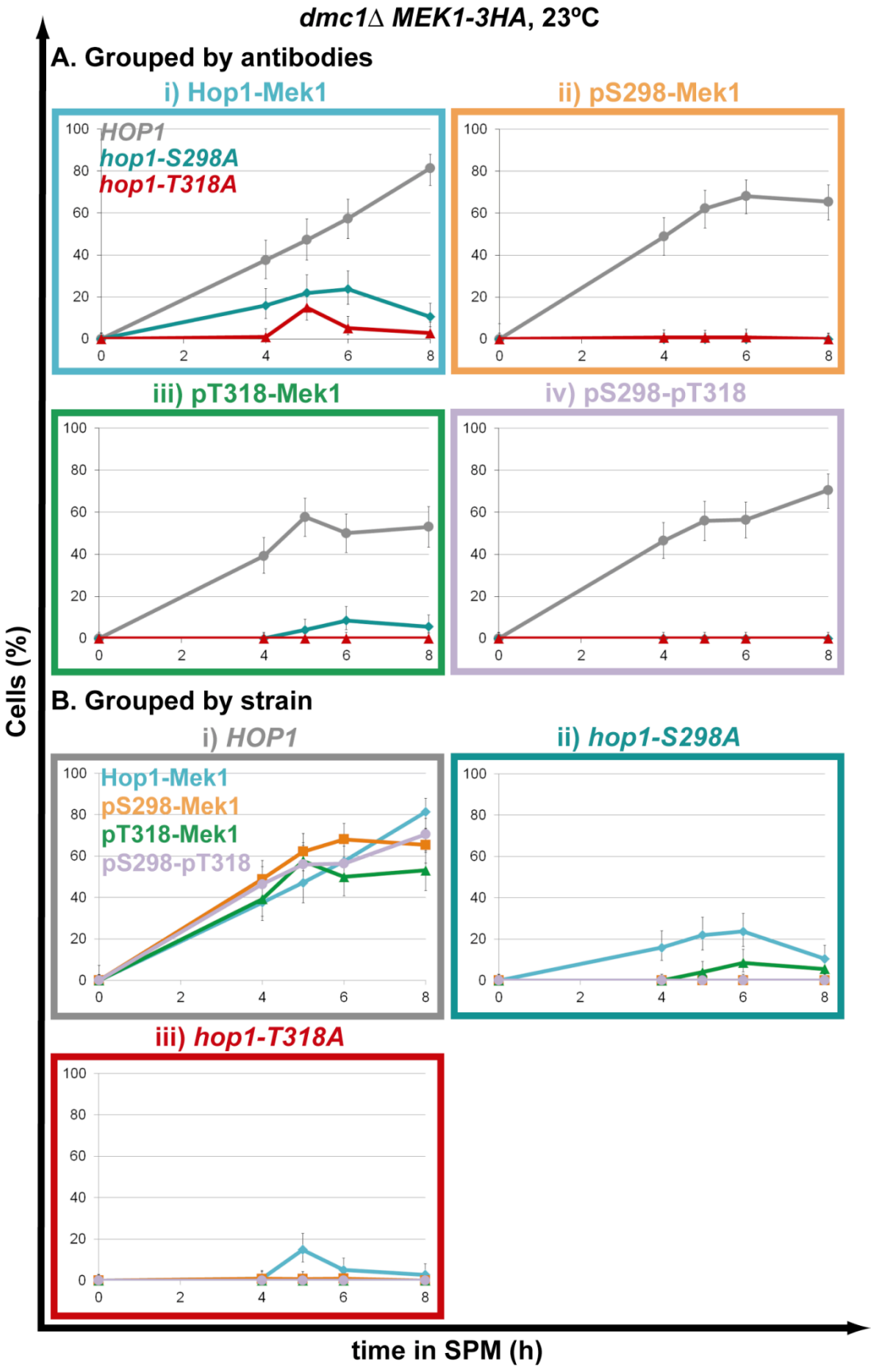
dmc1Δ MEK1-3HA, 23ºC
A. Grouped by antibodies
i) Hop1-Mek1
HOP1
hop1-S298A
hop1-T318A
ii) pS298-Mek1
iii) pT318-Mek1
iv) pS298-pT318
B. Grouped by strain
i) HOP1
Hop1-Mek1
pS298-Mek1
pT318-Mek1
pS298-pT318
ii) hop1-S298A
iii) hop1-T318A
Cells (%)
time in SPM (h)

6.2.5. Cytological analysis of Hop1-S298 and Hop1-T318 phosphorylation in *dmc1Δ*

Using the phospho-specific antibodies described in Section 2.5.4, the phosphorylation of residues S298 or T318 of Hop1 was studied in *HOP1*, *hop1-S298A* and *hop1-T318A* strains in *dmc1*Δ *MEK1-3HA* background. Meiotic nuclear spreads were prepared from synchronous meiotic cultures and immunostained with combinations of α-HA (Mek1-3HA), α-pS298 and α-pT318 antibodies. At least 100 cells per sample were examined as before (Sections 5.2.3 and 5.2.5).

As seen in Figure 6.3B, panel i, appearance of both Hop1 phosphorylations in *HOP1 dmc1*Δ follow Hop1 recruitment profile as expected. In this context, all antibodies are detected at the chromosomes 8h after meiosis induction and their levels are highest at this time point as a result of the arrest triggered by the absence of Dmc1.

In *hop1-S298A dmc1*Δ, α-pT318 signals reach their highest levels at 6h, when they can be detected in 31.6% of cells. By 8h, T318 phosphorylation is detected in 12.0% of *hop1-S298A dmc1*Δ cells (Figure 6.3B, panel ii). In *hop1-T318A dmc1*Δ, phosphorylation of S298 is greatest at 4h, when 28.0% of cells exhibit α-pS298 staining and detected in less than 9% of cells at later time points (Figure 6.3B, panel iii). The turnover of Hop1 phosphorylation in *hop1-S298A dmc1*Δ and *hop1-T318A dmc1*Δ strains correlates with the kinetics of meiotic progression of each phosphomutant in the context of *dmc1*Δ (Figure 6.1).

Notably, as in *DMC1* background (Figure 5.6B, panels ii and iii), Mek1 appears to co-localise more closely with α-pT318 antibody in *hop1-S298A dmc1*Δ than with α-pS298 antibody in *hop1-T318A dmc1*Δ (Figure 6.4B, panels ii and iii). Whilst in the latter, both Mek1 and pS298 peak at 4h (Figure 6.3B, panel iii), few cells show any co-localisation between the two antibodies at this time point. In *hop1-S298A* the curves of Mek1 loading, T318 phosphorylation and co-localisation between Mek1 and Hop1/pT318 are inter-dependent (Figures 6.3B, panel ii and 6.4B, panel ii).

6.2.6. Western blot analysis of Hop1-S298 and -T318 phosphorylation in *dmc1Δ*

Hop1 levels and phosphorylation were evaluated in *dmc1*Δ background in *HOP1*, *hop-S298A* and *hop1-T318A* using an anti-Hop1 antibody and the two phospho-specific antibodies, anti-pS298 and anti-pT318, as in Section 5.2.8.

Hop1 levels are comparable in the three strains, although the turnover of the protein is distinct. As previously reported (Carballo et al., 2008), high levels of Hop1 are detected 12h into meiosis in the context of *HOP1 dmc1*Δ (Figure 6.5) due to the activation of the recombination checkpoint. In *hop1-S298A dmc1*Δ, levels of the protein are slightly reduced by 10h, remaining at this level until the last time point analysed, 12h. In *hop1-T318A dmc1*Δ, Hop1 levels are reduced by 10h and the protein is no longer detected by 12h (Figure 6.5).

Hyperphosphorylation of Hop1 is observed 12h into meiosis in *HOP1 dmc1*Δ. In *hop1-S298A dmc1*Δ, Hop1 phosphorylation is detected at 4h, highest between 5 and 8h and reduced by 10h. However, the slowest migrating band of Hop1 is absent in the context of *hop1-S298A dmc1*Δ, likely due to the absence of S298 phosphorylation.

Hop1 phosphorylation is detected in *hop1-T318A dmc1*Δ at 4h, as in *HOP1 dmc1*Δ or *hop1-S298A dmc1*Δ. However, it is reduced by 6h and no longer detected by 8h. Phosphorylation levels also appear reduced in *hop1-T318A dmc1*Δ when compared to *HOP1 dmc1*Δ or *hop1-S298A dmc1*Δ (Figure 6.5), possibly due to the rapid repair of DSBs through IS recombination and fast meiotic progression in this context (Figure 6.1).

Both phospho-specific antibodies are detected in *HOP1 dmc1*Δ, where they are still present by 12h after meiosis induction (Figure 6.5). In *hop1-S298A dmc1*Δ, some phosphorylation of threonine 318 can be detected, albeit reduced and, as expected, no phosphorylation of serine 298 is observed (Figure 6.5). None of the phospho-specific antibodies can be detected *hop1-T318A dmc1*Δ. This differs from the results described above for the immunocytology experiments (Section 6.2.5; Figure 6.3B, panel iii), where signals from α-pS298 antibody were detected in this mutant. The difference may be due to the different sensitivities of the phospho-specific antibodies when used in each technique.

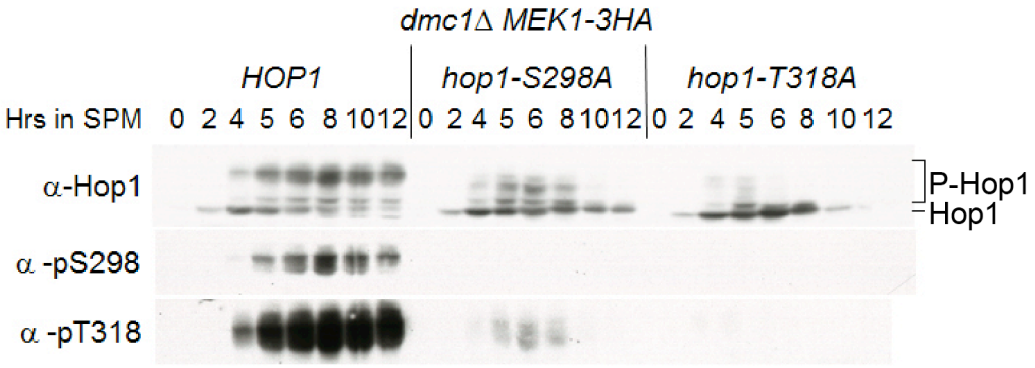

Figure 6.5 Hop1 phosphorylation in *hop1* phosphomutants in *dmc1*Δ background

Homozygous diploids of indicated genotypes were taken through synchronous meiosis at 23ºC. Samples were collected at indicated time points for further analysis. Crude protein extracts were prepared using the TCA method and run on a 10% polyacrylamide gel. Following blotting onto a nitrocellulose membrane, this was probed with α-Hop1, α-pS298 and α-pT318 antibodies.

6.2.7. Mek1 is partially activated in *hop1-S298A dmc1Δ*

In Section 5.2.9, it was observed that Mek1 phosphorylation occurs in *hop1-S298A* and is absent in *hop1-T318A*, which correlates with the spore viability of the two phosphomutants. Given that meiotic progression is delayed, but not arrested in *hop1-S298A dmc1*Δ and unaffected in *hop1-T318A dmc1*Δ, the status of Mek1 phosphorylation was assessed in this context. For this, samples collected from synchronous meiotic cultures of *HOP1*, *hop1-S298A* and *hop1-T318A* strains in a *dmc1*Δ *MEK1-3HA* background were analysed by Western blot as before (Section 5.2.9).

Like Hop1, Mek1 is hyperphosphorylated in *HOP1 dmc1*Δ strains (Figure 6.6). As in *DMC1* background (Section 5.2.9; Figure 5.9), no phosphorylation of Mek1 is detected in *hop1-T318A dmc1*Δ and the protein is no longer observed by 12h. In *hop1-S298A dmc1*Δ, a reduced mobility shift is observed, indicating that Mek1 is partially phosphorylated in this context. Notably, partial Mek1 phosphorylation is still observed at 12h in *hop1-S298A dmc1*Δ, probably leading to the delay observed in meiotic progression in this mutant (Figures 6.1 and 6.6).

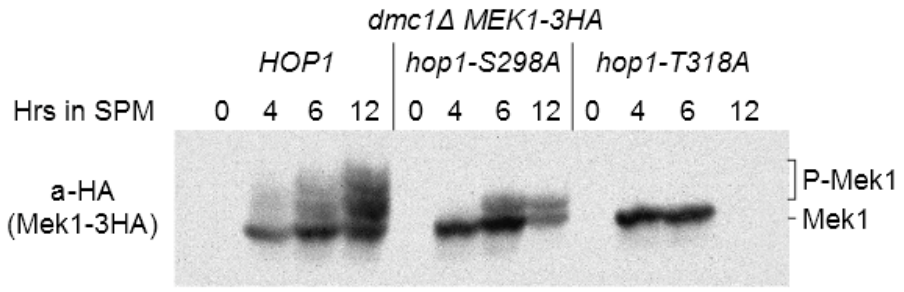

Figure 6.6 Mek1 phosphorylation in *hop1* phosphomutants in *dmc1*Δ background

Homozygous diploids of indicated genotypes were taken through synchronous meiosis at 23ºC. Samples were collected at indicated time points for further analysis. Crude protein extracts were prepared using the TCA method and run on a 7.5% polyacrylamide gel containing 4 µM Phos-tag. Following blotting onto a PVDF membrane, this was probed with α-HA (Mek1-3HA) antibody.

6.2.8. Genetic interaction between *hop1* and *mek1* phosphomutants

The kinase activity of Mek1 is crucial for its roles in meiotic recombination and checkpoint (Section 1.5). Activation of Mek1 is dependent on the phosphorylation of two conserved residues in the activation loop of the protein, threonines 327 and 331 (Figure 1.6). Mutating these residues to alanine, a nonphosphorylatable amino acid, leads to a *mek1*Δ-like phenotype, characterised by low spore viability and absence of *dmc1*Δ arrest (Niu et al., 2005, Wan et al., 2004).

A third residue, S320, has been shown to be specifically required for preventing *DMC1*-independent repair of DSBs. In a mutant where the serine residue at position 320 is replaced by alanine, *mek1-S320A*, spore viability is high in the context of *DMC1*, but no arrest is observed in *dmc1*Δ background. When this serine is replaced by a phosphomimetic aspartic acid residue (*mek1-S320D*), *dmc1*Δ arrest is restored (Niu et al., 2007).

The phenotype of *hop1-S298A* at low temperature resembles that of *mek1-S320A* in that both confer high viability in *DMC1* (86.5% of the spores produced by *hop1-S298A* at 18ºC and 93.6% of those generated by *mek1-S320A* at 30ºC are viable) and no arrest in *dmc1*Δ background (65.3 ± 9.0% sporulation efficiency in *hop1-S298A dmc1*Δ and 58.0 ± 5.3% in *mek1-S320A dmc1*Δ) (Niu et al., 2007). The observation above that Mek1 is not fully activated in *hop1-S298A dmc1*Δ (Figure 6.6) raised the possibility that the defects conferred by *hop1-S298A* could be due to inefficient phosphorylation of serine residue 320 of Mek1 in this mutant.

In order to test this hypothesis, double mutants expressing combinations of nonphosphorylatable and phosphomimetic alleles of *hop1-S298* and *mek1-S320* were generated (Sections 2.7.2 and 2.8.3; Table 2.8) and analysed for spore viability and sporulation efficiency in *DMC1* and *dmc1*Δ backgrounds, respectively.

6.2.8.1. Spore viability of hop1-S298 mek1-S320 *double mutants*

If *DMC1*-independent repair of DSBs in *hop1-S298A dmc1*Δ at 23ºC (Figure 4.2) is due to a failure in phosphorylating serine 320 of Mek1, introduction of the *mek1-S320D* allele might restore *dmc1*Δ arrest. On the other hand, expression of

mek1-S320A in *hop1-S298D*, which normally confers arrest in *dmc1*Δ, may revert this phenotype to that of *hop1-S298A dmc1*Δ.

First, viability of the double mutants in *DMC1* background was tested at 18, 30 and 36ºC as described above (Section 3.2.1). At least 40 tetrads (160 spores) were dissected for each condition. As previously reported (Niu et al., 2007), neither *mek1-S320A* nor *mek1-S320D* has a significant impact on the spore viability of *HOP1* at any of the temperatures tested. *HOP1 mek1-S320A* and *HOP1 mek1-S320D* produce more than 86% viable spores at 18, 30 and 36ºC (Figure 6.7A and D).

The two *mek1-S320* alleles exhibit genetic interaction with *hop1-S298* alleles. In the context of *hop1-S298A*, both *mek1-S320A* and *mek1-S320D* lead to a significant reduction in spore viability at 18 and 30ºC. 86.5% of *hop1-S298A* spores are viable at 18ºC, while in *hop1-S298A mek1-S320A* or *hop1-S298A mek1-S320D* spore viability is lower than 2.5% at this temperature (Figure 6.7B and D). A reduction in spore viability is also observed at 30ºC from 53.2% in the *hop1-S298A* single mutant to less than 6.3% in the double mutants.

*S*pore viability is also reduced in *hop1-S298D mek1-S320A* (Figure 6.7C and D) from values of 95% or over in *hop1-S298D* singe mutant to less than 15% in the double mutant. Notably, when *hop1-S298D* is combined with *mek1-S320D* a temperature-sensitive phenotype in terms of spore viability is observed. At 18ºC, 78.1% of the spores produced by *hop1-S298D mek1-S320D* are viable. The fraction of viable spores is significantly reduced at 30 and 36ºC, to 15.0 and 8.8%, respectively. This indicates that *hop1-S298D* confers a phenotype milder than that of *hop-S298A*, but not fully WT, which is in agreement with the results shown in Figures 3.3B and 4.1B.

Figure 6.7 Effect of temperature on spore viability in *hop1-S298 mek1-S320* double mutants

Homozygous diploids of indicated genotypes in *HOP1 DMC1* **(A)**, *hop1-S298A DMC1* **(B)** or *hop1-S298D DMC1* **(C)** backgrounds were incubated on SPM plates at 18, 30, and 36ºC for one (T≥30º) or two days (T<30ºC). Tetrads were dissected on YPD plates and incubated at 30ºC for 2 days. Spore viability is calculated as the number of visible spore colonies (e.g., Figure 3.1B) over the total number of spores dissected. For each strain, at least 40 tetrads (160 spores) were analysed. The spore viability values plotted in panels A, B and C are shown in panel **D**.

A

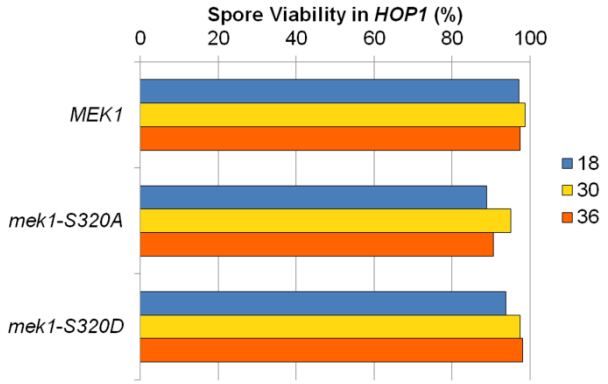

B

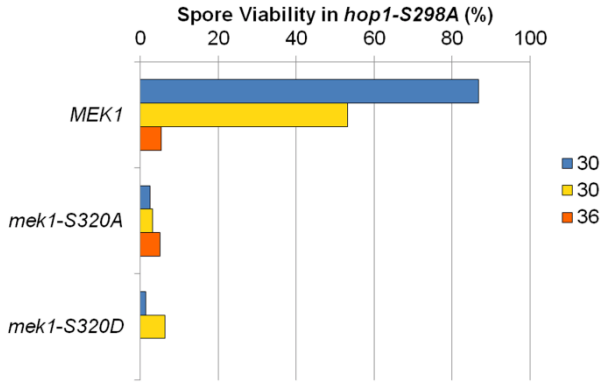

C

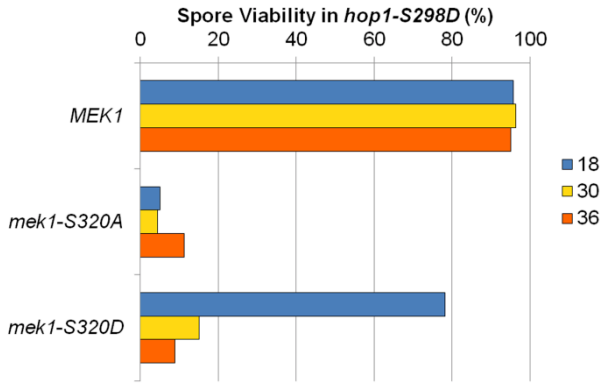

D

***HOP1* allele**	***MEK1* allele**	**Spore Viability (%)**		
		18°C	**30°C**	**36°C**
HOP1	*MEK1*	97.1	98.8	97.4
	mek1-S320A	88.8	95.0	90.6
	mek1-S320D	93.8	97.5	98.1
hop1-S298A	*MEK1*	86.8	53.2	5.4
	mek1-S320A	2.5	3.1	5.0
	mek1-S320D	1.3	6.3	<0.6
hop1-S298D	*MEK1*	95.7	96.3	95.0
	mek1-S320A	5.0	4.4	11.3
	mek1-S320D	78.1	15.0	8.8

6.2.8.2. Sporulation efficiency of **hop1-S298 mek1-S320** *mutants in* **dmc1Δ** *background*

The results obtained above (Section 6.2.8.1) indicate that *mek1-S320A* and *mek1-S320D* genetically interact with *hop1-S298A* and *hop1-S298D* in terms of spore viability in *DMC1* background. Next, their impact on *dmc1*Δ arrest was assessed at 30ºC (Niu et al., 2007).

Results show that *mek1-S320A* does alleviate *dmc1*Δ arrest in *HOP1* (less than 0.5% of *HOP1 MEK1 dmc1*Δ cells produce spores, compared to 17.7% of *HOP1 mek1-S320A dmc1*Δ cells; Figure 6.8A and D), consistent with the notion that phosphorylation at serine 320 of Mek1 is required for mediating *dmc1*Δ arrest (Niu et al., 2007).

Unexpectedly, sporulation efficiency is slightly higher in *hop1-S298A mek1-S320D dmc1*Δ than in *hop1-S298A mek1-S320A dmc1*Δ (41.5 ± 4.0 and 28.7 ± 6.5%, respectively; Figure 6.8B and D). No statistically significant difference is observed in the sporulation efficiency of *hop1-S298D mek1-S320A dmc1*Δ (35.0 ± 7.6%) and *hop1-S298D mek1-S320D dmc1*Δ (23.6 ± 6.2%) strains (Figure 6.8C and D).

Figure 6.8 Sporulation efficiency of *hop1-S298 mek1-S320* mutants in *dmc1*∆ background

Homozygous diploids of indicated genotypes in *HOP1 dmc1*∆ **(A)**, *hop1-S298A dmc1*∆ **(B)** or *hop1-S298D dmc1*∆ **(C)** backgrounds were incubated on SPM plates at 30ºC for one day. Sporulation efficiency is assessed as the fraction of cells containing two or more spores out of the total number of cells scored. For each genotype, 200 or more cells were scored in two independent experiments. Error bars represent the standard deviation from the mean. The sporulation efficiency and standard deviation values plotted in panels A, B and C are shown in panel **D**.

A

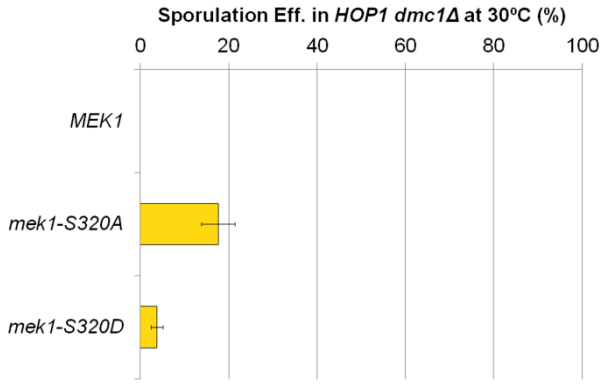

B

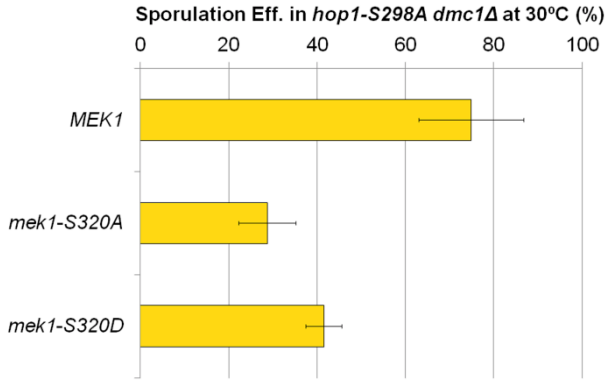

C

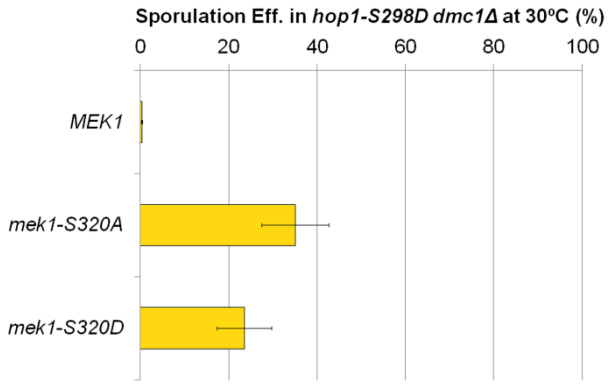

D

***HOP1* allele**	***MEK1* allele**	**Sporulation efficiency in *dmc1*△ ± SD (%)**
HOP1	*MEK1*	<0.5
	mek1-S320A	17.7 ± 3.8
	mek1-S320D	3.8 ± 1.3
hop1-S298A	*MEK1*	74.9 ± 11.9
	mek1-S320A	28.8 ± 6.5
	mek1-S320D	41.5 ± 4.0
hop1-S298D	*MEK1*	0.4 ± 0.1
	mek1-S320A	35.0 ± 7.6
	mek1-S320D	23.6 ± 6.2

6.3. Discussion

6.3.1. Full activation of Mek1 is required for *dmc1Δ* arrest

Co-localisation between Hop1 and Mek1 at chromosome axes correlates with the extent of delay in meiotic progression in *dmc1*Δ background, with higher residence times of Hop1/Mek1 at chromosomes leading to slower meiotic progression in the context of *dmc1*Δ (Figures 6.1 and 6.4A, panel i). This suggests that Mek1 recruitment is sufficient for initial establishment of IH bias, but stabilisation of Mek1 at chromosomes through interaction with phosphorylated serine 298 of Hop1 is required for preventing *DMC1*-independent repair of DSBs in *dmc1*Δ.

Additionally, Mek1 is partially phosphorylated in *hop1-S298A dmc1*Δ but not in *hop1-T318A dmc1*Δ (Figure 6.6). The presence of a partially phosphorylated form of Mek1 12h following meiotic induction in *hop1-S298A dmc1*Δ may be the cause of the delay observed in meiotic progression in this mutant. Phosphorylation of Hop1 at T318 is thus essential for activation of Mek1, sufficient to ensure IH bias in *DMC1* background at low temperature. Phosphorylation of Hop1 at S298 is required for full activation of Mek1, essential for ensuring IH bias in *dmc1*Δ background.

These results suggest that stabilisation of Hop1-Mek1 complexes through interaction of the second with phosphorylated serine 298 is required for full activation of Mek1. The higher local concentrations of Mek1 at chromosomes, achieved through more stable interaction with Hop1, then permit its full activation by transphosphorylation. Consistent with the notion that higher local chromosomal concentration of Mek1 is required for its full activation, the expression of a multicopy allele of *hop1-S298A* (*hop1-S298Ax2*) in *dmc1*Δ background rescues the defect in *dmc1*Δ arrest of *hop1-S298A* (Figure 4.1A). This is likely due to the increased availability of the mutant protein Hop1^{S298A} at the chromosomes, which would then lead to improved chromosomal recruitment of Mek1.

6.3.2. Genetic interaction between *hop1-S298* and *mek1-S320* alleles

The results presented above show that *hop1-S298* and *mek1-S320* alleles genetically interact. As described in Chapter 4, IH bias is compromised in *hop1-S298A*, with DSBs being repaired in a *DMC1*-independent manner in *hop1-S298A dmc1*Δ (Figure 4.2). Furthermore, deletion of another gene with impact on IH bias,

HED1, leads to a reduction in spore viability in the context of *hop1-S298A* (Figure 4.4A). It has also been shown that *hop1-S298D* confers a phenotype milder than that of *hop1-S298A*, which can only be observed when a single copy of *hop1-S298D* is expressed (Figures 3.3B and 4.1B), suggesting that, although improved, IH bias is not as robust in this phosphomutant as in *HOP1*.

It is possible that *mek1-S320* mutants, similarly to the *hed1*Δ mutant, confer mild defects in IH bias in a *DMC1* background which only translate into a reduction in spore viability when IH bias is further compromised. In the context of *HOP1*, no effect of *mek1-S320A* or *mek1-S320D* is observed on spore viability (Figure 6.7A). However, when combined with *hop1-S298A* or *hop1-S298D* alleles, where IH bias is not as robust, spore viability is compromised (Figure 6.7B and C).

Chapter 7: General Discussion

7.1. Summary of results

I have characterised two *HOP1* phosphomutants: *hop1-S298A* and *hop1-T318A*, in which a single serine or threonine residue comprised in the SCD of Hop1 were mutated to alanine. It was shown that *hop1-S298A* confers a temperature-sensitive defect in spore viability, while *hop1-T318A* produces dead spores at all tested temperatures.

The spore viability of *hop1-S298A* mutant is rescued when a phosphomimetic aspartic acid residue is introduced at position 298 of Hop1 (*hop1-S298D*) or when twice the number of copies of this allele is expressed (*hop1-S298Ax2*). A reduction in copy number of either allele (*hop1-S298D/hop1*Δ or *hop1-S298A/hop1*Δ) leads to decreased spore viability.

Deletion of *HED1* in the context of *hop1-S298A* exacerbates the spore viability defects of the *hop1-S298A* single mutant. The *hop1-S298A zip1*Δ double mutant also shows reduced spore viability comparatively to either single mutant.

A mild checkpoint bypass is observed in *hop1-S298A rad50S*. Bypass of checkpoint is more evident in a *zip1*Δ background, where most *hop1-S298A zip1*Δ cells progress through meiosis.

hop1-S298A sporulates efficiently in a *dmc1*Δ background at all temperatures tested and DSBs do not accumulate in the double mutant at low temperature, in contrast to *dmc1*Δ single mutant. Again, expression of *hop1-S298Ax2* or *hop1-S298D* restores arrest in *dmc1*Δ, which requires the presence of two copies of either allele.

Characterisation of meiosis at the permissive temperature shows no major differences in Hop1 chromosomal recruitment and phosphorylation in *HOP1*, *hop1-S298A* and *hop1-T318A* strains. However, Mek1 chromosomal levels are significantly reduced in *hop1-T318A*. In *hop1-S298A*, Mek1 recruitment to chromosomes appears to be as efficient as in WT, but co-localisation between Hop1 and Mek1 is reduced. Phosphorylation of Mek1 can be detected in *hop1-S298A*, but not in *hop1-T318A*.

In *dmc1*Δ background, few *HOP1* cells progress through the meiotic divisions, while most *hop1-S298A* and *hop1-T318A* cells do so. However, a delay is observed in meiotic divisions in *hop1-S298A dmc1*Δ. These observations correlate with the turnover of proteins at chromosomes. A faster turnover of Hop1, Hop1's phosphorylated forms, and Mek1 is observed in *hop1-T318A dmc1*Δ compared to *hop1-S298A dmc1*Δ. In *HOP1 dmc1*Δ, Hop1, phosphorylated Hop1 and Mek1 accumulate at the chromosome axes. Mek1 becomes hyperphosphorylated in *HOP1 dmc1*Δ, while only partial Mek1 phosphorylation can be detected in *hop1-S298A dmc1*Δ and none in *hop1-T318A dmc1*Δ.

7.2. The effect of temperature in meiosis

Changes in temperature impact protein-protein and protein-DNA interactions, often affecting the phenotype of mutants where these are compromised more strongly than that of wild-type. This may be due to alterations in protein structure and/or to a direct effect on protein interactions. Low temperatures tend to stabilise these, while high temperatures have the reverse effect.

It has been shown that *hop1-S298A* confers a temperature-sensitive defect in spore viability (Figure 3.1). Further characterisation of this mutant revealed that, regardless of the high spore viability levels detected at the permissive temperature (23ºC), co-localisation of the mutant protein with Mek1 is compromised (Figures 5.3B and 5.6A, panel i), suggesting that Hop1-Mek1 interaction is weaker in the mutant than in WT. Thus, it is likely that an increase in temperature will affect $Hop1^{S298A}$-Mek1 interaction further. It is probable that Hop1-Mek1 interaction becomes more transient at high temperature, preventing stable Mek1 accumulation at chromosomes and its subsequent activation.

Further experiments are required to test this hypothesis, including quantification of Mek1 chromosomal levels and Hop1-Mek1 co-localisation at 33ºC. Preliminary experiments indicate that Mek1 is not phosphorylated at this temperature, which is consistent with the reduced spore viability conferred by *hop1-S298A* at 33 and 36ºC. A system where Mek1 is constitutively bound to mutant proteins $Hop1^{T318A}$ and $Hop1^{S298A}$ could also provide additional insight on how the interaction between Hop1 and Mek1 is regulated by Mec1/Tel1-mediated phosphorylation of Hop1. If these fusion proteins rescued the phenotype of both mutants at high and low temperatures, it would support the notion that the meiotic

defects in the phosphomutants are a result of inefficient recruitment/interaction with Mek1.

7.3. Links between recombination and checkpoint

Mec1, the yeast orthologue of the mammalian ATR (Section 1.3.1), is involved in processes such as DNA replication and repair and cell cycle checkpoints (Abraham, 2001, Cha and Kleckner, 2002, Zhou and Elledge, 2000). During meiosis, it is essential for arrest in meiotic progression in response to defects in recombination (e.g., *dmc1*Δ) and synapsis (e.g., *zip1*Δ). Rad24 and Rad17 are also required for these checkpoint responses. In their absence, the cells progress through meiosis and produce inviable spores (Lydall et al., 1996, Xu et al., 1997).

In addition to defects in checkpoint response, *mec1-1*, *rad24* and *rad17* mutants also exhibit recombination defects. In these mutants, levels of ectopic and IS recombination are increased, which leads to aberrant synapsis with increased number of polycomplexes (Grushcow et al., 1999, Thompson and Stahl, 1999). The observation that Mec1 and its paralogue in budding yeast, Tel1, phosphorylate proteins with essential roles in recombination, such as Sae2 and Hop1 (Sections 1.2.3.1 and 1.4) (Carballo et al., 2008, Cartagena-Lirola et al., 2006), further suggests that recombination and checkpoint regulation are tightly linked. This is also supported by the fact that proteins initially thought to be mainly required for IH recombination, such as the axial components Red1, Hop1 and Mek1, have since been shown to be essential for checkpoint activation (Carballo et al., 2008, Grushcow et al., 1999, Hochwagen and Amon, 2006, Longhese et al., 2008) (Sections 1.4 and 1.5).

The study of two *hop1* phosphomutants, *hop1-S298A* and *hop1-T318A*, provides some clues on how recombination and checkpoint functions may be interlinked. In *hop1-T318A*, which confers constitutively low spore viability, Mek1 phosphorylation is absent. Contrastingly, in *hop1-S298A*, which produces highly viable spores at low temperature, activation of this kinase can be detected (Figures 3.1 and 5.9). Although *dmc1*Δ arrest is absent in both mutants (Figure 6.1), meiotic progression is delayed in *hop1-S298A dmc1*Δ. This is most likely a consequence of partial phosphorylation of Mek1 in the context of *hop1-S298A dmc1*Δ (Figure 6.6), suggesting that further Mek1 phosphorylation may be required for a robust IH bias. This prevents *DMC1*-independent repair of DSBs and consequently leads to checkpoint activation.

Hop1 and Mek1 can be seen as the functional homologues of Rad9 and Rad53 in meiosis (Section 1.3.2), triggering the prophase I checkpoint like their counterparts mediate the checkpoint response to DNA damage. In fact, activation of the DNA damage checkpoint requires phosphorylation of the SQ/TQ cluster domain of Rad9, which allows its interaction with the FHA domain of Rad53. The latter is then recruited to damage sites, where its oligomerization and phosphorylation by Mec1 can occur. Formation of Rad53 oligomers facilitates transphosphorylation and full checkpoint activation (Traven and Heierhorst, 2005, Usui et al., 2009).

Similarities with Hop1/Mek1 can be easily detected. Mek1 localisation to recombination sites is dependent on Mec1/Tel1 phosphorylation of Hop1's SCD (Carballo et al., 2008) and this recruitment requires the FHA domain of Mek1 (Wan et al., 2004). Furthermore, the C-terminus of Hop1 is required for Mek1 dimerization and, consequently, for its activation (Niu et al., 2005). Finally, it has been shown above that partial activation of Mek1 in *hop1-S298A dmc1*Δ at 23ºC is not sufficient for preventing *DMC1*-independent repair of DSBs (Figures 4.2 and 6.6). Similarly, extensive phosphorylation and formation of high order oligomers of Rad53 are required for DNA damage checkpoint response (Usui et al., 2009).

7.4. Mek1 chromosomal levels and activation

The extent of Hop1-Mek1 co-localisation in *hop1-S298A* is reduced in comparison to wild-type (Figure 5.6A, panel i) despite the fact that similar chromosomal levels of Mek1 are detected in *HOP1* and *hop1-S298A* strains (Figure 5.4A, panel ii). This suggests that phosphorylation at serine 298 of Hop1 by Mec1/Tel1 is required for the continued interaction with Mek1.

Further indication that Hop1-Mek1 interaction is compromised but not absent in *hop1-S298A* is provided by the experiments where overexpression of *hop1-S298A* rescues spore viability and *dmc1*Δ arrest (Figures 3.3A and 4.1A). The inefficient Hop1^{S298A}-Mek1 interaction would be compensated in this case by the higher levels of the mutant protein available at chromosomes to recruit Mek1 via interaction with phosphorylated threonine residue 318. To verify this, cytological analysis of *hop1-S298Ax2* meiosis must be carried out to determine Hop1 and Mek1 chromosomal levels.

The level of Mek1 at chromosomes, but not the overall amount of protein, is reduced in *hop1-T318A* (Figures 5.4A, panel ii, and 5.9). This suggests that T318 phosphorylation is essential for Mek1 recruitment whilst S298 phosphorylation is

required for stabilisation or maintenance of Hop1-Mek1 interaction. This would explain the reduced levels of co-localisation detected in *hop1-S298A*, as a more transient interaction would be detected less efficiently.

The fact that *hop1-S298A* shows high levels of spore viability despite the inefficient interaction with Mek1 might indicate that either (i) Mek1's role in promoting IH bias is not as relevant at low temperature or (ii) that Mek1 presence at chromosomes might be sufficient for its roles in unchallenged but not in challenged meiosis.

The first explanation is not supported by the fact that the phenotype conferred by *hop1-T318A* is not temperature-dependent. Furthermore, *MEK1* deletion leads to a cold-sensitive phenotype in terms of spore viability (Carballo and Cha, unpublished data). In support of the second hypothesis, increase in temperature or deletion of *hed1*Δ compromise spore viability of *hop1-S298A* (Figures 3.1 and 4.4A). Additionally, *hop1-S298A* confers defects in the activation of *rad50S* and *zip1*Δ checkpoints (Figures 4.5 and 4.6B). This may be due to inefficient Mek1 activation in these backgrounds. Further experiments are required to address this hypothesis.

Similar observations, revealing a correlation between protein levels and proficiency in its different roles, were previously reported in work carried out on a hemizygous *ZIP/zip1Δ* mutant (Klutstein et al., 2009). In this hemizygous diploid, nondisjunction of homologous chromosomes is increased and synapsis and meiotic interference are impaired, but, in contrast to *zip1Δ/zip1*Δ homozygous diploids, recombination is unaffected (Klutstein et al., 2009, Sym and Roeder, 1994).

7.5. IH bias models

The bias towards inter-homologue recombination in budding yeast meiosis may be imposed by several mechanisms: (i) imposition of a physical barrier for IS recombination, (ii) active promotion of IH recombination, (iii) kinetic impediments to IS recombination or (iv) local inhibition of cohesion.

The first model proposes that IS recombination is prevented by the presence of the meiosis-specific axis components Red1, Hop1 and Mek1. These proteins alter meiotic chromosomal structure, hampering the recombination activity of Rad51/Rad54. The meiosis-specific recombinase Dmc1 then assumes the predominant role in homology search and invasion of the homologue (Bishop et al., 1992, Shinohara et al., 1997a, Shinohara et al., 1992).

In support of this model, rescue of the *dmc1*Δ phenotype by Rad51 overexpression depends on Mek1 kinase activity. This suggests that IS recombination is blocked by Mek1, which in this manner directs Rad51 recombinase activity towards the homologue (Niu et al., 2005). Additionally, DSBs accumulate in haploid *dmc1*Δ strains induced to sporulate, while repair occurs via IS recombination in *mek1*Δ *dmc1*Δ haploids. These observations suggest that Mek1 actively prevents IS recombination (Callender and Hollingsworth, 2010).

In order to restrict Mek1 anti-recombination activity to sister chromatids, Mek1 activity would have to be limited to the region flanking the DSB (Goldfarb and Lichten, 2010, Niu et al., 2007). Interestingly, it has been shown that DSB-induced chromatin modifications mediated by Mec1/Tel1 occur in the proximity of DSBs (50-100 kb) (Shroff et al., 2004). Furthermore, Mek1 action appears to be more localised than that of its mitotic counterpart, Rad53. When fully activated, the latter is released from the complex it forms with Rad9, leading to checkpoint signal amplification (Gilbert et al., 2001).

A second way of explaining establishment of IH bias is through a positive enforcement of recombination with the homologous chromosomes. In this case, the active promotion of IH recombination by Red1, Hop1 and Mek1, and Dmc1's preference for the homologue as a recombination template result in the IH bias observed in budding yeast meiosis. However, this would not be applicable to other model systems, since only Rad51 orthologues are present in some organisms, such as *Caenorhabditis elegans*, *Sordaria macrospora*, *Neurospora crassa* and *Drosophila melanogaster* (Abdu et al., 2002, Borkovich et al., 2004, Garcia-Muse and Boulton, 2007, Nowrousian et al., 2010).

Observations that IS recombination events occur at a similar level and time as IH recombination events lead to the suggestion that, rather than blocking recombination with the sister-chromatid, Mek1 reduces the kinetics of IS strand invasion by 3-fold (Goldfarb and Lichten, 2010). This allows for competition between IH and IS recombination pathways that would otherwise not occur, given the constraints associated with homology search and invasion of the homologue in IH recombination. Additionally, inhibition of Rad51 activity through Hed1 and Mek1-mediated Rad54 phosphorylation, would further decrease the rate at which IS recombination events take place (Section 1.2.3.2) (Goldfarb and Lichten, 2010, Niu et al., 2009, Tsubouchi and Roeder, 2006).

Cohesion also plays a role in IH bias. Absence of the meiosis-specific cohesin subunit, Rec8, leads to loss of IH bias at the SEI to dHJ transition. A fourth model for IH bias proposes that IS recombination is by default the favoured pathway for DSB repair, due to proximity between sister chromatids and presence of cohesion. The local action of the Red1-Hop1-Mek1 complex relieves cohesion, thus allowing invasion into the homologue (Kim et al., 2010).

Notably, these models are not mutually exclusive. IH bias could be established through a combination of IS recombination inhibition (through both physical and kinetic barriers), promotion of IH recombination and modulation of cohesion.

The fact that full Mek1 activation is required for preventing *DMC1*-independent repair of DSBs in challenged meiosis (Chapters 4 and 6) supports the idea that the activity of this kinase somehow inhibits IS recombination. Reduced levels of Mek1 phosphorylation appear to be insufficient to ensure spore viability when further alleles compromising IH recombination (e.g., *hed1*Δ and *dmc1*Δ) are present. This is most likely due to *DMC1*-independent repair of DSBs as indicated by the low levels of DSBs detected in *hop1-S298A dmc1*Δ double mutant (Figure 4.2).

7.6. Establishment *versus* maintenance of IH bias

Partial Mek1 activation in *hop1-S298A* is sufficient for high levels of spore viability at low temperature. However, it leads to a reduction in spore viability in *hop1-S298A hed1*Δ and to *DMC1*-independent repair of DSBs in *hop1-S298A dmc1*Δ background (Figure 4.2). This suggests that two stages may be distinguished in the implementation of IH bias: establishment and maintenance.

In unchallenged meiosis, initial Mek1 activation is sufficient for establishment of the bias towards IH recombination. However, in challenged meiosis (e.g., *dmc1*Δ, *hed1*Δ, high temperature), Mek1 must remain at chromosomes and be fully active for maintenance of bias. This is supported by the fact that suppression of the phenotype conferred by *DMC1* deletion by overexpression of Rad51 requires Mek1 kinase activity (Niu et al., 2005). Additionally, mutation of S320 of Mek1 into an alanine residue causes no spore viability defects in *DMC1* background but leads to a bypass of *dmc1*Δ arrest (Section 1.5.3) (Niu et al., 2007, Wan et al., 2004), supporting that notion that IH bias must be reinforced in challenged meiosis. Furthermore, it has been shown that IH bias is initially established in a *rec8*Δ

mutant, but is then lost at the SEI to dHJ transition, which is also consistent with the notion of two distinct phases in the implementation of IH bias (Kim et al., 2010).

All genetic studies carried out so far suggest that Mek1 dimerization is required for its functions (Niu et al., 2005, Niu et al., 2007). However, co-IP experiments using differentially tagged Mek1 proteins have failed to detect Mek1 dimerization. It has been suggested that this failure is due to reduced levels of Mek1 dimers in the cell at any specific time point (Niu et al., 2005). Possibly, in unchallenged meiosis few Mek1 dimers are present at each time, imposing IH bias in a local manner. During challenged meiosis Mek1 dimers must be more abundant so that higher phosphorylation levels are obtained. Full Mek1 activation would then be required for maintaining IH bias and thus preventing DSB repair via IS recombination and triggering checkpoint.

It would be relevant to observe the effect of expressing GST-tagged Mek1 protein in *hop1-T318A* and *hop1-S298A*, as Mek1 dimerization is achieved artificially in these strains through GST-GST binding upon Mek1 recruitment (Niu et al., 2005). Mek1 dimers could thus be obtained in conditions where Red1-Hop1-Mek1 interactions are less stable. The expectation would be that expression of a *MEK1-GST* allele would improve IH bias and checkpoint functions in *hop1-S298A* but not in *hop1-T318A*, as the latter is ineffective in the recruitment of Mek1 to chromosomes.

7.7. A model

It has previously been shown that Hop1 phosphorylation by Tel1/Mec1 is required for its functions in IH bias and checkpoint (Carballo et al., 2008). Based on the results presented above, a model is proposed for the regulation of Hop1 function through Mec1/Tel1-dependent phosphorylation (Figure 7.1).

In *HOP1* cells, phosphorylation of Hop1 occurs upon DSB formation (Figure 7.1A, panel i). The presence of a phosphorylated threonine at position 318 allows interaction with Mek1, likely through its FHA domain (Figure 7.1A, panel ii). Once recruited, transient Mek1 dimers are formed (Figure 7.1A, panel iii), leading to Mek1 activation (Figure 7.1A, panel iv). In challenged meiosis, a more robust interaction between Hop1 and Mek1 is required to maintain high local concentrations of the kinase dimers at the chromosome axes. Phosphorylation at serine 298 is likely required for stabilising this interaction, allowing Mek1 hyperphosphorylation (Figure 7.1A, panel v). This is essential for preventing *DMC1*-independent repair of DSBs.

In a *dmc1*Δ background, unrepaired DSBs accumulate, triggering the prophase checkpoint.

In *hop1-S298A* (Figure 7.1B), Mek1 is recruited to the chromosomes, but its interaction with Hop1 is compromised, as shown by the reduced levels of Hop1-Mek1 co-localisation detected in this mutant (Figure 5.6A, panel i). This indicates that the complex formed by Red1, Hop1 and Mek1 may be less stable. Dimers of Mek1 would then form more transiently in the context of *hop1-S298A*, leading to inefficient activation of Mek1 by transphosphorylation. In turn, this would explain the absence of *dmc1*Δ checkpoint in *hop1-S298A* and the synergistic effects observed when additional mutations that affect IH bias (e.g., *hed1*Δ) are introduced in the context of this mutant.

hop1-T318A cells show inefficient recruitment of Mek1 (Figure 5.4A, panel ii), possibly due to the absence of a phosphorylated threonine residue with which FHA domains tend to interact (Figure 7.1C) (Durocher et al., 2000, Durocher and Jackson, 2002). In this situation, as Hop1-Mek1 interaction appears to be severely compromised, no phosphorylation of Mek1 is detected. This explains the more drastic phenotype of *hop1-T318A*, which resembles that of *hop1*^{SCD} (Carballo et al., 2008).

When *hop1-S298A* is overexpressed in *hop1-S298Ax2* (Figure 7.1D), spore viability and *dmc1*Δ arrest are rescued (Figures 3.3A and 4.1A). In this case, increased expression of the *hop1-S298A* allele is likely to lead to higher chromosomal levels of the mutant Hop1^{S298A} protein. This would result in the increase of Mek1 chromosomal levels, allowing for the establishment of more numerous Mek1-Mek1 interactions and, consequently, lead to full activation of this protein.

Figure 7.1 Regulation of Hop1 function by Mec1/Tel1 phosphorylation

Upon DSB catalysis, Mec1/Tel1 phosphorylate Hop1 at T318 and S298 (panel A, i). These phosphorylations allow efficient recruitment and interaction with Mek1 (panel A, ii), leading to Mek1 dimerization (panel A, iii) and activation (panel A, iv). In challenged meiosis, stable Mek1 dimers at the chromosomes are required for the hyperphosphorylation of Mek1 (panel A, i).
In the *HOP1* conditional allele, *hop1-S298A*, Hop1-Mek1 interaction is compromised, leading to more transient Mek1 dimers, thus preventing hyperphosphorylation of the kinase (panel B).
Absence of phosphorylation at the amino acid residue 318 of Hop1 in *hop1-T318A* results in failure in Mek1 recruitment, conferring a $hop1^{SCD}$-like phenotype (panel C) (Carballo et al., 2008).
Overexpression of *hop1-S298A* in *hop1-S298Ax2* (panel D) results in increased levels of the mutant protein $Hop1^{S298A}$ available to interact with Mek1. This leads to higher local concentrations of Mek1 at the axes, allowing its dimerization and hyperphosphorylation.

(i) Mec1/Tel1 phosphorylation of Hop1 at S298 and T318 upon DSB formation
(ii) Hop1-Mek1 interaction via pT318 and FHA domain of Mek1
(iii) Mek1 dimerization
(iv) Mek1 activation
(v) Mek1 hyperphosphorylation

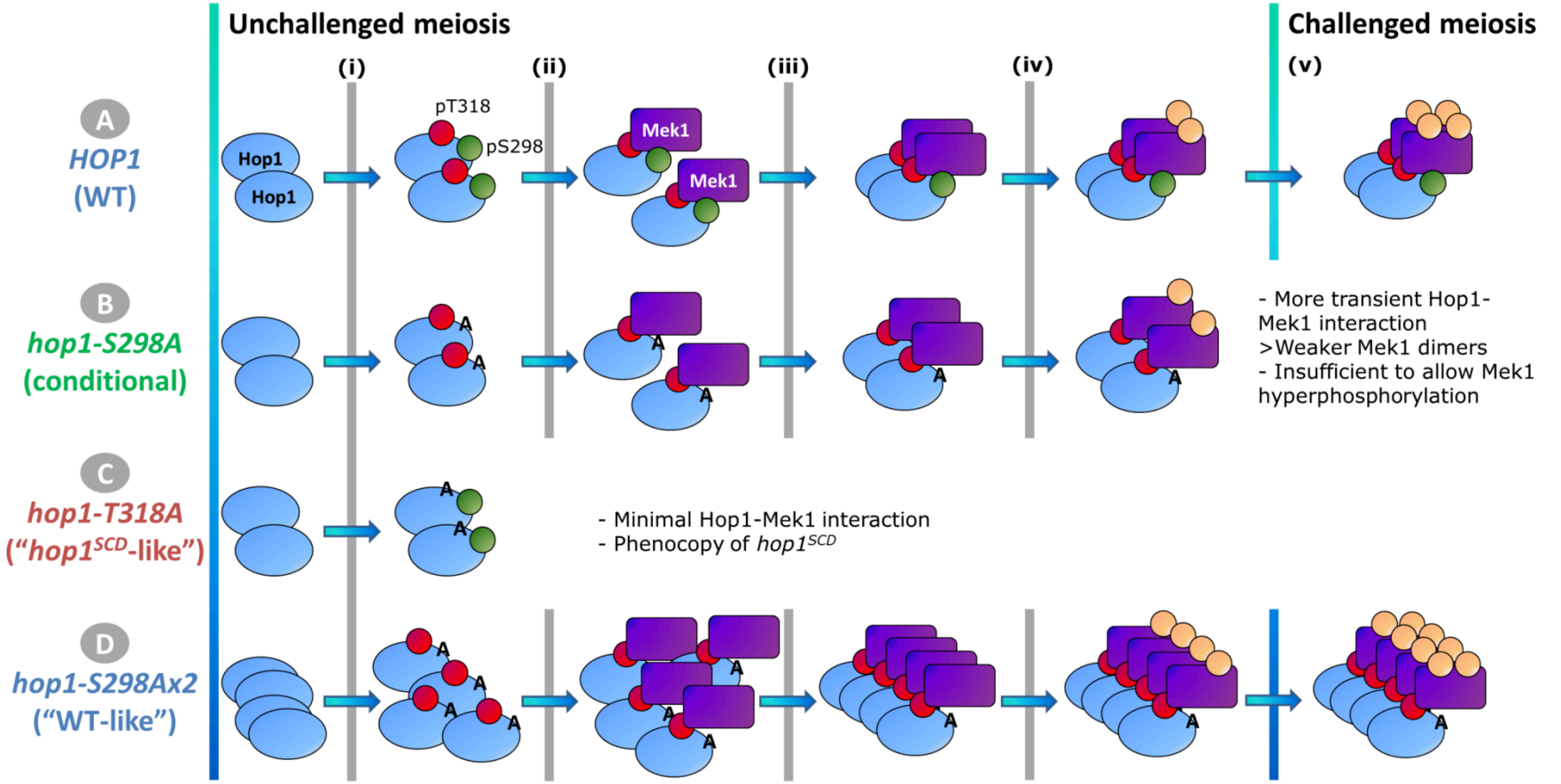

7.8. Future work

In order to confirm that the phenotype conferred by *hop1-S298A* and *hop1-T318A* phosphomutants stems from defects in Hop1-Mek1 interaction, a co-immunoprecipitation experiment (co-IP) should be carried out. If the hypothesis is correct, higher levels of Mek1 should be detected in *HOP1* strains, no Mek1 should precipitate with $Hop1^{T318A}$ mutant protein and an intermediate level of Mek1 would be bound to $Hop1^{S298A}$. Additionally, fusion proteins of mutant Hop1 protein and Mek1 could be obtained and, if these rescued the phenotype of both mutants, this would also support the proposed hypothesis. Expression of self-dimerising GST-Mek1 in *hop1-S298A* should restore spore viability and checkpoint if the defects conferred by this mutant are due to reduced levels of Mek1 dimerisation.

It is also relevant to address the status of DSBs in (i) *hop1-S298A rad50S* and (ii) *hop1-S298A rad51*Δ *dmc1*Δ in order to prove that (i) DSBs are formed to normal levels in *hop1-S298A* and (ii) repair of DSBs in *hop1-S298A dmc1*Δ is due to IS recombination.

Further experiments to address the rescue of spore viability and checkpoint conferred by *hop1-S298Ax2* are also required. First, overall and chromosomal levels of $Hop1^{S298A}$ mutant protein must be determined, by Western blot and immuno-cytology experiments, respectively. Chromosomal levels of Mek1 should also be analysed. If higher amounts of $Hop1^{S298A}$ and Mek1 proteins were present at the chromosomes in this mutant, it would favour the notion that Hop1-Mek1 interaction is less efficient when serine 298 of Hop1 cannot be phosphorylated.

Finally, western blot detection of Mek1 phosphorylation in *hop1-S298A* at 33ºC is needed to establish whether the reduced levels of spore viability at this temperature result from the absence of Mek1 phosphorylation. Analysis of Mek1 phosphorylation in *hop1-S298Ax2* and *hop1-S298D* at 23 and 33ºC would also provide valuable insight into how Mek1 phosphorylation contributes to IH bias in unchallenged or challenged meiosis.

References

ABDU, U., BRODSKY, M. & SCHUPBACH, T. (2002) Activation of a meiotic checkpoint during Drosophila oogenesis regulates the translation of Gurken through Chk2/Mnk. *Curr Biol,* 12**,** 1645-51.

ABRAHAM, R. T. (2001) Cell cycle checkpoint signaling through the ATM and ATR kinases. *Genes Dev,* 15**,** 2177-96.

AJIMURA, M., LEEM, S. H. & OGAWA, H. (1993) Identification of new genes required for meiotic recombination in Saccharomyces cerevisiae. *Genetics,* 133**,** 51-66.

ALANI, E., PADMORE, R. & KLECKNER, N. (1990) Analysis of wild-type and rad50 mutants of yeast suggests an intimate relationship between meiotic chromosome synapsis and recombination. *Cell,* 61**,** 419-36.

ALLERS, T. & LICHTEN, M. (2001) Differential timing and control of noncrossover and crossover recombination during meiosis. *Cell,* 106**,** 47-57.

ALPI, A., PASIERBEK, P., GARTNER, A. & LOIDL, J. (2003) Genetic and cytological characterization of the recombination protein RAD-51 in Caenorhabditis elegans. *Chromosoma,* 112**,** 6-16.

ANDERSEN, S. L. & SEKELSKY, J. (2010) Meiotic versus mitotic recombination: two different routes for double-strand break repair: the different functions of meiotic versus mitotic DSB repair are reflected in different pathway usage and different outcomes. *Bioessays,* 32**,** 1058-66.

ANURADHA, S. & MUNIYAPPA, K. (2004) Saccharomyces cerevisiae Hop1 zinc finger motif is the minimal region required for its function in vitro. *J Biol Chem,* 279**,** 28961-9.

ARAVIND, L. & KOONIN, E. V. (1998) The HORMA domain: a common structural denominator in mitotic checkpoints, chromosome synapsis and DNA repair. *Trends Biochem Sci,* 23**,** 284-6.

ARBEL, A., ZENVIRTH, D. & SIMCHEN, G. (1999) Sister chromatid-based DNA repair is mediated by RAD54, not by DMC1 or TID1. *EMBO J,* 18**,** 2648-58.

ARGUESO, J. L., WANAT, J., GEMICI, Z. & ALANI, E. (2004) Competing crossover pathways act during meiosis in Saccharomyces cerevisiae. *Genetics,* 168**,** 1805-16.

ARORA, C., KEE, K., MALEKI, S. & KEENEY, S. (2004) Antiviral protein Ski8 is a direct partner of Spo11 in meiotic DNA break formation, independent of its cytoplasmic role in RNA metabolism. *Mol Cell,* 13**,** 549-59.

BAILIS, J. M. & ROEDER, G. S. (1998) Synaptonemal complex morphogenesis and sister-chromatid cohesion require Mek1-dependent phosphorylation of a meiotic chromosomal protein. *Genes Dev,* 12**,** 3551-63.

BAILIS, J. M., SMITH, A. V. & ROEDER, G. S. (2000) Bypass of a meiotic checkpoint by overproduction of meiotic chromosomal proteins. *Mol Cell Biol,* 20**,** 4838-48.

BARCHI, M., MAHADEVAIAH, S., DI GIACOMO, M., BAUDAT, F., DE ROOIJ, D. G., BURGOYNE, P. S., JASIN, M. & KEENEY, S. (2005) Surveillance of different recombination defects in mouse spermatocytes yields distinct responses despite elimination at an identical developmental stage. *Mol Cell Biol,* 25**,** 7203-15.

BARONI, E., VISCARDI, V., CARTAGENA-LIROLA, H., LUCCHINI, G. & LONGHESE, M. P. (2004) The functions of budding yeast Sae2 in the DNA damage response require Mec1- and Tel1-dependent phosphorylation. *Mol Cell Biol,* 24**,** 4151-65.

BARTRAND, A. J., IYASU, D., MARINCO, S. M. & BRUSH, G. S. (2006) Evidence of meiotic crossover control in Saccharomyces cerevisiae through Mec1-mediated phosphorylation of replication protein A. *Genetics,* 172**,** 27-39.

BAUDAT, F., MANOVA, K., YUEN, J. P., JASIN, M. & KEENEY, S. (2000) Chromosome synapsis defects and sexually dimorphic meiotic progression in mice lacking Spo11. *Mol Cell,* 6**,** 989-98.

BAUDRIMONT, A., PENKNER, A., WOGLAR, A., MAMNUN, Y. M., HULEK, M., STRUCK, C., SCHNABEL, R., LOIDL, J. & JANTSCH, V. (2011) A New Thermosensitive smc-3 Allele Reveals Involvement of Cohesin in Homologous Recombination in C. elegans. *PLoS One,* 6**,** e24799.

BENDER, C. F., SIKES, M. L., SULLIVAN, R., HUYE, L. E., LE BEAU, M. M., ROTH, D. B., MIRZOEVA, O. K., OLTZ, E. M. & PETRINI, J. H. (2002) Cancer predisposition and hematopoietic failure in Rad50(S/S) mice. *Genes Dev,* 16**,** 2237-51.

BENNETT, M. D. (1977) The time and duration of meiosis. *Philos Trans R Soc Lond B Biol Sci,* 277**,** 201-26.

BERCHOWITZ, L. E., FRANCIS, K. E., BEY, A. L. & COPENHAVER, G. P. (2007) The role of AtMUS81 in interference-insensitive crossovers in A. thaliana. *PLoS Genet,* 3**,** e132.

BERCHOWITZ, L. E., HANLON, S. E., LIEB, J. D. & COPENHAVER, G. P. (2009) A positive but complex association between meiotic double-strand break hotspots and open chromatin in Saccharomyces cerevisiae. *Genome Res,* 19**,** 2245-57.

BHALLA, N. & DERNBURG, A. F. (2005) A conserved checkpoint monitors meiotic chromosome synapsis in Caenorhabditis elegans. *Science,* 310**,** 1683-6.

BISHOP, D. K. (1994) RecA homologs Dmc1 and Rad51 interact to form multiple nuclear complexes prior to meiotic chromosome synapsis. *Cell,* 79**,** 1081-92.

BISHOP, D. K., NIKOLSKI, Y., OSHIRO, J., CHON, J., SHINOHARA, M. & CHEN, X. (1999) High copy number suppression of the meiotic arrest caused by a dmc1 mutation: REC114 imposes an early recombination block and RAD54 promotes a DMC1-independent DSB repair pathway. *Genes Cells,* 4**,** 425-44.

BISHOP, D. K., PARK, D., XU, L. & KLECKNER, N. (1992) DMC1: a meiosis-specific yeast homolog of E. coli recA required for recombination, synaptonemal complex formation, and cell cycle progression. *Cell,* 69**,** 439-56.

BLAT, Y., PROTACIO, R. U., HUNTER, N. & KLECKNER, N. (2002) Physical and functional interactions among basic chromosome organizational features govern early steps of meiotic chiasma formation. *Cell,* 111**,** 791-802.

BORDE, V., GOLDMAN, A. S. & LICHTEN, M. (2000) Direct coupling between meiotic DNA replication and recombination initiation. *Science,* 290**,** 806-9.

BORKOVICH, K. A., ALEX, L. A., YARDEN, O., FREITAG, M., TURNER, G. E., READ, N. D., SEILER, S., BELL-PEDERSEN, D., PAIETTA, J., PLESOFSKY, N., PLAMANN, M., GOODRICH-TANRIKULU, M., SCHULTE, U., MANNHAUPT, G., NARGANG, F. E., RADFORD, A., SELITRENNIKOFF, C., GALAGAN, J. E., DUNLAP, J. C., LOROS, J. J., CATCHESIDE, D., INOUE, H., ARAMAYO, R., POLYMENIS, M., SELKER,

E. U., SACHS, M. S., MARZLUF, G. A., PAULSEN, I., DAVIS, R., EBBOLE, D. J., ZELTER, A., KALKMAN, E. R., O'ROURKE, R., BOWRING, F., YEADON, J., ISHII, C., SUZUKI, K., SAKAI, W. & PRATT, R. (2004) Lessons from the genome sequence of Neurospora crassa: tracing the path from genomic blueprint to multicellular organism. *Microbiol Mol Biol Rev,* 68**,** 1-108.

BORNER, G. V., BAROT, A. & KLECKNER, N. (2008) Yeast Pch2 promotes domainal axis organization, timely recombination progression, and arrest of defective recombinosomes during meiosis. *Proc Natl Acad Sci U S A,* 105**,** 3327-32.

BORNER, G. V., KLECKNER, N. & HUNTER, N. (2004) Crossover/noncrossover differentiation, synaptonemal complex formation, and regulatory surveillance at the leptotene/zygotene transition of meiosis. *Cell,* 117**,** 29-45.

BUHLER, C., BORDE, V. & LICHTEN, M. (2007) Mapping meiotic single-strand DNA reveals a new landscape of DNA double-strand breaks in Saccharomyces cerevisiae. *PLoS Biol,* 5**,** e324.

BULLARD, S. A., KIM, S., GALBRAITH, A. M. & MALONE, R. E. (1996) Double strand breaks at the HIS2 recombination hot spot in Saccharomyces cerevisiae. *Proc Natl Acad Sci U S A,* 93**,** 13054-9.

BURNS, N., GRIMWADE, B., ROSS-MACDONALD, P. B., CHOI, E. Y., FINBERG, K., ROEDER, G. S. & SNYDER, M. (1994) Large-scale analysis of gene expression, protein localization, and gene disruption in Saccharomyces cerevisiae. *Genes Dev,* 8**,** 1087-105.

BUSYGINA, V., SARO, D., WILLIAMS, G., LEUNG, W. K., SAY, A. F., SEHORN, M. G., SUNG, P. & TSUBOUCHI, H. (2012) Novel Attributes of Hed1 Affect Dynamics and Activity of the Rad51 Presynaptic Filament during Meiotic Recombination. *J Biol Chem,* 287**,** 1566-75.

BUSYGINA, V., SEHORN, M. G., SHI, I. Y., TSUBOUCHI, H., ROEDER, G. S. & SUNG, P. (2008) Hed1 regulates Rad51-mediated recombination via a novel mechanism. *Genes Dev,* 22**,** 786-95.

CALLENDER, T. L. & HOLLINGSWORTH, N. M. (2010) Mek1 suppression of meiotic double-strand break repair is specific to sister chromatids, chromosome autonomous and independent of Rec8 cohesin complexes. *Genetics,* 185**,** 771-82.

CAO, L., ALANI, E. & KLECKNER, N. (1990) A pathway for generation and processing of double-strand breaks during meiotic recombination in S. cerevisiae. *Cell,* 61**,** 1089-101.

CARBALLO, J. A. & CHA, R. S. (2007) Meiotic roles of Mec1, a budding yeast homolog of mammalian ATR/ATM. *Chromosome Res,* 15**,** 539-50.

CARBALLO, J. A., JOHNSON, A. L., SEDGWICK, S. G. & CHA, R. S. (2008) Phosphorylation of the axial element protein Hop1 by Mec1/Tel1 ensures meiotic interhomolog recombination. *Cell,* 132**,** 758-70.

CARTAGENA-LIROLA, H., GUERINI, I., MANFRINI, N., LUCCHINI, G. & LONGHESE, M. P. (2008) Role of the Saccharomyces cerevisiae Rad53 checkpoint kinase in signaling double-strand breaks during the meiotic cell cycle. *Mol Cell Biol,* 28**,** 4480-93.

CARTAGENA-LIROLA, H., GUERINI, I., VISCARDI, V., LUCCHINI, G. & LONGHESE, M. P. (2006) Budding Yeast Sae2 is an In Vivo Target of the Mec1 and Tel1 Checkpoint Kinases During Meiosis. *Cell Cycle,* 5**,** 1549-59.

CARYL, A. P., ARMSTRONG, S. J., JONES, G. H. & FRANKLIN, F. C. (2000) A homologue of the yeast HOP1 gene is inactivated in the Arabidopsis meiotic mutant asy1. *Chromosoma,* 109**,** 62-71.

CHA, R. S. & KLECKNER, N. (2002) ATR homolog Mec1 promotes fork progression, thus averting breaks in replication slow zones. *Science,* 297**,** 602-6.

CHEN, S. Y., TSUBOUCHI, T., ROCKMILL, B., SANDLER, J. S., RICHARDS, D. R., VADER, G., HOCHWAGEN, A., ROEDER, G. S. & FUNG, J. C. (2008) Global analysis of the meiotic crossover landscape. *Dev Cell,* 15**,** 401-15.

CHEN, Y. T., VENDITTI, C. A., THEILER, G., STEVENSON, B. J., ISELI, C., GURE, A. O., JONGENEEL, C. V., OLD, L. J. & SIMPSON, A. J. (2005) Identification of CT46/HORMAD1, an immunogenic cancer/testis antigen encoding a putative meiosis-related protein. *Cancer Immun,* 5**,** 9.

COLAIACOVO, M. P., MACQUEEN, A. J., MARTINEZ-PEREZ, E., MCDONALD, K., ADAMO, A., LA VOLPE, A. & VILLENEUVE, A. M. (2003) Synaptonemal complex assembly in C. elegans is dispensable for loading strand-exchange proteins but critical for proper completion of recombination. *Dev Cell,* 5**,** 463-74.

COUTEAU, F., NABESHIMA, K., VILLENEUVE, A. & ZETKA, M. (2004) A component of C. elegans meiotic chromosome axes at the interface of homolog alignment, synapsis, nuclear reorganization, and recombination. *Curr Biol,* 14**,** 585-92.

CROMIE, G. A., HYPPA, R. W., TAYLOR, A. F., ZAKHARYEVICH, K., HUNTER, N. & SMITH, G. R. (2006) Single Holliday junctions are intermediates of meiotic recombination. *Cell,* 127**,** 1167-78.

DANIEL, K., LANGE, J., HACHED, K., FU, J., ANASTASSIADIS, K., ROIG, I., COOKE, H. J., STEWART, A. F., WASSMANN, K., JASIN, M., KEENEY, S. & TOTH, A. (2011) Meiotic homologue alignment and its quality surveillance are controlled by mouse HORMAD1. *Nat Cell Biol,* 13**,** 599-610.

DE LOS SANTOS, T. & HOLLINGSWORTH, N. M. (1999) Red1p, a MEK1-dependent phosphoprotein that physically interacts with Hop1p during meiosis in yeast. *J Biol Chem,* 274**,** 1783-90.

DE LOS SANTOS, T., HUNTER, N., LEE, C., LARKIN, B., LOIDL, J. & HOLLINGSWORTH, N. M. (2003) The Mus81/Mms4 endonuclease acts independently of double-Holliday junction resolution to promote a distinct subset of crossovers during meiosis in budding yeast. *Genetics,* 164**,** 81-94.

DERNBURG, A. F., MCDONALD, K., MOULDER, G., BARSTEAD, R., DRESSER, M. & VILLENEUVE, A. M. (1998) Meiotic recombination in C. elegans initiates by a conserved mechanism and is dispensable for homologous chromosome synapsis. *Cell,* 94**,** 387-98.

DI GIACOMO, M., BARCHI, M., BAUDAT, F., EDELMANN, W., KEENEY, S. & JASIN, M. (2005) Distinct DNA-damage-dependent and -independent responses drive the loss of oocytes in recombination-defective mouse mutants. *Proc Natl Acad Sci U S A,* 102**,** 737-42.

DRESSER, M. E. & GIROUX, C. N. (1988) Meiotic chromosome behaviour in spread preparations of yeast. *J Cell Biol,* 106**,** 567-73.

DUROCHER, D. & JACKSON, S. P. (2002) The FHA domain. *FEBS Lett,* 513**,** 58-66.

DUROCHER, D., TAYLOR, I. A., SARBASSOVA, D., HAIRE, L. F., WESTCOTT, S. L., JACKSON, S. P., SMERDON, S. J. & YAFFE, M. B. (2000) The molecular basis of FHA domain:phosphopeptide binding specificity and

implications for phospho-dependent signaling mechanisms. *Mol Cell,* 6**,** 1169-82.

EHMSEN, K. T. & HEYER, W. D. (2008) Saccharomyces cerevisiae Mus81-Mms4 is a catalytic, DNA structure-selective endonuclease. *Nucleic Acids Res,* 36**,** 2182-95.

EICHINGER, C. S. & JENTSCH, S. (2010) Synaptonemal complex formation and meiotic checkpoint signaling are linked to the lateral element protein Red1. *Proc Natl Acad Sci U S A,* 107**,** 11370-5.

FALK, J. E., CHAN, A. C., HOFFMANN, E. & HOCHWAGEN, A. (2010) A Mec1- and PP4-dependent checkpoint couples centromere pairing to meiotic recombination. *Dev Cell,* 19**,** 599-611.

FRIEDEL, A. M., PIKE, B. L. & GASSER, S. M. (2009) ATR/Mec1: coordinating fork stability and repair. *Curr Opin Cell Biol,* 21**,** 237-44.

FRIEDMAN, D. B., HOLLINGSWORTH, N. M. & BYERS, B. (1994) Insertional mutations in the yeast HOP1 gene: evidence for multimeric assembly in meiosis. *Genetics,* 136**,** 449-64.

FUKUDA, T., DANIEL, K., WOJTASZ, L., TOTH, A. & HOOG, C. (2009) A novel mammalian HORMA domain-containing protein, HORMAD1, preferentially associates with unsynapsed meiotic chromosomes. *Exp Cell Res*.

GARCIA, V., PHELPS, S. E., GRAY, S. & NEALE, M. J. (2011) Bidirectional resection of DNA double-strand breaks by Mre11 and Exo1. *Nature,* 479**,** 241-4.

GARCIA-MUSE, T. & BOULTON, S. J. (2007) Meiotic recombination in Caenorhabditis elegans. *Chromosome Res,* 15**,** 607-21.

GARTNER, A., MILSTEIN, S., AHMED, S., HODGKIN, J. & HENGARTNER, M. O. (2000) A conserved checkpoint pathway mediates DNA damage--induced apoptosis and cell cycle arrest in C. elegans. *Mol Cell,* 5**,** 435-43.

GASIOR, S. L., WONG, A. K., KORA, Y., SHINOHARA, A. & BISHOP, D. K. (1998) Rad52 associates with RPA and functions with rad55 and rad57 to assemble meiotic recombination complexes. *Genes Dev,* 12**,** 2208-21.

GHABRIAL, A. & SCHUPBACH, T. (1999) Activation of a meiotic checkpoint regulates translation of Gurken during Drosophila oogenesis. *Nat Cell Biol,* 1**,** 354-7.

GIETZ, R. D. & WOODS, R. A. (2002) Transformation of yeast by lithium acetate/single-stranded carrier DNA/polyethylene glycol method. *Methods Enzymol,* 350**,** 87-96.

GILBERT, C. S., GREEN, C. M. & LOWNDES, N. F. (2001) Budding yeast Rad9 is an ATP-dependent Rad53 activating machine. *Mol Cell,* 8**,** 129-36.

GLYNN, E. F., MEGEE, P. C., YU, H. G., MISTROT, C., UNAL, E., KOSHLAND, D. E., DERISI, J. L. & GERTON, J. L. (2004) Genome-wide mapping of the cohesin complex in the yeast Saccharomyces cerevisiae. *PLoS Biol,* 2**,** E259.

GODDARD, M. R., GODFRAY, H. C. & BURT, A. (2005) Sex increases the efficacy of natural selection in experimental yeast populations. *Nature,* 434**,** 636-40.

GOLDFARB, T. & LICHTEN, M. (2010) Frequent and efficient use of the sister chromatid for DNA double-strand break repair during budding yeast meiosis. *PLoS Biol,* 8**,** e1000520.

GOLDSTEIN, A. L. & MCCUSKER, J. H. (1999) Three new dominant drug resistance cassettes for gene disruption in Saccharomyces cerevisiae. *Yeast,* 15**,** 1541-53.

GRELON, M., VEZON, D., GENDROT, G. & PELLETIER, G. (2001) AtSPO11-1 is necessary for efficient meiotic recombination in plants. *EMBO J,* 20**,** 589-600.

GRUSHCOW, J. M., HOLZEN, T. M., PARK, K. J., WEINERT, T., LICHTEN, M. & BISHOP, D. K. (1999) Saccharomyces cerevisiae checkpoint genes MEC1, RAD17 and RAD24 are required for normal meiotic recombination partner choice. *Genetics,* 153**,** 607-20.

HABER, J. E. (1998) The many interfaces of Mre11. *Cell,* 95**,** 583-6.

HASHASH, N., JOHNSON, A. L. & CHA, R. S. (2011) Regulation of fragile sites expression in budding yeast by MEC1, RRM3 and hydroxyurea. *J Cell Sci,* 124**,** 181-5.

HASSOLD, T. & HUNT, P. (2001) To err (meiotically) is human: the genesis of human aneuploidy. *Nat Rev Genet,* 2**,** 280-91.

HENDERSON, D. S., WIEGAND, U. K., NORMAN, D. G. & GLOVER, D. M. (2000) Mutual correction of faulty PCNA subunits in temperature-sensitive lethal mus209 mutants of Drosophila melanogaster. *Genetics,* 154**,** 1721-33.

HENDERSON, K. A., KEE, K., MALEKI, S., SANTINI, P. A. & KEENEY, S. (2006) Cyclin-dependent kinase directly regulates initiation of meiotic recombination. *Cell,* 125**,** 1321-32.

HIDETAKA, K. (2009) Phos-tag Western blotting for detecting stoichiometric protein phosphorylation in cells. *Nature protocols*.

HO, H. C. & BURGESS, S. M. (2011) Pch2 Acts through Xrs2 and Tel1/ATM to Modulate Interhomolog Bias and Checkpoint Function during Meiosis. *PLoS Genet,* 7**,** e1002351.

HOCHWAGEN, A. & AMON, A. (2006) Checking your breaks: surveillance mechanisms of meiotic recombination. *Curr Biol,* 16**,** R217-28.

HOLLINGSWORTH, N. M. & BYERS, B. (1989) HOP1: a yeast meiotic pairing gene. *Genetics,* 121**,** 445-62.

HOLLINGSWORTH, N. M., GOETSCH, L. & BYERS, B. (1990) The HOP1 gene encodes a meiosis-specific component of yeast chromosomes. *Cell,* 61**,** 73-84.

HOLLINGSWORTH, N. M. & JOHNSON, A. D. (1993) A conditional allele of the Saccharomyces cerevisiae HOP1 gene is suppressed by overexpression of two other meiosis-specific genes: RED1 and REC104. *Genetics,* 133**,** 785-97.

HOLLINGSWORTH, N. M. & PONTE, L. (1997) Genetic interactions between HOP1, RED1 and MEK1 suggest that MEK1 regulates assembly of axial element components during meiosis in the yeast Saccharomyces cerevisiae. *Genetics,* 147**,** 33-42.

HONG, E. J. & ROEDER, G. S. (2002) A role for Ddc1 in signaling meiotic double-strand breaks at the pachytene checkpoint. *Genes Dev,* 16**,** 363-76.

HUNTER, N. & KLECKNER, N. (2001) The single-end invasion: an asymmetric intermediate at the double-strand break to double-holliday junction transition of meiotic recombination. *Cell,* 106**,** 59-70.

IVANOV, E. L., KOROLEV, V. G. & FABRE, F. (1992) XRS2, a DNA repair gene of Saccharomyces cerevisiae, is needed for meiotic recombination. *Genetics,* 132**,** 651-64.

JIAO, K., BULLARD, S. A., SALEM, L. & MALONE, R. E. (1999) Coordination of the initiation of recombination and the reductional division in meiosis in Saccharomyces cerevisiae. *Genetics,* 152**,** 117-28.

JIAO, K., SALEM, L. & MALONE, R. (2003) Support for a meiotic recombination initiation complex: interactions among Rec102p, Rec104p, and Spo11p. *Mol Cell Biol,* 23**,** 5928-38.

JOHZUKA, K. & OGAWA, H. (1995) Interaction of Mre11 and Rad50: two proteins required for DNA repair and meiosis-specific double-strand break formation in Saccharomyces cerevisiae. *Genetics,* 139**,** 1521-32.

JOSHI, N., BAROT, A., JAMISON, C. & BORNER, G. V. (2009) Pch2 links chromosome axis remodeling at future crossover sites and crossover distribution during yeast meiosis. *PLoS Genet,* 5**,** e1000557.

KEE, K. & KEENEY, S. (2002) Functional interactions between SPO11 and REC102 during initiation of meiotic recombination in Saccharomyces cerevisiae. *Genetics,* 160**,** 111-22.

KEENEY, S., GIROUX, C. N. & KLECKNER, N. (1997) Meiosis-specific DNA double-strand breaks are catalyzed by Spo11, a member of a widely conserved protein family. *Cell,* 88**,** 375-84.

KIM, K. P., WEINER, B. M., ZHANG, L., JORDAN, A., DEKKER, J. & KLECKNER, N. (2010) Sister cohesion and structural axis components mediate homolog bias of meiotic recombination. *Cell,* 143**,** 924-37.

KIRONMAI, K. M., MUNIYAPPA, K., FRIEDMAN, D. B., HOLLINGSWORTH, N. M. & BYERS, B. (1998) DNA-binding activities of Hop1 protein, a synaptonemal complex component from Saccharomyces cerevisiae. *Mol Cell Biol,* 18**,** 1424-35.

KLAPHOLZ, S. & ESPOSITO, R. E. (1980a) Isolation of SPO12-1 and SPO13-1 from a natural variant of yeast that undergoes a single meiotic division. *Genetics,* 96**,** 567-88.

KLAPHOLZ, S. & ESPOSITO, R. E. (1980b) Recombination and chromosome segregation during the single division meiosis in SPO12-1 and SPO13-1 diploids. *Genetics,* 96**,** 589-611.

KLEIN, F., MAHR, P., GALOVA, M., BUONOMO, S. B., MICHAELIS, C., NAIRZ, K. & NASMYTH, K. (1999) A central role for cohesins in sister chromatid cohesion, formation of axial elements, and recombination during yeast meiosis. *Cell,* 98**,** 91-103.

KLEIN, H. L. (1997) RDH54, a RAD54 homologue in Saccharomyces cerevisiae, is required for mitotic diploid-specific recombination and repair and for meiosis. *Genetics,* 147**,** 1533-43.

KLUTSTEIN, M., XAVER, M., SHEMESH, R., ZENVIRTH, D., KLEIN, F. & SIMCHEN, G. (2009) Separation of roles of Zip1 in meiosis revealed in heterozygous mutants of Saccharomyces cerevisiae. *Mol Genet Genomics*.

LANGE, A., MILLS, R. E., LANGE, C. J., STEWART, M., DEVINE, S. E. & CORBETT, A. H. (2007) Classical nuclear localization signals: definition, function, and interaction with importin alpha. *J Biol Chem,* 282**,** 5101-5.

LATYPOV, V., ROTHENBERG, M., LORENZ, A., OCTOBRE, G., CSUTAK, O., LEHMANN, E., LOIDL, J. & KOHLI, J. (2010) Roles of Hop1 and Mek1 in meiotic chromosome pairing and recombination partner choice in Schizosaccharomyces pombe. *Mol Cell Biol,* 30**,** 1570-81.

LEEM, S. H. & OGAWA, H. (1992) The MRE4 gene encodes a novel protein kinase homologue required for meiotic recombination in Saccharomyces cerevisiae. *Nucleic Acids Res,* 20**,** 449-57.

LI, J., HOOKER, G. W. & ROEDER, G. S. (2006) Saccharomyces cerevisiae Mer2, Mei4 and Rec114 form a complex required for meiotic double-strand break formation. *Genetics,* 173**,** 1969-81.

LIBBY, B. J., DE LA FUENTE, R., O'BRIEN, M. J., WIGGLESWORTH, K., COBB, J., INSELMAN, A., EAKER, S., HANDEL, M. A., EPPIG, J. J. & SCHIMENTI, J. C. (2002) The mouse meiotic mutation mei1 disrupts chromosome synapsis with sexually dimorphic consequences for meiotic progression. *Dev Biol,* 242**,** 174-87.

LOIDL, J., KLEIN, F. & SCHERTHAN, H. (1994) Homologous pairing is reduced but not abolished in asynaptic mutants of yeast. *J Cell Biol,* 125**,** 1191-200.

LONGHESE, M. P., GUERINI, I., BALDO, V. & CLERICI, M. (2008) Surveillance mechanisms monitoring chromosome breaks during mitosis and meiosis. *DNA Repair (Amst),* 7**,** 545-57.

LONGTINE, M. S., MCKENZIE, A., 3RD, DEMARINI, D. J., SHAH, N. G., WACH, A., BRACHAT, A., PHILIPPSEN, P. & PRINGLE, J. R. (1998) Additional modules for versatile and economical PCR-based gene deletion and modification in Saccharomyces cerevisiae. *Yeast,* 14**,** 953-61.

LORENZ, A., WELLS, J. L., PRYCE, D. W., NOVATCHKOVA, M., EISENHABER, F., MCFARLANE, R. J. & LOIDL, J. (2004) S. pombe meiotic linear elements contain proteins related to synaptonemal complex components. *J Cell Sci,* 117**,** 3343-51.

LYDALL, D., NIKOLSKY, Y., BISHOP, D. K. & WEINERT, T. (1996) A meiotic recombination checkpoint controlled by mitotic checkpoint genes. *Nature,* 383**,** 840-3.

MANCERA, E., BOURGON, R., BROZZI, A., HUBER, W. & STEINMETZ, L. M. (2008) High-resolution mapping of meiotic crossovers and non-crossovers in yeast. *Nature,* 454**,** 479-85.

MANFRINI, N., GUERINI, I., CITTERIO, A., LUCCHINI, G. & LONGHESE, M. P. (2010) Processing of meiotic DNA double strand breaks requires cyclin-dependent kinase and multiple nucleases. *J Biol Chem,* 285**,** 11628-37.

MAO-DRAAYER, Y., GALBRAITH, A. M., PITTMAN, D. L., COOL, M. & MALONE, R. E. (1996) Analysis of meiotic recombination pathways in the yeast Saccharomyces cerevisiae. *Genetics,* 144**,** 71-86.

MARTINEZ-PEREZ, E. & VILLENEUVE, A. M. (2005) HTP-1-dependent constraints coordinate homolog pairing and synapsis and promote chiasma formation during C. elegans meiosis. *Genes Dev,* 19**,** 2727-43.

MCKEE, A. H. & KLECKNER, N. (1997) A general method for identifying recessive diploid-specific mutations in Saccharomyces cerevisiae, its application to the isolation of mutants blocked at intermediate stages of meiotic prophase and characterization of a new gene SAE2. *Genetics,* 146**,** 797-816.

MCKIM, K. S. & HAYASHI-HAGIHARA, A. (1998) mei-W68 in Drosophila melanogaster encodes a Spo11 homolog: evidence that the mechanism for initiating meiotic recombination is conserved. *Genes Dev,* 12**,** 2932-42.

MIECZKOWSKI, P. A., DOMINSKA, M., BUCK, M. J., LIEB, J. D. & PETES, T. D. (2007) Loss of a histone deacetylase dramatically alters the genomic distribution of Spo11p-catalyzed DNA breaks in Saccharomyces cerevisiae. *Proc Natl Acad Sci U S A,* 104**,** 3955-60.

MIMITOU, E. P. & SYMINGTON, L. S. (2008) Sae2, Exo1 and Sgs1 collaborate in DNA double-strand break processing. *Nature,* 455**,** 770-4.

MIMITOU, E. P. & SYMINGTON, L. S. (2009) DNA end resection: many nucleases make light work. *DNA Repair (Amst),* 8**,** 983-95.

MIZUNO, K., EMURA, Y., BAUR, M., KOHLI, J., OHTA, K. & SHIBATA, T. (1997) The meiotic recombination hot spot created by the single-base substitution

ade6-M26 results in remodeling of chromatin structure in fission yeast. *Genes Dev,* 11**,** 876-86.

MOREAU, S., FERGUSON, J. R. & SYMINGTON, L. S. (1999) The nuclease activity of Mre11 is required for meiosis but not for mating type switching, end joining, or telomere maintenance. *Mol Cell Biol,* 19**,** 556-66.

MUNIYAPPA, K., ANURADHA, S. & BYERS, B. (2000) Yeast meiosis-specific protein Hop1 binds to G4 DNA and promotes its formation. *Mol Cell Biol,* 20**,** 1361-9.

MURAKAMI, H. & KEENEY, S. (2008) Regulating the formation of DNA double-strand breaks in meiosis. *Genes Dev,* 22**,** 286-92.

NAG, D. K., SCHERTHAN, H., ROCKMILL, B., BHARGAVA, J. & ROEDER, G. S. (1995) Heteroduplex DNA formation and homolog pairing in yeast meiotic mutants. *Genetics,* 141**,** 75-86.

NAIRZ, K. & KLEIN, F. (1997) mre11S--a yeast mutation that blocks double-strand-break processing and permits nonhomologous synapsis in meiosis. *Genes Dev,* 11**,** 2272-90.

NAVADGI-PATIL, V. M. & BURGERS, P. M. (2009) A tale of two tails: activation of DNA damage checkpoint kinase Mec1/ATR by the 9-1-1 clamp and by Dpb11/TopBP1. *DNA Repair (Amst),* 8**,** 996-1003.

NAVADGI-PATIL, V. M. & BURGERS, P. M. (2011) Cell-cycle-specific activators of the Mec1/ATR checkpoint kinase. *Biochem Soc Trans,* 39**,** 600-5.

NISHANT, K. T., CHEN, C., SHINOHARA, M., SHINOHARA, A. & ALANI, E. (2010) Genetic analysis of baker's yeast Msh4-Msh5 reveals a threshold crossover level for meiotic viability. *PLoS Genet,* 6.

NIU, H., LI, X., JOB, E., PARK, C., MOAZED, D., GYGI, S. P. & HOLLINGSWORTH, N. M. (2007) Mek1 kinase is regulated to suppress double-strand break repair between sister chromatids during budding yeast meiosis. *Mol Cell Biol,* 27**,** 5456-67.

NIU, H., WAN, L., BAUMGARTNER, B., SCHAEFER, D., LOIDL, J. & HOLLINGSWORTH, N. M. (2005) Partner choice during meiosis is regulated by Hop1-promoted dimerization of Mek1. *Mol Biol Cell,* 16**,** 5804-18.

NIU, H., WAN, L., BUSYGINA, V., KWON, Y., ALLEN, J. A., LI, X., KUNZ, R. C., KUBOTA, K., WANG, B., SUNG, P., SHOKAT, K. M., GYGI, S. P. & HOLLINGSWORTH, N. M. (2009) Regulation of meiotic recombination via Mek1-mediated Rad54 phosphorylation. *Mol Cell,* 36**,** 393-404.

NOVAK, J. E., ROSS-MACDONALD, P. B. & ROEDER, G. S. (2001) The budding yeast Msh4 protein functions in chromosome synapsis and the regulation of crossover distribution. *Genetics,* 158**,** 1013-25.

NOWROUSIAN, M., STAJICH, J. E., CHU, M., ENGH, I., ESPAGNE, E., HALLIDAY, K., KAMEREWERD, J., KEMPKEN, F., KNAB, B., KUO, H. C., OSIEWACZ, H. D., POGGELER, S., READ, N. D., SEILER, S., SMITH, K. M., ZICKLER, D., KUCK, U. & FREITAG, M. (2010) De novo assembly of a 40 Mb eukaryotic genome from short sequence reads: Sordaria macrospora, a model organism for fungal morphogenesis. *PLoS Genet,* 6**,** e1000891.

NYBERG, K. A., MICHELSON, R. J., PUTNAM, C. W. & WEINERT, T. A. (2002) Toward maintaining the genome: DNA damage and replication checkpoints. *Annu Rev Genet,* 36**,** 617-56.

OH, S. D., LAO, J. P., HWANG, P. Y., TAYLOR, A. F., SMITH, G. R. & HUNTER, N. (2007) BLM ortholog, Sgs1, prevents aberrant crossing-over by suppressing formation of multichromatid joint molecules. *Cell,* 130**,** 259-72.

PADMORE, R., CAO, L. & KLECKNER, N. (1991) Temporal comparison of recombination and synaptonemal complex formation during meiosis in S. cerevisiae. *Cell,* 66**,** 1239-56.

PAGE, S. L. & HAWLEY, R. S. (2004) The genetics and molecular biology of the synaptonemal complex. *Annu Rev Cell Dev Biol,* 20**,** 525-58.

PALAND, S. & LYNCH, M. (2006) Transitions to asexuality result in excess amino acid substitutions. *Science,* 311**,** 990-2.

PANIZZA, S., MENDOZA, M. A., BERLINGER, M., HUANG, L., NICOLAS, A., SHIRAHIGE, K. & KLEIN, F. (2011) Spo11-accessory proteins link double-strand break sites to the chromosome axis in early meiotic recombination. *Cell,* 146**,** 372-83.

PECINA, A., SMITH, K. N., MEZARD, C., MURAKAMI, H., OHTA, K. & NICOLAS, A. (2002) Targeted stimulation of meiotic recombination. *Cell,* 111**,** 173-84.

PHADNIS, N., HYPPA, R. W. & SMITH, G. R. (2011) New and old ways to control meiotic recombination. *Trends Genet,* 27**,** 411-21.

PRINZ, S., AMON, A. & KLEIN, F. (1997) Isolation of COM1, a new gene required to complete meiotic double-strand break-induced recombination in Saccharomyces cerevisiae. *Genetics,* 146**,** 781-95.

REINHOLDT, L. G. & SCHIMENTI, J. C. (2005) Mei1 is epistatic to Dmc1 during mouse meiosis. *Chromosoma,* 114**,** 127-34.

ROCKMILL, B., ENGEBRECHT, J. A., SCHERTHAN, H., LOIDL, J. & ROEDER, G. S. (1995) The yeast MER2 gene is required for chromosome synapsis and the initiation of meiotic recombination. *Genetics,* 141**,** 49-59.

ROCKMILL, B. & ROEDER, G. S. (1988) RED1: a yeast gene required for the segregation of chromosomes during the reductional division of meiosis. *Proc Natl Acad Sci U S A,* 85**,** 6057-61.

ROCKMILL, B. & ROEDER, G. S. (1990) Meiosis in asynaptic yeast. *Genetics,* 126**,** 563-74.

ROCKMILL, B. & ROEDER, G. S. (1991) A meiosis-specific protein kinase homolog required for chromosome synapsis and recombination. *Genes Dev,* 5**,** 2392-404.

ROEDER, G. S. (1997) Meiotic chromosomes: it takes two to tango. *Genes Dev,* 11**,** 2600-21.

ROEDER, G. S. & BAILIS, J. M. (2000) The pachytene checkpoint. *Trends Genet,* 16**,** 395-403.

ROMANIENKO, P. J. & CAMERINI-OTERO, R. D. (2000) The mouse Spo11 gene is required for meiotic chromosome synapsis. *Mol Cell,* 6**,** 975-87.

SANCHEZ-MORAN, E., OSMAN, K., HIGGINS, J. D., PRADILLO, M., CUNADO, N., JONES, G. H. & FRANKLIN, F. C. (2008) ASY1 coordinates early events in the plant meiotic recombination pathway. *Cytogenet Genome Res,* 120**,** 302-12.

SASANUMA, H., HIROTA, K., FUKUDA, T., KAKUSHO, N., KUGOU, K., KAWASAKI, Y., SHIBATA, T., MASAI, H. & OHTA, K. (2008) Cdc7-dependent phosphorylation of Mer2 facilitates initiation of yeast meiotic recombination. *Genes Dev,* 22**,** 398-410.

SCHWACHA, A. & KLECKNER, N. (1994) Identification of joint molecules that form frequently between homologs but rarely between sister chromatids during yeast meiosis. *Cell,* 76**,** 51-63.

SCHWACHA, A. & KLECKNER, N. (1997) Interhomolog bias during meiotic recombination: meiotic functions promote a highly differentiated interhomolog-only pathway. *Cell,* 90**,** 1123-35.

SCHWARZACHER, T. (2003) Meiosis, recombination and chromosomes: a review of gene isolation and fluorescent in situ hybridization data in plants. *J Exp Bot,* 54**,** 11-23.

SHARIF, W. D., GLICK, G. G., DAVIDSON, M. K. & WAHLS, W. P. (2002) Distinct functions of S. pombe Rec12 (Spo11) protein and Rec12-dependent crossover recombination (chiasmata) in meiosis I; and a requirement for Rec12 in meiosis II. *Cell Chromosome,* 1**,** 1.

SHIN, Y. H., CHOI, Y., ERDIN, S. U., YATSENKO, S. A., KLOC, M., YANG, F., WANG, P. J., MEISTRICH, M. L. & RAJKOVIC, A. (2010) Hormad1 mutation disrupts synaptonemal complex formation, recombination, and chromosome segregation in mammalian meiosis. *PLoS Genet,* 6**,** e1001190.

SHINOHARA, A., GASIOR, S., OGAWA, T., KLECKNER, N. & BISHOP, D. K. (1997a) Saccharomyces cerevisiae recA homologues RAD51 and DMC1 have both distinct and overlapping roles in meiotic recombination. *Genes Cells,* 2**,** 615-29.

SHINOHARA, A., OGAWA, H. & OGAWA, T. (1992) Rad51 protein involved in repair and recombination in S. cerevisiae is a RecA-like protein. *Cell,* 69**,** 457-70.

SHINOHARA, M., OH, S. D., HUNTER, N. & SHINOHARA, A. (2008) Crossover assurance and crossover interference are distinctly regulated by the ZMM proteins during yeast meiosis. *Nat Genet,* 40**,** 299-309.

SHINOHARA, M., SHITA-YAMAGUCHI, E., BUERSTEDDE, J. M., SHINAGAWA, H., OGAWA, H. & SHINOHARA, A. (1997b) Characterization of the roles of the Saccharomyces cerevisiae RAD54 gene and a homologue of RAD54, RDH54/TID1, in mitosis and meiosis. *Genetics,* 147**,** 1545-56.

SHROFF, R., ARBEL-EDEN, A., PILCH, D., IRA, G., BONNER, W. M., PETRINI, J. H., HABER, J. E. & LICHTEN, M. (2004) Distribution and dynamics of chromatin modification induced by a defined DNA double-strand break. *Curr Biol,* 14**,** 1703-11.

SMITH, A. V. & ROEDER, G. S. (1997) The yeast Red1 protein localizes to the cores of meiotic chromosomes. *J Cell Biol,* 136**,** 957-67.

SUN, H., TRECO, D. & SZOSTAK, J. W. (1991) Extensive 3'-overhanging, single-stranded DNA associated with the meiosis-specific double-strand breaks at the ARG4 recombination initiation site. *Cell,* 64**,** 1155-61.

SWEENEY, F. D., YANG, F., CHI, A., SHABANOWITZ, J., HUNT, D. F. & DUROCHER, D. (2005) Saccharomyces cerevisiae Rad9 acts as a Mec1 adaptor to allow Rad53 activation. *Curr Biol,* 15**,** 1364-75.

SYM, M., ENGEBRECHT, J. A. & ROEDER, G. S. (1993) ZIP1 is a synaptonemal complex protein required for meiotic chromosome synapsis. *Cell,* 72**,** 365-78.

SYM, M. & ROEDER, G. S. (1994) Crossover interference is abolished in the absence of a synaptonemal complex protein. *Cell,* 79**,** 283-92.

SYM, M. & ROEDER, G. S. (1995) Zip1-induced changes in synaptonemal complex structure and polycomplex assembly. *J Cell Biol,* 128**,** 455-66.

TERASAWA, M., OGAWA, T., TSUKAMOTO, Y. & OGAWA, H. (2008) Sae2p phosphorylation is crucial for cooperation with Mre11p for resection of DNA double-strand break ends during meiotic recombination in Saccharomyces cerevisiae. *Genes Genet Syst,* 83**,** 209-17.

TERENTYEV, Y., JOHNSON, R., NEALE, M. J., KHISROON, M., BISHOP-BAILEY, A. & GOLDMAN, A. S. (2010) Evidence that MEK1 positively promotes interhomologue double-strand break repair. *Nucleic Acids Res*.

THOMPSON, D. A. & STAHL, F. W. (1999) Genetic control of recombination partner preference in yeast meiosis. Isolation and characterization of mutants elevated for meiotic unequal sister-chromatid recombination. *Genetics,* 153**,** 621-41.

TOUGAN, T., KASAMA, T., OHTAKA, A., OKUZAKI, D., SAITO, T. T., RUSSELL, P. & NOJIMA, H. (2010) The Mek1 phosphorylation cascade plays a role in meiotic recombination of Schizosaccharomyces pombe. *Cell Cycle,* 9**,** 4688-702.

TRAVEN, A. & HEIERHORST, J. (2005) SQ/TQ cluster domains: concentrated ATM/ATR kinase phosphorylation site regions in DNA-damage-response proteins. *Bioessays,* 27**,** 397-407.

TSUBOUCHI, H. & OGAWA, H. (1998) A novel mre11 mutation impairs processing of double-strand breaks of DNA during both mitosis and meiosis. *Mol Cell Biol,* 18**,** 260-8.

TSUBOUCHI, H. & OGAWA, H. (2000) Exo1 roles for repair of DNA double-strand breaks and meiotic crossing over in Saccharomyces cerevisiae. *Mol Biol Cell,* 11**,** 2221-33.

TSUBOUCHI, H. & ROEDER, G. S. (2003) The importance of genetic recombination for fidelity of chromosome pairing in meiosis. *Dev Cell,* 5**,** 915-25.

TSUBOUCHI, H. & ROEDER, G. S. (2006) Budding yeast Hed1 down-regulates the mitotic recombination machinery when meiotic recombination is impaired. *Genes Dev,* 20**,** 1766-75.

USUI, T., FOSTER, S. S. & PETRINI, J. H. (2009) Maintenance of the DNA-damage checkpoint requires DNA-damage-induced mediator protein oligomerization. *Mol Cell,* 33**,** 147-59.

USUI, T., OGAWA, H. & PETRINI, J. H. (2001) A DNA damage response pathway controlled by Tel1 and the Mre11 complex. *Mol Cell,* 7**,** 1255-66.

VERSHON, A. K., HOLLINGSWORTH, N. M. & JOHNSON, A. D. (1992) Meiotic induction of the yeast HOP1 gene is controlled by positive and negative regulatory sites. *Mol Cell Biol,* 12**,** 3706-14.

WAN, L., DE LOS SANTOS, T., ZHANG, C., SHOKAT, K. & HOLLINGSWORTH, N. M. (2004) Mek1 kinase activity functions downstream of RED1 in the regulation of meiotic double strand break repair in budding yeast. *Mol Biol Cell,* 15**,** 11-23.

WAN, L., NIU, H., FUTCHER, B., ZHANG, C., SHOKAT, K. M., BOULTON, S. J. & HOLLINGSWORTH, N. M. (2008) Cdc28-Clb5 (CDK-S) and Cdc7-Dbf4 (DDK) collaborate to initiate meiotic recombination in yeast. *Genes Dev,* 22**,** 386-97.

WOJTASZ, L., DANIEL, K., ROIG, I., BOLCUN-FILAS, E., XU, H., BOONSANAY, V., ECKMANN, C. R., COOKE, H. J., JASIN, M., KEENEY, S., MCKAY, M. J. & TOTH, A. (2009) Mouse HORMAD1 and HORMAD2, two conserved meiotic chromosomal proteins, are depleted from synapsed chromosome axes with the help of TRIP13 AAA-ATPase. *PLoS Genet,* 5**,** e1000702.

WOLTERING, D., BAUMGARTNER, B., BAGCHI, S., LARKIN, B., LOIDL, J., DE LOS SANTOS, T. & HOLLINGSWORTH, N. M. (2000) Meiotic segregation, synapsis, and recombination checkpoint functions require physical

interaction between the chromosomal proteins Red1p and Hop1p. *Mol Cell Biol,* 20**,** 6646-58.

WU, T. C. & LICHTEN, M. (1994) Meiosis-induced double-strand break sites determined by yeast chromatin structure. *Science,* 263**,** 515-8.

WU, T. C. & LICHTEN, M. (1995) Factors that affect the location and frequency of meiosis-induced double-strand breaks in Saccharomyces cerevisiae. *Genetics,* 140**,** 55-66.

XU, L., WEINER, B. M. & KLECKNER, N. (1997) Meiotic cells monitor the status of the interhomolog recombination complex. *Genes Dev,* 11**,** 106-18.

YAMADA, T., MIZUNO, K., HIROTA, K., KON, N., WAHLS, W. P., HARTSUIKER, E., MUROFUSHI, H., SHIBATA, T. & OHTA, K. (2004) Roles of histone acetylation and chromatin remodeling factor in a meiotic recombination hotspot. *EMBO J,* 23**,** 1792-803.

YU, H. G. & KOSHLAND, D. E. (2003) Meiotic condensin is required for proper chromosome compaction, SC assembly, and resolution of recombination-dependent chromosome linkages. *J Cell Biol,* 163**,** 937-47.

ZANDERS, S. & ALANI, E. (2009) The pch2Delta mutation in baker's yeast alters meiotic crossover levels and confers a defect in crossover interference. *PLoS Genet,* 5**,** e1000571.

ZANDERS, S., SONNTAG BROWN, M., CHEN, C. & ALANI, E. (2011) Pch2 Modulates Chromatid Partner Choice During Meiotic Double-Strand Break Repair in Saccharomyces cerevisiae. *Genetics,* 188**,** 511-21.

ZETKA, M. C., KAWASAKI, I., STROME, S. & MULLER, F. (1999) Synapsis and chiasma formation in Caenorhabditis elegans require HIM-3, a meiotic chromosome core component that functions in chromosome segregation. *Genes Dev,* 13**,** 2258-70.

ZHOU, B. B. & ELLEDGE, S. J. (2000) The DNA damage response: putting checkpoints in perspective. *Nature,* 408**,** 433-9.

ZICKLER, D. & KLECKNER, N. (1998) The leptotene-zygotene transition of meiosis. *Annu Rev Genet,* 32**,** 619-97.

ZIMMER, C. (2009) Origins. On the origin of sexual reproduction. *Science,* 324**,** 1254-6.

ZIMMERING, S. (1963) The effect of temperature on meiotic loss of the Y chromosome in the male Drosophila. *Genetics,* 48**,** 133-8.